LEVEL

THE EFFECT OF WINGLETS ON THE KC-135A AIRCRAFT

George W. Loptien
Flight Vehicle Branch
Aeromechanics Division

D D C
MAY 8 1979
C

November 1978

TECHNICAL REPORT AFFDL-TR-78-124

Final Report for Period June 1975 - October 1977

AIR FORCE FLIGHT DYNAMICS LABORATORY
AIR FORCE WRIGHT AERONAUTICAL LABORATORIES
AIR FORCE SYSTEMS COMMAND
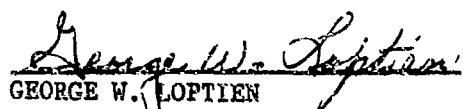WRIGHT-PATTERSON AIR FORCE BASE, OHIO 45433

79 05 07 019

NOTICE

When Government drawings, specifications, or other data are used for any purpose other than in connection with a definitely related Government procurement operation, the United States Government thereby incurs no responsibility nor any obligation whatsoever; and the fact that the government may have formulated, furnished, or in any way supplied the said drawings, specifications, or other data, is not to be regarded by implication or otherwise as in any manner licensing the holder or any other person or corporation, or conveying any rights or permission to manufacture, use, or sell any patented invention that may in any way be related thereto.

This report has been reviewed by the Information Office (OI) and is releasable to the National Technical Information Service (NTIS). At NTIS, it will be available to the general public, including foreign nations.

This technical report has been reviewed and is approved for publication.
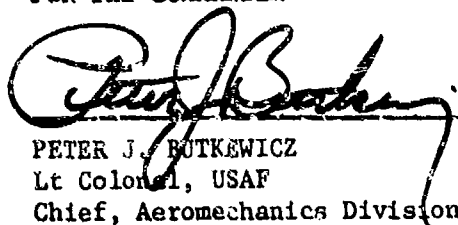
GEORGE W. LOPTIEN
Project Engineer
Flight Vehicle Branch
Aeromechanics Division

CHARLES J. COSENZA
Chief, Flight Vehicle Branch
Aeromechanics Division

FOR THE COMMANDER

PETER J. BUTKEWICZ
Lt Colonel, USAF
Chief, Aeromechanics Division

"If your address has changed, if you wish to be removed from our mailing list, or if the addressee is no longer employed by your organization please notify AFFDL/FXS ,W-PAFB, OH 45433 to help us maintain a current mailing list".

Copies of this report should not be returned unless return is required by security considerations, contractual obligations, or notice on a specific document.

AIR FORCE/56780/24 April 1979 — 100

REPORT DOCUMENTATION PAGE		READ INSTRUCTIONS BEFORE COMPLETING FORM
1. REPORT NUMBER AFFDL-TR-78-124	2. GOVT ACCESSION NO.	3. RECIPIENT'S CATALOG NUMBER
4. TITLE (and Subtitle) THE EFFECT OF WINGLETS ON THE KC-135 AIRCRAFT		5. TYPE OF REPORT & PERIOD COVERED Final Report. June 1975 - October 1977
		6. PERFORMING ORG. REPORT NUMBER
7. AUTHOR(s) George W. Loptien		8. CONTRACT OR GRANT NUMBER(s)
9. PERFORMING ORGANIZATION NAME AND ADDRESS Air Force Flight Dynamics Laboratory (AFFDL/FXS) Air Force Wright Aeronautical Laboratories Wright-Patterson Air Force Base, Ohio 45433		10. PROGRAM ELEMENT, PROJECT, TASK AREA & WORK UNIT NUMBERS Project 2404, Task 240416, Work Unit 24041603
11. CONTROLLING OFFICE NAME AND ADDRESS Air Force Flight Dynamics Laboratory (AFFDL/FXS) Air Force Wright Aeronautical Laboratories Wright-Patterson Air Force Base, Ohio 45433		12. REPORT DATE November 1978
		13. NUMBER OF PAGES 118
14. MONITORING AGENCY NAME & ADDRESS(if different from Controlling Office)		15. SECURITY CLASS. (of this report) Unclassified
		15a. DECLASSIFICATION/DOWNGRADING SCHEDULE

16. DISTRIBUTION STATEMENT (of this Report)

Approved for public release; distribution unlimited.

17. DISTRIBUTION STATEMENT (of the abstract entered in Block 20, if different from Report)

18. SUPPLEMENTARY NOTES

19. KEY WORDS (Continue on reverse side if necessary and identify by block number)

KC-135, Winglets, Drag Reduction, Fuel Savings

20. ABSTRACT (Continue on reverse side if necessary and identify by block number)

To investigate the effects of winglets on the aerodynamic characteristics of the KC-135 aircraft, semispan and full-span wind tunnel models with winglets have been investigated in the NASA/LRC 8-Foot Transonic Pressure Tunnel. At cruise conditions, the full-span tests indicated a total drag reduction of 5.3 percent for the model with the Boeing and NASA upper plus lower winglet configurations and 6.5 percent for the model with the NASA upper winglet configuration. A wing-tip-extension configuration tested on the semispan model
(over)

DD _{1 JAN 73} FORM **1473** EDITION OF 1 NOV 65 IS OBSOLETE

20. Abstract (Continued)

had a drag reduction of about 3 percent compared to about 5 to 7 percent for the winglet configurations, however, the tip extension was not optimized for drag reduction. At cruise conditions, the wing tip extension produced the greatest increase in the wing root bending moment and the upper winglets the least. The increase in wing root bending moment at cruise conditions varied from about 2.5 percent with the Boeing winglets, to about 3.5 percent with the tip extension. At cruise flight conditions, winglets on the KC-135A aircraft were estimated to reduce the drag about 8.2 percent and increase the maximum lift-drag ratio about 9.5 percent.

ACCESSION for

NTIS   White Section
DDC   B ff Section
UNANNOUNCED
JUSTIFICATION

BY
DISTRIBUTION

FOREWORD

This report was prepared by Mr. George W. Loptien of the Flight Vehicle Branch, Aeromechanics Division, Air Force Flight Dynamics Laboratory, Wright-Patterson Air Force Base, Ohio, under Project 2404, Aerodynamic Synthesis and Flight Research, Task 240416, Unified Flight Mechanics Technology, Work Unit 24041603, Analysis and Evaluation of Aero Configuration Advancements.

Winglets appear to offer significant improvement in aerodynamic efficiency and fuel and operating cost savings. This Report summarizes basic information concerning winglets and is part of an overall plan to develop winglet technology for flight test demonstration.

Winglets have been investigated using semispan and full span KC-135A models in the NASA/LaRC 8-Foot Transonic Pressure Tunnel. Basic results from this investigation are presented in this Report. Mr. Stuart G. Flechner, NASA/LaRC, was the project engineer.

TABLE OF CONTENTS

ILLUSTRATIONS

ILLUSTRATIONS (CONTINUED)

ILLUSTRATIONS (CONTINUED)

ILLUSTRATIONS (CONTINUED)

ILLUSTRATIONS (CONTINUED)

ILLUSTRATIONS (CONTINUED)

ILLUSTRATIONS (CONTINUED)

SYMBOLS

$$\Delta C_L = C_{L_{\substack{\text{WITH} \\ \text{WINGLET}}}} - C_{L_{\substack{\text{WITHOUT} \\ \text{WINGLET}}}}$$ Incremental lift coefficient

$$\Delta C_D = C_{D_{\substack{\text{WITH} \\ \text{WINGLET}}}} - C_{D_{\substack{\text{WITHOUT} \\ \text{WINGLET}}}}$$ Incremental drag coefficient

$$\Delta C_m = C_{m_{\substack{\text{WITH} \\ \text{WINGLET}}}} - C_{m_{\substack{\text{WITHOUT} \\ \text{WINGLET}}}}$$ Incremental pitching moment coefficient

$$\Delta C_b = C_{b_{\substack{\text{WITH} \\ \text{WINGLET}}}} - C_{b_{\substack{\text{WITHOUT} \\ \text{WINGLET}}}}$$ Incremental wing root bending moment coefficient

$$\Delta C_n = C_{n_{\substack{\text{WITH} \\ \text{WINGLET}}}} - C_{n_{\substack{\text{WITHOUT} \\ \text{WINGLET}}}}$$ Incremental yawing moment coefficient

$$\Delta C_l = C_{l_{\substack{\text{WITH} \\ \text{WINGLET}}}} - C_{l_{\substack{\text{WITHOUT} \\ \text{WINGLET}}}}$$ Incremental rolling moment coefficient

$$\Delta \alpha = \alpha_{\substack{\text{WITH} \\ \text{WINGLET}}} - \alpha_{\substack{\text{WITHOUT} \\ \text{WINGLET}}}$$ Incremental angle of attack

$$C_L = \frac{L}{qS}$$ Lift coefficient

$$C_D = \frac{D}{qS}$$ Drag coefficient

$$C_m = \frac{M\alpha}{qS\bar{c}}$$ Pitching moment coefficient

$$C_b = \frac{B}{qSb}$$ Wing root bending moment coefficient

$$C_n = \frac{N}{qSb}$$ Yawing moment coefficient

$$C_l = \frac{R}{qSb}$$ Rolling moment coefficient

$$L$$ Lift

SYMBOLS (CONTINUED)

D   Drag

Mα   Pitching moment, about an axis perpen-
                                           dicular to plane of symmetry and through
                                           the quarter chord position of the wing
                                           mean aerodynamic chord, positive nose
                                           up

B   Wing root bending moment (rolling
                                           moment of one-half of model), about a
                                           longitudinal axis parallel to plane of
                                           symmetry at the wing-fuselage juncture,
                                           positive up

N   Yawing moment, about a vertical axis
                                           parallel to plane of symmetry, positive
                                           nose right

R   Rolling moment, about a longitudinal axis
                                           parallel to plane of symmetry, positive
                                           right wing down

q   Free stream dynamic pressure

S   Wing reference area

                                               $S = 5.003 \ ft^2$ (semispan model, exposed
                                                               basic wing, NASA wing-
                                                               lets)
                                               $S = 5.038 \ ft^2$ (semispan model, exposed
                                                               basic wing, Boeing
                                                               winglets)
                                               $S = 2.91 ft^2$ (full span model)

$\bar{c}$ Wing reference chord

                                               $\bar{c} = 15.74$ in. (semispan model, exposed
                                                               basic wing, NASA wing-
                                                               lets)
                                               $\bar{c} = 15.69$ in. (semispan model, exposed
                                                               basic wing, Boeing
                                                               winglets)
                                               $\bar{c} = 8.28$ in. (full span model)

SYMBOLS (CONTINUED)

b	Wing reference span
	b = 54.60 in. (full span model)
b´	Exposed basic wing semispan
	b´ = 48.92 in. (semispan model,NASA wing)
	b´ = 49.56 in. (semispan model, Boeing wing)
ℓ	Winglet length or span
M	Mach number
R/ft	Reynolds number per foot
α	Angle of attack, angle between fuselage centerline and flow direction, positive nose up
β	Angle of sideslip, angle between fuselage centerline and flow direction, positive nose left
i_u	Upper winglet incidence angle, angle between upper winglet root chord and plane of symmetry, positive nose toward plane of symmetry (toe in)
i_L	Lower winglet incidence angle, angle between lower winglet root chord and plane of symmetry, positive nose away from plane of symmetry (toe out)
ϕ_U	Upper winglet cant angle, angle between upper winglet and vertical, positive cant outward
ϕ_L	Lower winglet cant angle, angle between lower winglet and vertical, positive cant outward
i_H	Horizontal tail incidence angle, angle between horizontal tail chord line and fuselage centerline, positive nose up

SYMBOLS (CONTINUED)

δ_F Wing flap deflection angle, angle
between flap chord and wing chord,
positive flaps down

δ_A Aileron deflection angle, angle between
aileron chord and wing chord, positive
trailing edge down

Aileron deflection is designated by two
numbers separated by a slash mark, e.g.,
δ_A = 0/0. The number to the left of the
slash mark indicates left aileron deflec-
tion and the number to the right, the
right aileron deflection.

Subscripts:

WING   Semispan model wing without winglets

B   Basic KC-135A model without winglets
(Wing tips clipped to accommodate mounting
winglets)

INTRODUCTION

The USAF is interested in reducing the fuel requirements and operational costs of existing and future aircraft. Methods for improving aircraft efficiency are continually being investigated and innovative aerodynamic drag reduction technologies are constantly being sought. A method suitable for retrofit to existing fleet aircraft is highly desirable.

The winglet concept, developed by NASA/LRC, appears to offer significant improvement in aircraft efficiency by reducing aircraft drag, fuel requirements, and operating costs. Winglets represent the latest state-of-the-art aerodynamic drag reduction technology and offer significant improvement in aircraft efficiency. Total drag reductions up to 8 percent have been estimated for the KC-135A aircraft at cruise.

The feasibility of winglets on the KC-135 aircraft has been investigated by the Boeing Commercial Airplane Company under Air Force contract (Reference 1). This investigation has indicated no basic aerodynamic, structural, or dynamic problems from winglets on the KC-135. The investigation has indicated a fuel savings of 68,000 gallons per aircraft per year, which results in a fleet fuel savings of 44 million gallons per year at a cost savings of 17.5 million dollars (40¢/gallon). A KC-135 winglet retrofit investigation indicated the cost for retrofitting winglets to be $66,000 (1977 dollars) per aircraft, or a fleet retrofit cost of about 42.5 million dollars.

The aerodynamic characteristics of semispan and full-span KC-135A wind tunnel models with different winglet concepts have been investigated in the

1

NASA/LRC 8-Foot Transonic Pressure Tunnel. Data from these investigations
have been provided to the Air Force Flight Dynamics Laboratory and some
basic results are presented in this Report.

MODEL AND TEST APPARATUS

Semispan Model.

An 0.070-scale semispan wind tunnel model was constructed by NASA/LRC
(Figures 1 and 2).* A semispan model configuration was selected to obtain
maximum Reynolds number on the winglets.

The 0.070-scale semispan model consisted of the right half of the
KC-135A aircraft. The wing was constructed basically of aluminum and was
designed to deflect under airloads to simulate aeroelastic deflection. The
wing was designed so that the tip deflected approximately the same as the
tip of the full-scale airplane at cruise conditions. The model included
the wing, flow-through nacelles, and fuselage (no tail), although only the
wing and nacelles were attached to the balance system. The basic KC-135A
aircraf: wing has a sweep angle at the quarter chord of 35 degrees, an aspect
ratio of 7.035, a taper ratio of 0.33, a 7-degree dihedral, two degrees
positive incidence at the root, and no geometric twist. The thickness/chord
ratio varies non-linearly from 15 percent at the wing-fuselage juncture to
9 percent at the trailing edge break station and then remains constant at
9 percent to the tip.

To accommodate mounting the winglets, a small portion of the model wing
tip was cut off, reducing the aspect ratio of the basic wing slightly. In
addition, the NASA and Boeing winglets were mounted at slightly different
spanwise locations so that the span of the basic wing was slightly different.

*Figures are located at end of report.

The exposed model wing semispan was 43.92 inches for the NASA basic wing (Figure 2) and 49.56 for the Boeing basic wing. The aspect ratio of the KC-135A wing was reduced from 7.035 to 6.86 for the NASA basic wing and 6.98 for the Boeing basic wing. The slightly different spanwise location of the winglets should have only minimal effect on the aerodynamic characteristics. A simple analysis (Appendix A) indicated a loss in aircraft lift-drag ratio of about -0.07, or about 0.4 percent, with removal of the tip portion of the basic wing.

The original NASA winglet concept was composed of upper and lower winglet fins (Figure 3); however, both upper winglets (only) and upper plus lower winglet combinations were investigated. The Boeing winglet configuration tested (Figure 4) was slightly different from the configuration investigated analytically (Reference 1) because of an error in model fabrication. As a result, the winglet configuration tested had a cant angle of 6 degrees instead of 20 degrees. The wing tip extension model (Figure 2) was an extension of the basic wing sized to produce approximately the same increase in wing root bending moment as the NASA upper plus lower winglet configuration. The span of the tip extension was 3.0 inches.

Fixed-position leading and trailing edge flap configurations were investigated on the semispan KC-135A model (Figure 5). These flaps were only representative and did not conform to the flap geometry of the KC-135A airplane. The trailing edge flaps were located just inboard of the nacelle centerlines and had a chord of 10% of the wing chord. Flap deflection for the leading edge flaps was 70 degrees and for the trailing edge flaps 25 degrees.

3

Full Span Model.

The basic 0.035 scale full span KC-135A model for the low speed
investigation (M = 0.3) (Figure 6) was equipped with a wing having flaps
and ailerons. The wings were constructed from steel and were not designed
to deflect aeroelastically. Three wing flap deflections 0, 30, and 50 degrees,
and three aileron deflections 0, ±10, and ±20 degrees could be set (Figure 7).
The model had four strut-mounted, flow-through nacelles attached to the wings.
To accommodate mounting the winglets, a small portion of the model wing tips
were cut off, reducing the aspect ratio of the basic wing from 7.035 to 6.98.
A variable incidence horizontal tail could be set at incidence angles of 0,
-4, and -10 degrees.

Because of the basic KC-135A model body construction, the strain gage
balance was located so far aft that the balance pitching moment limit was
exceeded at very low lift values at high speed. Consequently, the KC-135A
model body was replaced with a body that located the balance further forward.
This body was slightly larger than the KC-135A model body and was circular
instead of oval in cross section; however, these slight differences should
have only minimal effect on the aerodynamic characteristics. Because of the
construction of the body, the horizontal and vertical tails could not be
attached, and all high-speed tests were made without horizontal and vertical
tails. The wing for the high-speed model was constructed from steel and was
not designed to deflect aeroelastically. The wing was constructed without
flaps or ailerons and had a portion of the wing tips cut off to accommodate
mounting the winglets. Four strut-mounted, flow-through nacelles were
attached to the wings.

Test Apparatus.

The experimental investigation was conducted in the NASA/LRC 8 Foot
Transonic Pressure Tunnel, a continuous-flow, single-return, variable-
pressure facility with a closed slotted test section. The Mach number
range is from about 0.3 to 1.35.

The 0.070-scale semispan KC-135A model was attached to a balance system
located outside the left wall of the tunnel test section and was mounted in
the upright position. Only the wing, nacelles, and winglets were attached
to the balance. The fuselage was attached to a turntable in the left wall
of the test section and pitched with the wing, however, the fuselage was
completely isolated and no fuselage loads were recorded by the balance. The
fuselage had a slot through which the wing passed.

The 0.035-scale full-span KC-135A model was mounted in the center of
the tunnel test section on a sting-supported six-component strain gage balance
system. Aerodynamic forces and moments were read out on magnetic tape which
was computer processed.

<div align="center">DISCUSSION</div>

Winglets

Winglets are small, cambered fins located at the wing tips (Figures 1
and 6). Two winglet configurations developed by NASA/LRC and the Boeing
Commercial Airplane Company are shown in Figures 3 and 4. The original NASA
winglet configuration had fins both above and below the wing plane (Figure 3).
The upper fin was larger and was located rearward on the tip chord; the
trailing edge of the root chord section was located at the wing tip trailing
edge. The Boeing Company configuration was developed analytically and had

<div align="center">5</div>

only an upper fin (Figure 4) located rearward on the tip chord. A basic difference is the leading-edge strake which is intended to reduce the twist required at the winglet root and facilitate blending the winglet into the wing. The NASA upper winglets had a trapezoidal planform with an area 3.8% of the exposed basic wing area, a root chord 65% of the wing tip chord, a tip chord 21% of the wing tip chord, a height equal to the wing tip chord, and a leading edge sweep angle of 38 degrees. The upper winglets were untwisted, cambered outward (upper surface inboard), inclined outward from vertical, and were positioned so that the trailing edge of the root section was located at the wing tip trailing edge. The lower surface winglets had a trapezoidal planform with an area 0.6% of the exposed basic wing area, a span 23% of the wing tip chord, a root chord 40% of the wing tip chord, and a leading edge sweep angle of 52 degrees. The lower winglets were cambered inward, inclined outward from the vertical, had an incidence of -7 degrees (toed in), were twisted about the leading edge with 4 degrees of washout at the tip, and were positioned so that the leading edge was located at the wing tip leading edge. Both upper and lower winglets had 9% thick GA(W)-2 airfoil sections.

The Boeing winglets had a trapezoidal planform with an area of 3.5% of the exposed basic wing area, a root chord 60% of the wing tip chord, a height 13.5% of the wing (not exposed) semispan, and a winglet leading edge sweep angle of 37 degrees. The Boeing winglets had a strake at the leading edge, were cambered outward, were inclined 6 degrees outward from vertical, and were positioned so that the trailing edge of the root chord was located at the wing trailing edge. The winglets had a 6% thick, Boeing developed, supercritical airfoil and incorporated twist in the winglet root.

6

Results of Boeing Investigations

In Reference 1, potential performance improvements from winglets were investigated analytically. Results of this investigation indicated an 8.4 percent improvement in cruise M(L/D), a net improvement in range factor of 8.1 percent, and an increase in overall empty weight of 592 lb. Performance improvements from equal area tip extensions were also investigated.

The primary effect of winglets and tip extensions is to reduce induced drag, and, consequently, reduce total aircraft drag. However, in addition to performance gains from winglets or tip extensions, their effects on the aircraft structure must be considered. The weight of the winglets and their attachment structure will cancel some aerodynamic benefit and the local and wing root bending moments will be increased, possibly increasing wing weight.

Various winglet parameters were investigated analytically to determine the potential aerodynamic improvement on the KC-135 aircraft at cruise conditions. For all cases investigated, the winglets were located at the tip on the upper wing surface only. This investigation indicated that winglet chordwise location, sweep, taper ratio, and area do not significantly affect the overall aerodynamic characteristics of the KC-135 aircraft. Winglet length and cant angle appear to be the most significant parameters (Figures 8 and 9).

For the winglet length selected for the KC-135 aircraft (0.135 $^b/2$), a reduction in the induced drag of about 14 percent and an increase in the wing root bending moment of about 4 percent was indicated at cruise (Figure 8) for a winglet with no cant. As the winglet is canted outward (Figure 9), the induced drag is further reduced; however, the wing root bending moment is

increased. For the KC-135 winglets (cant 20 degrees), the induced drag reduction was about 17 percent and the wing root bending moment increase about 6 percent.

A number of different equal area tip extensions were also investigated (Figure 10). Comparison of the induced drag reduction and wing root bending moment increase for zero cant winglets and wing tip extensions is shown in Figure 11. When the winglet and tip extension produce the same induced drag improvement (14% for an 0.135 $^b/2$ winglet with no cant), the tip extension had 31 percent greater wing root bending moment than the winglet. When the root bending moment of the winglet and tip extension are equal, the induced drag was reduced about 22.9 percent more by the winglet than by the tip extension. The winglet gives greater aerodynamic improvement or a lighter structure.

Both winglets and wing tip extensions increase the aircraft nose-down pitching moment. Figure 12 shows that the nose-down pitching moment change of the KC-135 was considerably greater for a tip extension than for a corresponding zero cant winglet. When the winglet and tip extension produce the same induced drag improvement (14%), the pitching moment change from the tip extension was about 80 percent greater than that of the winglet. For equal wing root bending moment, the pitching moment change from the tip extension was about 35.7 percent. Both winglets and tip extensions increased the aircraft longitudinal stability.

Aerodynamic Data

Aerodynamic force and moment measurements obtained on the KC-135A models are presented in coefficient form in the stability axis system and are referenced to the wing area, span, and wing reference chord. The data

have been corrected for tunnel flow angularity, tunnel wall, and blockage
effects. Moments are presented about orthogonal axes through the moment
reference center. The wing root bending moment is the rolling moment of the
projecting semispan wing about an axis parallel to the plans of symmetry at
the wing fuselage juncture. The incremental aerodynamic characteristics of
the different configurations have been obtained from large-scale plots.
Data without winglets are for the wing tip clipped configuration.

At cruise conditions, $M = 0.77$ at 30,000 feet, the overall KC-135A
airplane cruise lift coefficient is about 0.426. At take off, flaps are
deflected 30 degrees and the lift coefficient is about 1.22, and at landing,
the flap deflection is 50 degrees and the lift coefficient about 1.0.

Winglet Configuration.

Results from the semispan wind tunnel tests at high subsonic speed
(Figure 13) indicated the greatest drag reductions with the NASA upper plus
lower winglet configuration; however, drag reductions of similar magnitude
were found with the upper winglet configurations at cruise lift coefficients.
For a cruise lift coefficient of 0.426, a total drag reduction of about 5.4
percent was indicated with the Boeing winglet configuration ($\phi_U = 6$ degrees)
and about 6.9 percent with the NASA upper ($\phi_U = 15$ degrees) and the NASA upper
plus lower ($\phi_U = 15$ degrees, $\phi_L = 36$ degrees) winglet configurations.

At low speed, contrary to the high-speed results, the greatest drag
reduction was found with the NASA upper winglet configuration (Figure 14).
Analytical results from the Nonplanar Lifting Systems Program (Reference 2)
also indicated the single upper winglet configuration to be slightly superior
in reducing induced drag. References 1 and 3 indicate that the effect of the

lower winglet is generally favorable, but that improvement in overall performance is only marginal. Because gains from the lower winglet are small and structural complexity increased, the lower winglet was eliminated from later NASA KC-135 winglet configurations. However, winglet effects are most likely configuration dependent, and the dual winglet configuration could prove advantageous for other aircraft.

Contrary to results from the semispan model tests, the full-span KC-135A model tests indicated the greatest drag reduction generally with the NASA upper winglet configuration (Figures 15 to 20); however, drag reductions of similar magnitude were achieved with the other winglet configurations investigated. In addition, it must be considered that the cant angle of the Boeing winglet configuration was six degrees, and that greater drag reduction could be achieved if the cant angle was increased. For cruise conditions, $M = 0.78$ and $C_L = 0.426$ (Figure 19), a total drag reduction of about 5.3 percent was obtained with the Boeing and NASA upper plus lower winglet configurations and about 6.5 percent with the NASA upper winglet configuration. At low speed (Figure 15), drag reduction of the KC-135A model with NASA upper winglets at $C_L = 0.426$ was approximately 3.0 percent, about half of the drag reduction achieved at cruise.

For lift coefficients less than about 0.2, the incremental winglet drag was positive, indicating the profile drag increase to be greater than the induced drag decrease generated by the winglets. For lift coefficients greater than about 0.2, the incremental total drag becomes negative indicating the decrease induced drag from the winglets to be greater than the increase in profile drag, resulting in an overall drag reduction for the KC-135A

model. As the drag reduction from winglets is primarily induced drag, these devices can be expected to be more effective at higher lift coefficients, and, as shown by Figures 15 to 20, drag reduction was considerably greater at higher lift coefficients. At cruise Mach number (Figure 19), drag reduction varied from about one percent at $C_L = 0.2$ to about 13 per cent at $C_L = 0.8$ for the NASA upper winglet configuration. The drag reduction achieved with the different winglet configurations on the KC-135A model at $C_L = 0.426$ with Mach number is shown in Figure 21.

The effect of the different winglet configurations on the lift of the KC-135A model (Figures 22 to 27) was to generally increase the lift about one to three percent. At cruise lift conditions (Figure 26), the increase in lift of the KC-135A model was about 2.5 percent with all of the winglet configurations investigated. Variation of the incremental lift of the KC-135A model with the different winglet configurations with Mach number is shown in Figure 28 and variation of the incremental lift curve slope with Mach number is shown in Figure 29. The lift curve slope of the KC-135A model was generally increased about one to three percent by the different winglet configurations. At low Mach numbers, the increase in lift curve slope appears to be slightly greater with the NASA upper plus lower winglet configuration; however, at higher Mach numbers, the increase is about the same as with the upper winglet configurations. Because of the increased lift with the winglets, the aircraft can fly at a reduced angle of attack which will reduce the profile drag. At cruise conditions, the reduction in angle of attack of the KC-135A model with winglets was about -0.1 degree (Figure 30).

A measure of the aerodynamic efficiency is the lift-drag ratio. The increase in the maximum untrimmed lift-drag ratio of the KC-135A model with

11

the different winglet configurations is shown in Figure 31 for different
Mach numbers. The increase in maximum untrimmed lift-drag ratio was about
the same with all of the different winglet configurations investigated.
At cruise conditions, the increase in the model maximum untrimmed lift-
drag ratio because of winglets was about 8 percent.

The effect of the different winglet configurations on the pitching
moment was to increase the nose down pitching moment and increase the longi-
tudinal stability of the KC-135A model (Figures 32 to 37). At cruise lift
conditions, the increase in nose-down pitching moment was about 13 percent
for the model with the NASA upper and Boeing winglet configurations and about
16 percent for the NASA upper plus lower winglet configuration. Variation of
the increase in nose-down pitching moment of the KC-135A model with the differ-
ent winglet configurations with Mach number is shown in Figure 38 for $C_L = 0.426$.

The effect of winglet configuration on the model aerodynamic characteris-
tics at low speed was also investigated at a flap deflection of 50 degrees and
a horizontal tail incidence angle of -10 degrees (Figures 39 to 41). The
greatest drag reduction was found with the upper winglet configurations
(Figure 39), and, as shown, the drag reduction was essentially the same for
both configurations investigated. At $C_L = 1.0$ (landing condition), Figure 39
indicates a total drag reduction of about 2.5 percent for the upper winglet
configurations and about 1.0 percent for the NASA upper plus lower winglet
configuration. Because of the difference in cant angle, the model tests at
$\delta_F = 0$ (tail off) generally indicate a slightly greater drag reduction with
the NASA upper winglet configuration than with the Boeing winglet configuration.
No explanation is known for the different behavior at $\delta_F = 50$ degrees. The
effect of the different winglet configurations on the lift of the model at

12

δ_F= 50 degrees, i_H= -10 degrees (Figure 40) was to generally increase the lift about 1 to 2 percent, except at very high lift coefficients. The effect of the winglets on the pitching moment at δ_F= 50 degrees, i_H= -10 degrees (Figure 41) was to increase the nose-down pitching moment and increase the longitudinal stability of the model.

Wing Root Bending Moment

Potential aerodynamic benefits from winglets appear to be significant; however, their total impact on the performance and structure of an aircraft has to be evaluated. The weight of the winglets and their attachment structure offset some of the aerodynamic benefit, and both the local and wing root bending moment will be increased. To accommodate the increased moments, wing weight may have to be increased, and an assessment between the benefits of improved aerodynamic performance and increased wing weight must be made.

To evaluate the effects of winglets on the KC-135 aircraft, all effects on the aircraft structure have been assumed to be proportional to measured model wing root bending moments. The wing root bending moments of the semi-span KC-135A model with and without winglets were measured by a strain gage built into the model wing. For this case, the wing root bending moment was the rolling moment of the exposed semispan wing. At cruise conditions (M = 0.78, C_L= 0.426) (Figure 42), the measured increase in the wing root bending moment of the semispan KC-135A model was about 2.5 percent with the Boeing winglet configuration and about 3 percent with both the NASA upper and the NASA upper plus lower winglet configurations. The Boeing analytical investigation indicated an increase of about 4.8 percent (Figure 9) in the wing root bending moment for a cant angle of 6 degrees at cruise conditions, a value

13

somewhat greater than the measured wing root bending moment. At low speed
(Figure 43), the increase in the wing root bending moment of the KC-135A
model with the NASA upper plus lower winglet configuration was approximately
6 percent for wing lift coefficients from about 0.6 to 0.95.

Winglet Incidence

As winglets are basically small, cambered, wings flying at an angle of
attack determined by the wing tip cross flow, winglet incidence can affect
the efficiency. To determine winglet incidence angle, the different winglet
configurations were investigated at several incidence angles.

The effect of winglet incidence on the drag of the KC-135A model with
the NASA upper and the Boeing winglet configurations at near cruise conditions
is shown in Figures 44 to 46. Incidence angle, within the range investigated,
influenced the drag reduction characteristics of the winglets only very slightly.
An incidence angle of -4 degrees was selected for the KC-135A model with the
NASA upper winglet configuration and an angle of -1 degree was selected for
the model with the Boeing winglet configuration. The bulk of the data obtained
from the KC-135A model with winglets was for these incidence angles. Results
from the semispan KC-135A model tests with the NASA upper plus lower winglet
configuration also indicated the greatest drag reductions for an upper wing-
let incidence angle of -4 degrees.

The effect of lower winglet incidence on the drag of the KC-135A model
with the NASA upper plus lower winglet configuration at near cruise conditions
is shown in Figures 47 and 48. The upper winglet incidence angle was fixed
at -4 degrees. The drag reduction of the NASA upper plus lower winglet con-
figuration was improved slightly as the lower winglet incidence angle was
reduced. At M = 0.78, the drag of the model was reduced about 4.7 percent

14

at a lower winglet incidence angle of ~8 degrees and about 5.1 percent
for incidence angles from about -7 to -5 degrees. A lower winglet incidence
angle of -7 degrees was selected for the NASA upper plus lower winglet
configuration and most data are for this incidence angle.

Winglet Cant

As indicated by the Boeing analytical investigations, winglet length
and cant angle appear to be the most significant geometric parameters affect-
ing the overall aircraft aerodynamic characteristics. All of the (upper)
winglets investigated were essentially the same length, and winglet cant angle,
per se, was not investigated. However, as the cant angles of the different
winglet configurations varied somewhat, some deductions concerning cant angle
can be made. Because the basic purpose of winglets is to reduce drag, drag
reduction at cruise has been selected at the primary criterion for winglets.

The effect of cant angle on the drag of the KC-135A model with the
different upper winglet configurations at cruise lift conditions (Figures 49
and 50) was to reduce the drag as the winglet was canted. The drag of the
model was reduced about 5.3 percent with a cant angle of 6 degrees, and about
6.5 percent with a cant angle of 12 degrees (Figure 50). Linear extrapolation
of the curve to zero cant (vertical winglets) indicated a drag reduction of
about 4.1 percent.

The effect of lower winglet cant angle on the drag of the KC-135A model
with the NASA upper plus lower winglet configuration at cruise lift conditions
(Figures 51 and 52) shows only a very slight change in the drag of the model
as the lower winglet is canted. Figure 52 indicates a drag reduction of about
5.3 percent with a lower winglet cant angle of 12 degrees and about 5.9 percent

15

with a cant angle of 36 degrees. Linear extrapolation to zero cant angle indicates a drag reduction of about 5 percent with the lower winglet vertical.

Wing Tip Extensions

The effect of wing tip extensions on the KC-135 aircraft was investigated analytically in Reference 1. Results of this investigation indicate that an equal area wing tip extension can reduce the induced drag about 10 percent more than an 0.135 ^{b}/2 zero cant winglet (Figure 9), but that the wing root bending moment is more than doubled.

A wing tip extension was investigated with the semispan KC-135A model. The configuration investigated (Figure 2) was designed to produce wing root bending moments similar to those of winglets and was not optimized for maximum drag reduction.

Comparison of the drag reduction of the semispan model with the tip extension and with the different winglet configurations (Figure 53) shows that the drag reduction from the tip extension was considerably less than from the winglets. At cruise conditions, the total drag reduction with the tip extension was about 3 percent, while that from the winglets varied from about 5.4 percent with the Boeing configuration to about 7 percent with the NASA upper and upper plus lower winglet configurations.

Comparison of the measured wing root bending moments of the semispan model with the tip extension and with the different winglet configurations (Figure 54) shows that the bending moment from the tip extension is greater than those from the winglet configurations. At cruise conditions, the measured increase in the model wing root bending moment was about 3.5 percent

16

for the tip extension, about 3.0 percent for the NASA upper and upper plus lower winglet configurations, and about 2.5 percent for the Boeing winglet configuration.

Comparison of the increase in lift and nose-down pitching moment of the semispan model with winglets and tip extension is shown in Figures 55 and 56, respectively. The increase in lift was approximately the same with both the tip extension and the winglet configurations. At cruise conditions, the increase in lift was about 2-3 percent. However, as shown by Figure 56, the change in nose down pitching moment was considerably greater with the tip extension. Both the tip extension and the winglets increase the nose down pitching moment and increase the longitudinal stability of the model.

Flaps and Horizontal Tail Deflection

Comparison of the drag reduction achieved with the NASA upper winglet configuration at low speed and $C_L = 1.0$ (Figure 57) for different horizontal tail and flap deflections indicated horizontal tail incidence angle to have only small influence on the drag reduction, and that the drag reduction was proportional to flap deflection, varying from about 12 percent at zero deflection to about 2.5 percent at 50 degrees deflection. The increase in lift from the winglets ($C_L = 1.0$) (Figure 58) was basically not affected by horizontal tail incidence, but becomes greater with increased flap deflection, varying from about 0.5 percent at $\delta_F = 0$ to about 2 percent at $\delta_F = 50$ degrees. The increase in lift curve slope (Figure 59) varied from about 1 to 3 percent with the greatest increase occurring at 30 degrees flap deflection. The increase in untrimmed maximum lift-drag ratio of the model (Figure 60) was essentially not influenced by tail incidence, but was decreased by flap

17

deflection. The increase in lift-drag ratio ranged from about 7.5 per-
cent at zero flap deflection to about 3.5 percent at 50 degrees flap deflec-
tion. The effect of horizontal tail incidence and flap deflection on the
model incremental pitching moment is shown in Figure 61. The model incre-
mental pitching moment was not greatly affected by flap deflection, but
was somewhat more negative at a tail incidence angle of -4 degrees than
at zero and -10 degrees.

Lateral-Directional Stability

An important consideration of winglets is their effect on the lateral
and directional stability characteristics. The effect of the different wing-
let configurations on the lateral and directional characteristics of the
KC-135A model is shown in Figures 62 and 63 for δ_F = 50 degrees. All of the
winglet configurations affected the lateral-directional characteristics about
the same and always increased the lateral and directional stability of the
model.

Aileron Deflection

The effect of aileron deflection on the lateral-directional character-
istics of the KC-135A model with winglets is shown in Figures 64 to 69.

The effect of aileron deflection on the rolling moment of the model
with and without winglets is shown in Figures 64 and 65 for flap deflections
of 30 and 50 degrees, respectively. The winglets increased the outboard
aileron effectiveness and the increase in effectiveness is essentially con-
stant across most of the lift range. At C_L = 1.0 to 30 degrees flap deflection
(Figure 64), the increase in the rolling moment was about 3 and 6 percent for
aileron deflections of 10 and 20 degrees, respectively. At C_L = 1.0 and 50
degrees deflection (Figure 65), the increase in the rolling moment was about
10 and 7 percent for 10 and 20 degrees aileron deflection, respectively.

18

The effect of aileron deflection on the yawing moment of the model with and without winglets is shown in Figures 66 to 69 for flap deflections of 30 to 50 degrees. There is essentially no change in yawing moment with aileron deflection.

Winglet Loss

The loss of one winglet, e.g., structural failure or combat, could quite possibly be detrimental to the aircraft safety or performance.

To investigate the effect of winglet loss, the KC-135A model was tested with a NASA upper winglet on the left wing tip only. This investigation was made for a flap deflection of 50 degrees and a horizontal tail incidence angle of -10 degrees.

The most obvious effect of the loss of a winglet is on the aircraft lateral and directional characteristics. Consider, for example, a KC-135 aircraft with winglets flying in equilibrium, and suddenly the right winglet is lost. The change in yawing moment and rolling moment with the loss of the right winglet is shown in Figures 70 and 71, respectively. The change in yawing moment of the KC-135A model was always negative over the lift coefficient range investigated, while the change in rolling moment was always positive, requiring right rudder and left ailerons to maintain aircraft equilibrium. As shown by Figure 72, there was essentially no change in the yawing moment slope parameter, C_{n_β} of the KC-135A model when one winglet was lost; however, as shown by Figure 73, there was a slight positive shift of the rolling moment parameter, C_{l_β}. At $C_L = 1.0$, the change in C_{l_β} was about 25 percent.

The effect of the loss of a winglet on the longitudinal aerodynamic characteristics is shown in Figures 74 to 76. The lift of the KC-135A model

19

was decreased up to about 1 percent (Figure 74) and the drag increased up to
about 2 percent with the loss of a winglet (Figure 75). The effect of the
pitching moment (Figure 76) was to increase the nose-down pitching moment
even more than the original two winglet configuration. At $C_L = 1.0$, the
change in nose-down pitching moment was about 50 percent greater than for
the model with two winglets. In view of the large nose-down pitching moment
introduced by winglets on the KC-135A model, it is surprising that removal of
one of the winglets further increased the nose-down pitching moment. It would
be expected that removal of one winglet would relieve the nose-down pitching
moment somewhat, but the data do not indicate this.

Full-Scale Winglet Performance

At full-scale flight conditions, the total drag reduction from winglets
should be somewhat greater than that measured at test conditions because of
decreased skin friction drag and the increased lift from winglets which per-
mits the aircraft to fly at a lower angle of attack decreasing the profile
drag. Additional effects which influence the full-scale aircraft drag in-
clude trim drag changes and excrescence drag. The effect of winglets on the
full-scale aircraft can therefore be assumed to be expressed by the following
equation,

$$C_{D \text{ WITH} \atop \text{WINGLETS}} = C_{D \text{ WITHOUT} \atop \text{WINGLETS}} + \Delta C_{D_{\text{WINGLETS}}} + \Delta C_{D_{\text{SCALE}}} + \Delta C_{D_{\text{EXCRES}}} + \Delta C_{D_{\text{PROFILE}}} + \Delta C_{D_{\text{TRIM}}}$$

Full-scale drag polars for the KC-135 aircraft with winglets have
been derived from wind tunnel and flight test data using the above equation
(Figure 77). The aircraft has been assumed to be equipped with winglets
having the NASA upper winglet configuration. The winglet incremental drag

20

as been taken from the data shown in Figure 19. $\Delta C_{D_{TRIM}}$ and $\Delta C_{D_{EXCRES}}$ have been shown to be close to zero and estimates of $\Delta C_{D_{SCALE}}$ and $\Delta C_{D_{PROFILE}}$ have indicated values of -0.00022 and -0.00015 for these coefficients. As shown by Figure 77, the full-scale drag improvement with winglets has been estimated to be about ΔC_D= -0.0020 or about 8.2 percent of the aircraft cruise drag. The improvement in the aircraft maximum lift-drag ratio because of the winglets (Figure 78) was about 1.68 or about 9.5 percent.

CONCLUSIONS

The aerodynamic characteristics of semispan and full-span KC-135A models with winglets and a tip extension have been investigated in the NASA/ LRC 8-Foot Transonic Pressure Tunnel. Some basic results from these investigations have been presented in this Report. The following conclusions have been derived.

1. Results from semispan wind tunnel tests at high subsonic speeds indicated the greatest drag reductions from the NASA upper plus lower winglet configuration; however, drag reductions of similar magnitude were found with the upper winglet configurations at cruise lift coefficients.

2. Contrary to the semispan model tests, full-span model tests indicated the greatest drag reductions at high subsonic speeds with the NASA upper winglet configuration. At cruise conditions, a total drag reduction of about 5.3 percent was found for the model with the Boeing and NASA upper plus lower winglet configurations and a reduction of about 6.5 percent for the model with the NASA upper winglet configuration.

3. At low speeds, a total drag reduction of about 3.0 percent was found for the full-span model with the NASA upper winglet configuration.

4. Drag was decreased with upper winglet cant. The drag of the full-span model was decreased about 5.3 percent with an upper winglet cant angle of 6 degrees and about 6.5 percent with a cant angle of 12 degrees.

5. Drag was decreased with lower winglet cant. The drag of the full-span model was decreased about 5.3 percent with a lower winglet cant angle of 12 degrees and about 5.9 percent with a cant angle of 36 degrees.

6. Results from semispan model tests at high subsonic speeds indicate the drag reduction from winglets to be greater than from a wing tip extension configuration. At cruise conditions, the total drag reduction of the semispan model with the tip extension was about 3 percent while reduction from the winglets varied from about 5.4 to 7 percent.

7. At high subsonic speeds, the increase in wing root bending moment of the semispan KC-135A model was greatest with a wing tip extension and least with the upper winglet configurations. At cruise conditions, the increase in wing root bending moment varied from about 2.5 percent with the Boeing winglet configuration to about 3.5 percent with the tip extension.

8. At cruise conditions, winglets generally increased the lift of the model about 1 to 3 percent.

9. At cruise conditions, winglets increased the model untrimmed maximum lift-drag ratio about 8 percent.

10. Both winglets and tip extensions increase the nose-down pitching moment and increase the longitudinal stability; however, the increase in pitching moment was considerably greater for the tip extension. At cruise conditions, the increase in nose-down pitching moment was about 13 percent for the full-span model with NASA upper and Boeing winglets and about 16 percent with the NASA upper plus lower winglet configuration.

11. At $M = 0.30$ and $C_L = 1.0$, total drag reduction of the full-span model varied from about 12 percent at zero flap deflection to about 2.5 percent at 50 degrees flap deflection.

12. At $M = 0.30$, the untrimmed maximum lift-drag ratio of the full-span KC-135A model with winglets was increased about 7.5 percent at zero flap deflection and about 4 percent at 50 degrees flap deflection.

13. Winglets increased the directional and lateral stability of the full-span KC-135A model.

14. Winglets increased the aileron effectiveness of the full span model. At $M = 0.30$ and $C_L = 1.0$, the increase in rolling moment was about 10 and 7 percent for 10 and 20 degrees aileron deflection, respectively.

15. The change in the aerodynamic characteristics of the KC-135A with the loss of one winglet appears to be sufficiently small so as not to impair aircraft capability or safety.

16. Estimated winglet effects at cruise flight conditions indicated a reduction in drag of 8.2 percent and an increase in $(L/D)_{MAX}$ of 9.5 percent.

APPENDIX A

EFFECT OF WING TIP REMOVAL
ON BASIC KC-135A WING

To accommodate mounting the winglets, a small portion of the model wing was removed, changing the wing span, area, and aspect ratio. Consider the following sketch, where subscript 1 denotes the original wing and 2 denotes the wing shortened to accommodate the attachment of winglets.
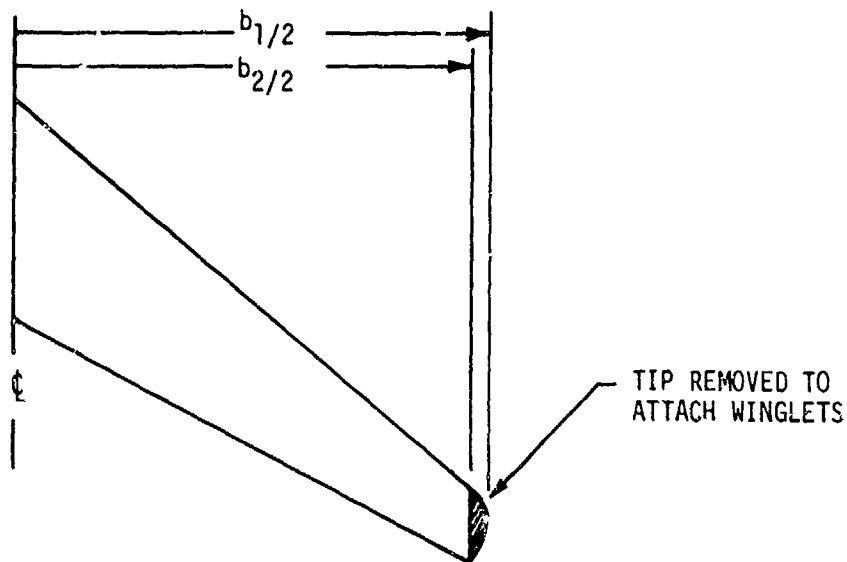
Lift can be expressed as

$$C_{L_1} = \frac{L_1}{qS_1} \quad , \quad C_{L_2} = \frac{L_2}{qS_2} \tag{1}$$

where, at cruise, $L_1 = L_2 = W$, and

$$C_{L_2} = C_{L_1} \frac{S_1}{S_2} \tag{2}$$

Drag for the corresponding conditions can be expressed as,

25

$$C_{D_1} = C_{D_{o_1}} + \frac{C_{L_1}^2}{\pi AR_1 e_1} \quad , \quad C_{D_2} = C_{D_{o_2}} + \frac{C_{L_2}^2}{\pi AR_2 e_2} \tag{3}$$

where, $C_{D_{0_2}} = C_{D_{0_1}} \dfrac{S_1}{S_2}$ (4)

and, $C_{D_2} = C_{D_{0_1}} \dfrac{S_1}{S_2} + \dfrac{C_{L_1}^2 \; S_1^2}{\pi \; S_2^2 \; AR_2 \; e_2}$ (5)

From flight data for the KC-135 aircraft at a cruise C_L of 0.426, $M = 0.78$, and a Reynolds number based on the mean aerodynamic chord of 42×10^6,

$$C_{L_1} = 0.4260, \; C_{D_1} = 0.0241, \; e_1 = 0.7491$$

which gives

$$C_{D_1} = C_{D_{P_1}} + \frac{C_{L_1}^2}{\pi AR_1 e_1} = 0.0241$$

or, $\quad C_{D_{P_1}} = 0.0241 - \dfrac{(0.4260)^2}{\pi(7.035)(0.7491)} = 0.0241 - 0.0110 = 0.0131$

From equation (2) the corresponding lift coefficient for the aircraft with the tip removed is

$$C_{L_2} = 0.4260 \left(\frac{2433}{2422}\right) = 0.4279$$

and the corresponding drag coefficient from equation (3) for the same wing efficiency factor

$$C_{D_2} = 0.0131 \left(\frac{2433}{2422}\right) + \frac{(0.4279)^2}{\pi(6.98)(0.7491)}$$

$$= 0.0132 + 0.0111 = 0.0243$$

Consequently,

$$(L/D)_2 = \frac{0.4279}{0.0243} = 17.609$$

and, $(L/D)_1 = \frac{0.4260}{0.0241} = 17.676$

a loss in aircraft lift-drag ratio of -0.067 or a loss of 0.4 percent.

APPENDIX B

CHARACTERISTICS OF THE BASIC KC-135A MODEL

To investigate the aerodynamic effects of different winglet configurations on the KC-135A model, it was necessary to determine the aerodynamic characteristics of the basic KC-135A model. To accommodate mounting the winglets a small portion of the model wing tips were cut off, reducing the aspect ratio of the basic wing from 7.035 to 6.98. An analysis (Appendix A) indicated a loss in aircraft lift-drag ratio of about -0.067, or about 0.4 percent, with the wing tips removed.

The variation of the lift of the basic model with angle of attack is shown in Figures 79, 80, and 81 for flap deflection of zero, 30 and 50 degrees. Extrapolation of Figure 79 (M = 0.30) to zero lift indicates the angle of zero lift of the model at zero flap deflection and zero horizontal tail incidence angle to be about -3 degrees. The lift curve slope varied from about 0.0796 at M = 0.30 to about 0.1008 at M = 0.80 for the model with the tail off. Variation of the drag with lift is shown in Figures 82, 83, and 84. At zero flap deflection and zero horizontal tail incidence, Figure 82 indicates the zero lift drag coefficient at M = 0.30 to be about 0.0218, the minimum drag coefficient to be about 0.0210, and the lift coefficient corresponding to the minimum drag coefficient to be about 0.075. For cruise conditions, Figure 84 indicates the drag coefficient of the model without tail to be about 0.0260. Variation of the model pitching moment with lift is shown in Figures 85, 86, and 87. At low speed (Figures 85 and 86), the slope of the pitching moment curves in the linear region was essentially unaffected by horizontal tail incidence or flap deflection.

28

For zero flap deflection (Figure 85), the zero-lift pitching moment coefficient was about -0.047 and the slope, dCm/dC_L, about -0.220. As shown by Figures 88 to 91, horizontal tail incidence and flap deflection had only small effect on the yawing and rolling moment of the basic KC-135A model except at high lift coefficients. Figures 92 and 93 show that the slope of the yawing and rolling moment curves was also little affected by horizontal tail incidence except for high lift coefficients.

APPENDIX C

COMPARISON OF FULL-SPAN AND SEMISPAN MODEL DATA

Aerodynamic coefficients are normally referenced to the theoretical wing area, although other areas may be used, and careful definition is required. The aerodynamic coefficients of wall-mounted semispan wing (or panel) models are generally referenced to the exposed wing area, and the results are normally comparable with full-span wind tunnel or flight data.

The KC-135A semispan model wing was directly attached to the wall mounted balance system; however, that portion next to the tunnel wall was shielded by the model body. The body pitched as the wing angle of attack was changed; however, the fuselage was completely isolated and no body loads were recorded. The body had a slot through which the wing passed. The wing was designed so that the tip deflected approximately the same as the tip of the full-scale airplane at cruise conditions. The aerodynamic coefficients of the KC-135A semispan model are referenced to the area of that portion of the wing outboard of the body, i.e., the exposed wing area. Data obtained are, therefore, for the exposed wing (plus winglets) in the presence of, but not attached to, the model body.

The full-span KC-135A model was mounted in the center of the tunnel test section on a sting-supported six-component balance system. The model wings were rigid and did not deflect aeroelastically. The aerodynamic coefficients are referenced to the theoretical wing area.

Comparison of the incremental lift and drag obtained with the 0.035-scale full-span model and the 0.07-scale semispan model with different

30

winglet configurations is shown in Figures 94 to 97 for Mach numbers of 0.70 and 0.78. Agreement of the data from the two different models is generally very good, however, some differences exist in the lift at M = 0.78.

Figure 1. Semispan KC-135A Model in the NASA/LaRC 8-Foot
Transonic Pressure Tunnel
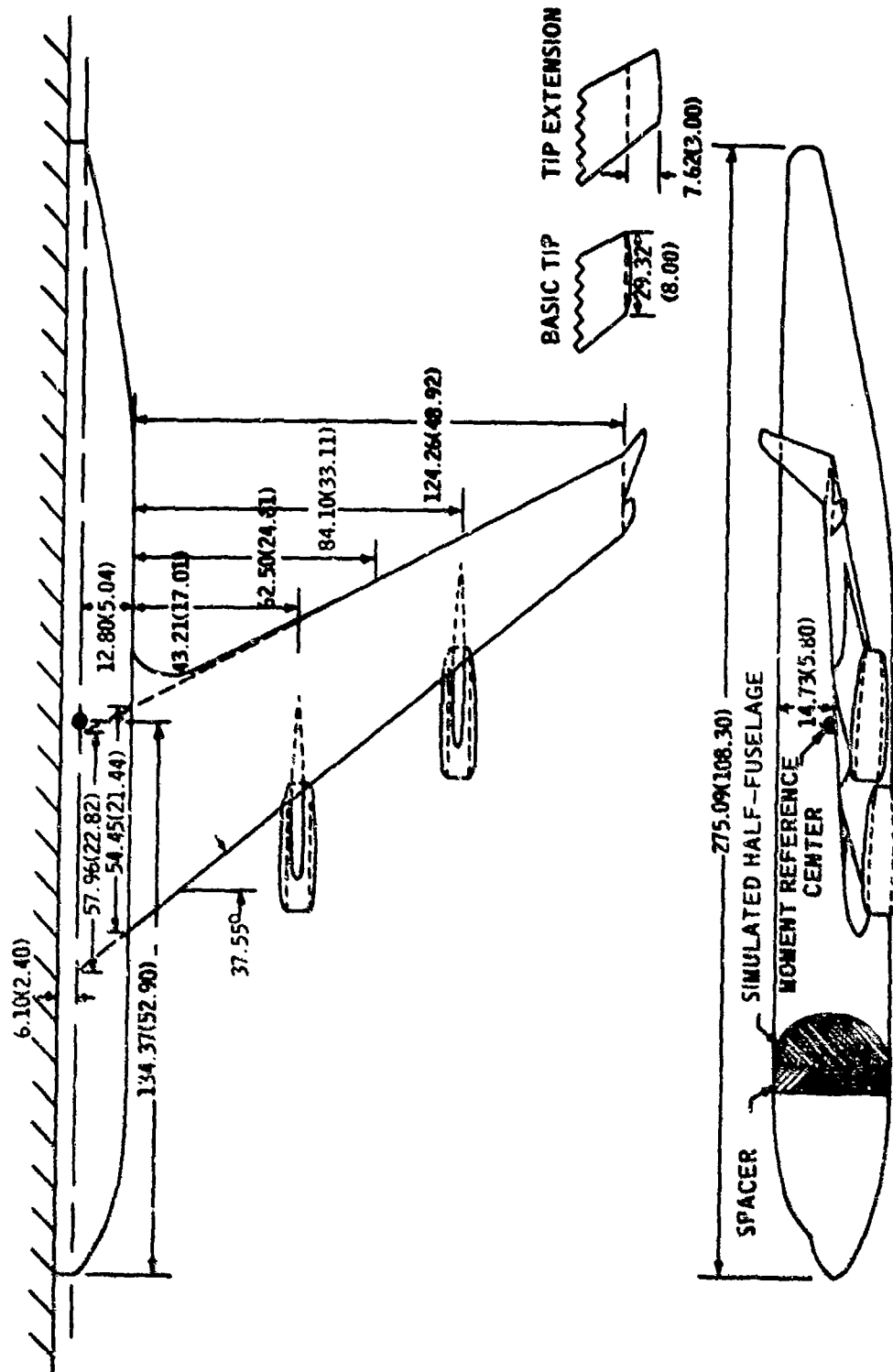
Figure 2. Basic Dimensions of KC-135A Semispan Model (Dimensions in centimeters (inches))
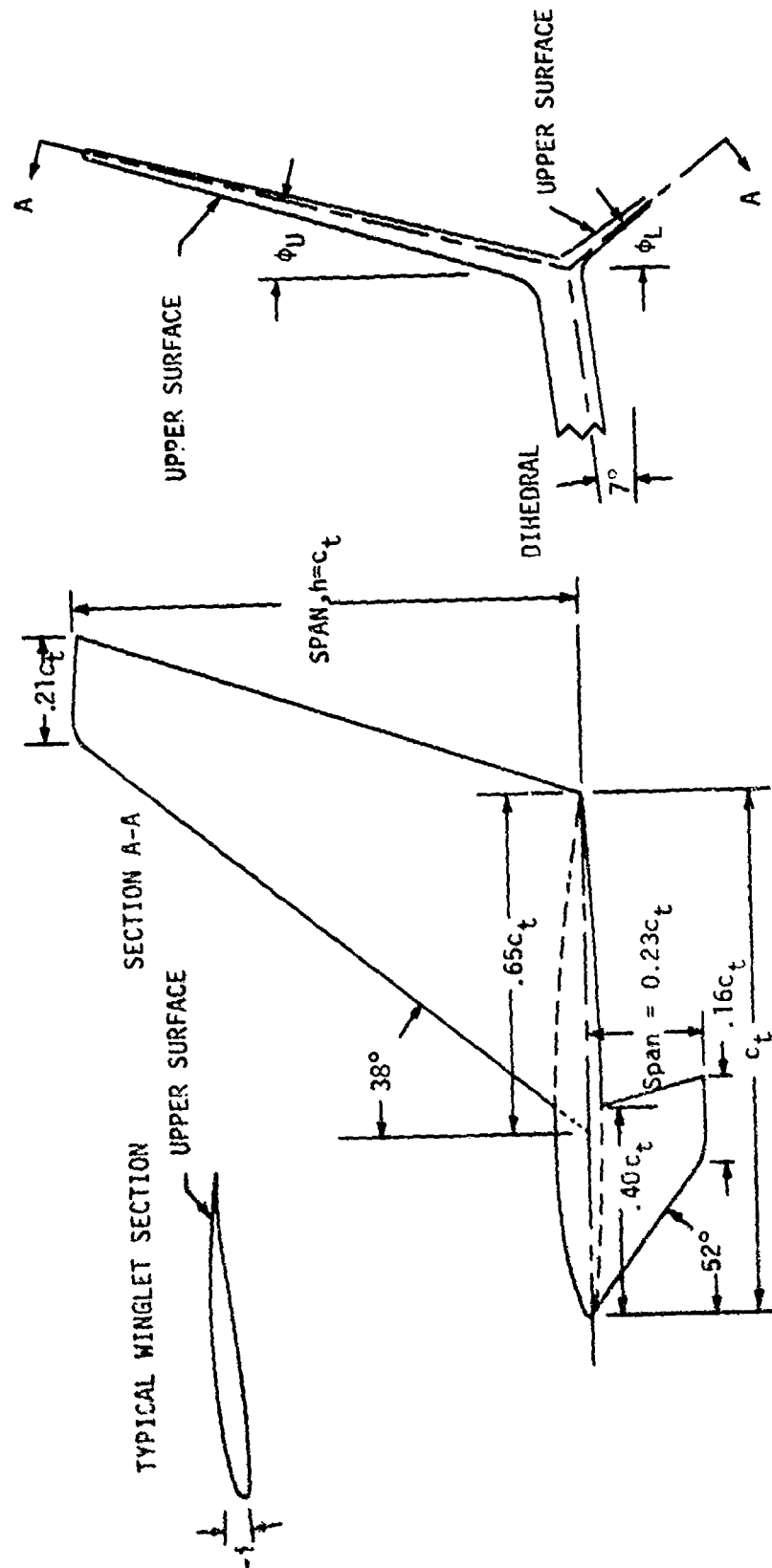
Figure 3. NASA Winglet Configurations

34

TYPICAL SECTION, A-A

TOP VIEW

SIDE VIEW

REAR VIEW

.135 b/2

6°

A

A
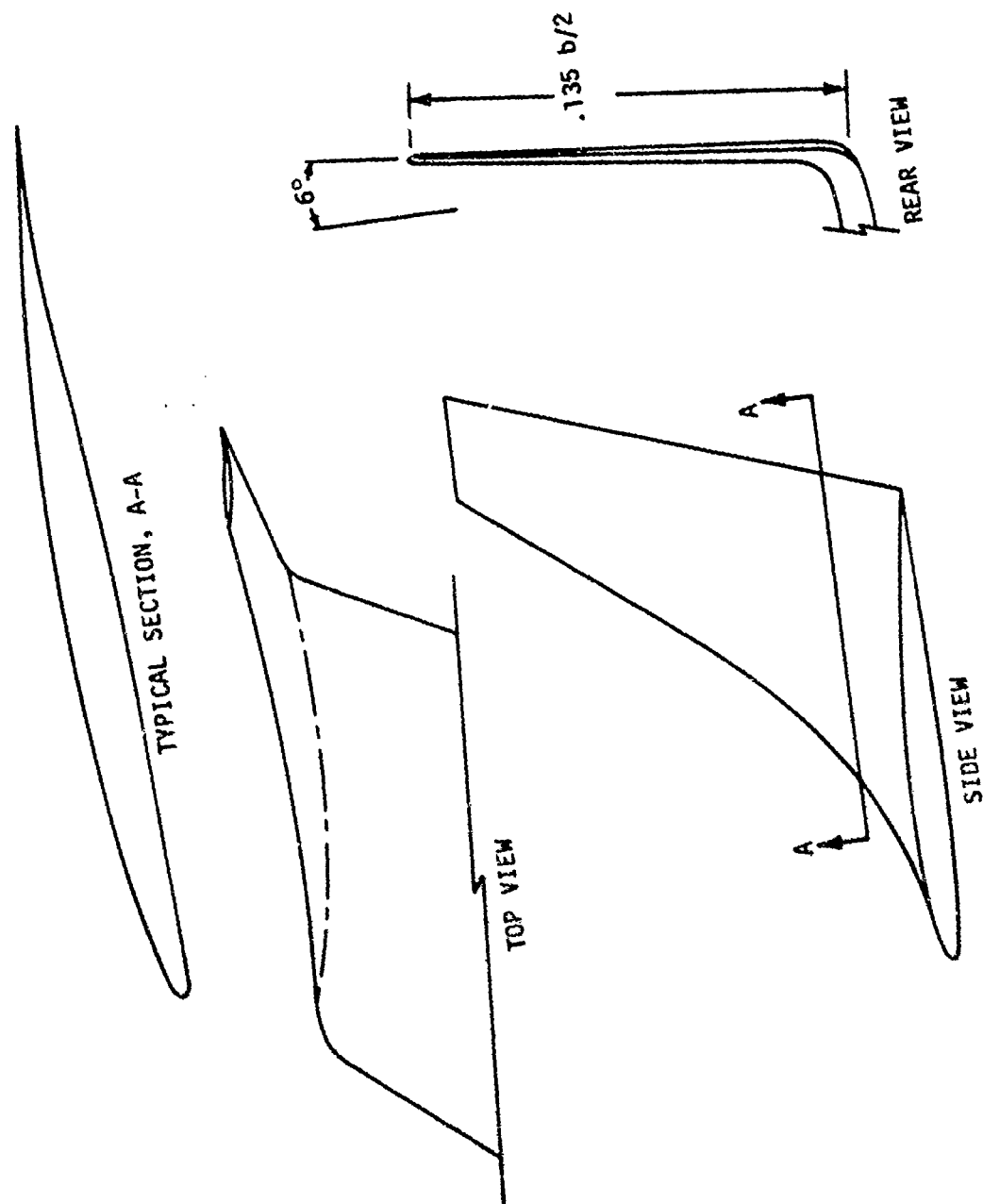
Figure 4. Boeing Winglet Configuration
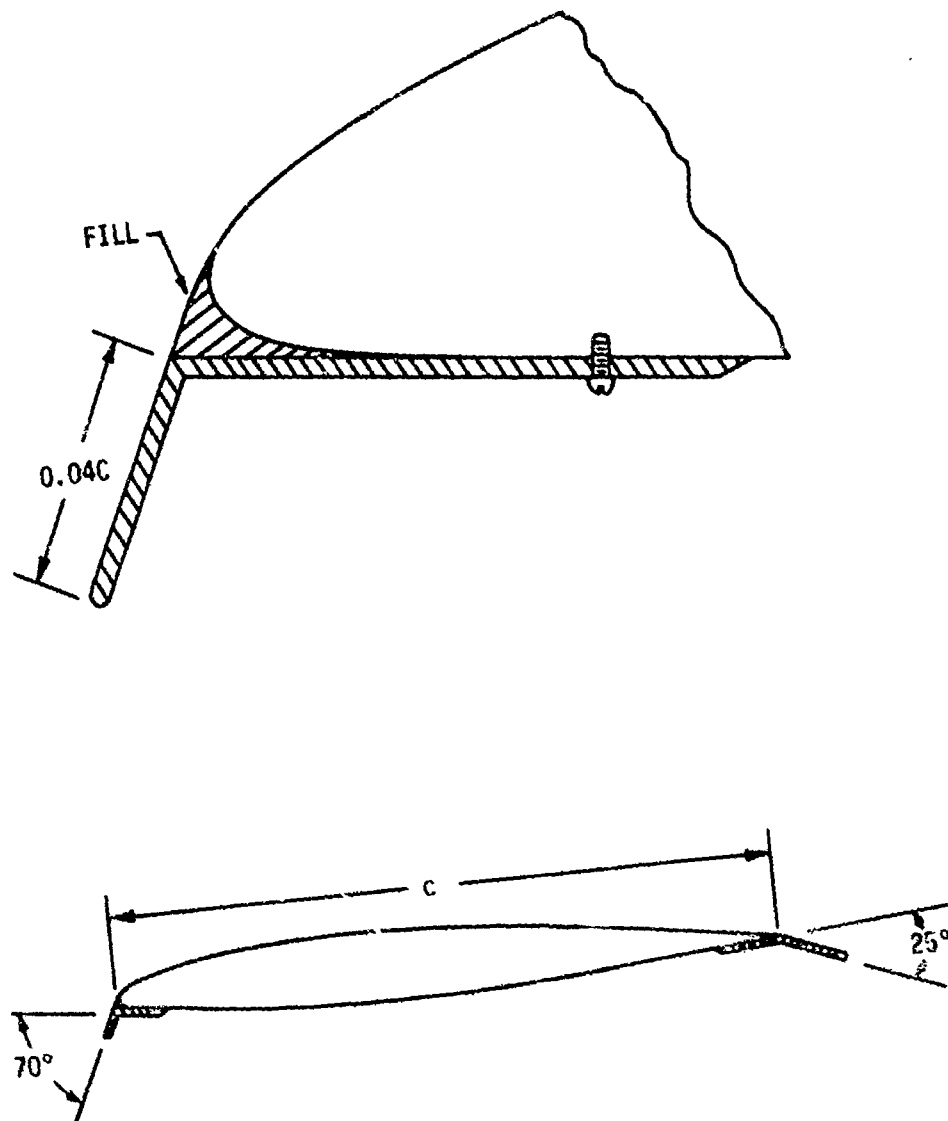
Figure 5. Leading and Trailing Edge Flaps for Semispan KC-135A Model

Figure 6. Full Span 0.035 Scale KC-135A Model With Low
Speed Wing and Winglets
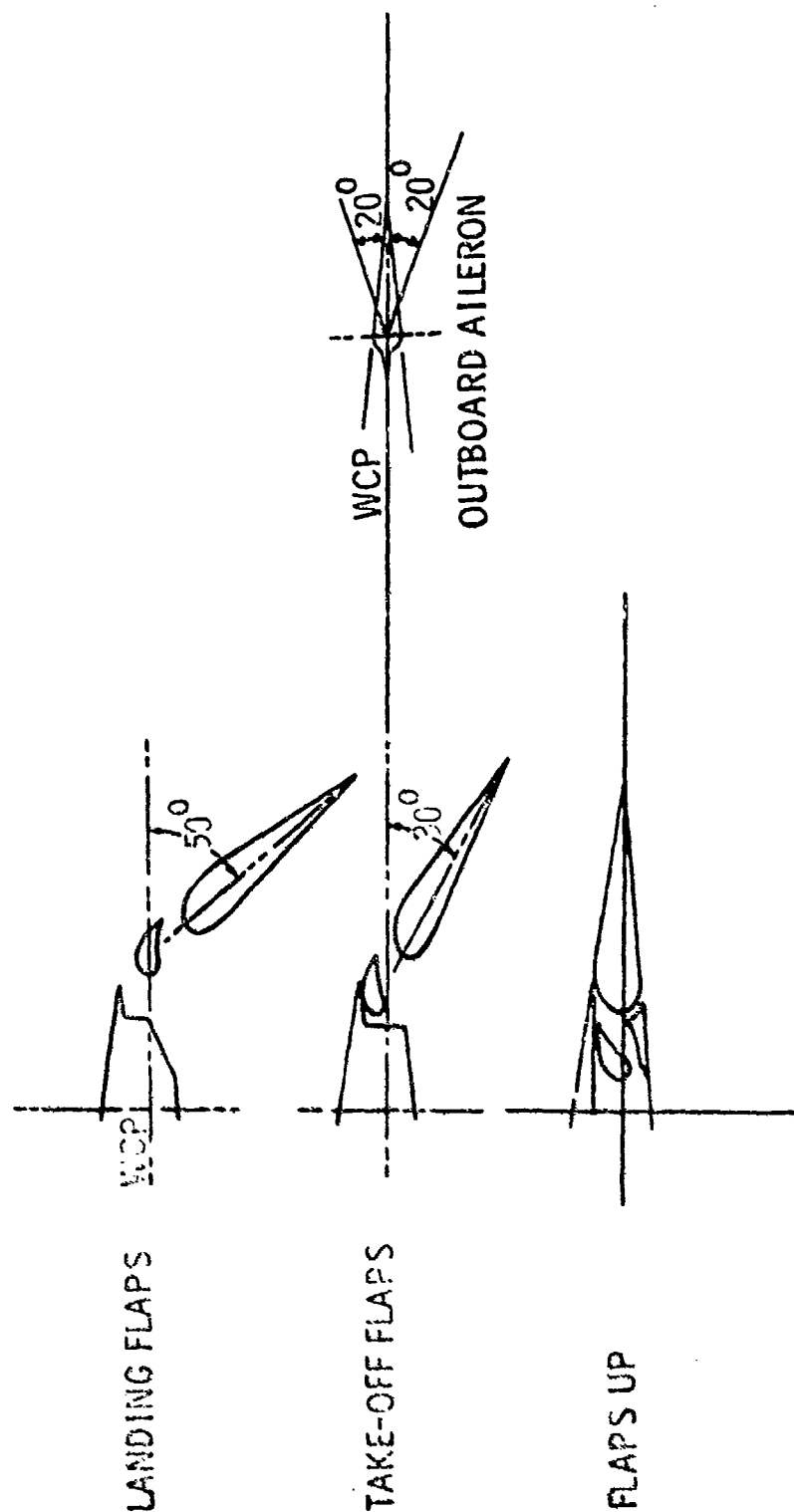
Figure 7. Wing Flap and Aileron Geometry of Full-Span
KC-135A Model
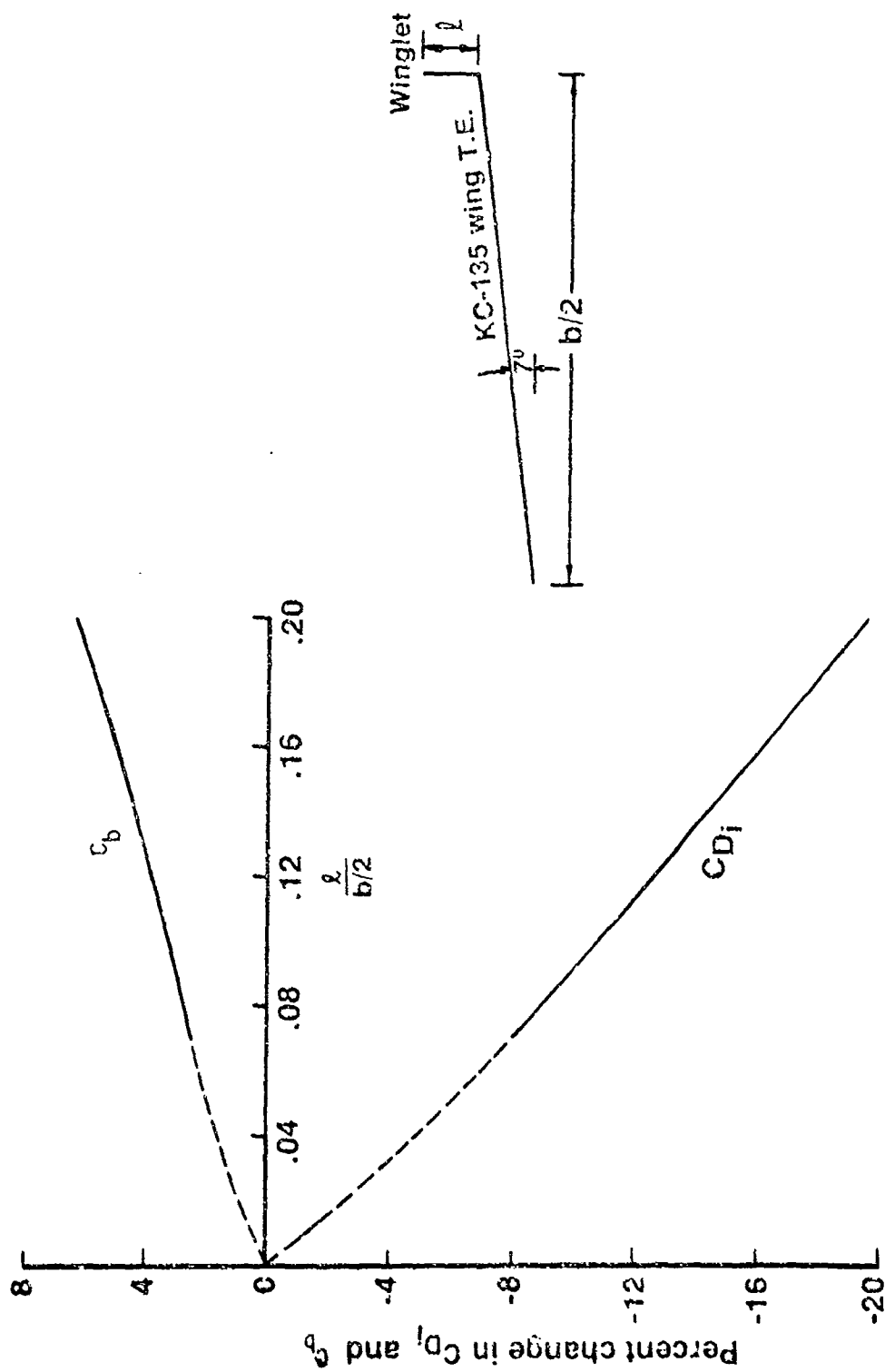
Figure 8. Effect of Winglet Length at Zero Cant
$C_{L_{CONFIG}} = 0.426$ (Reference 1)
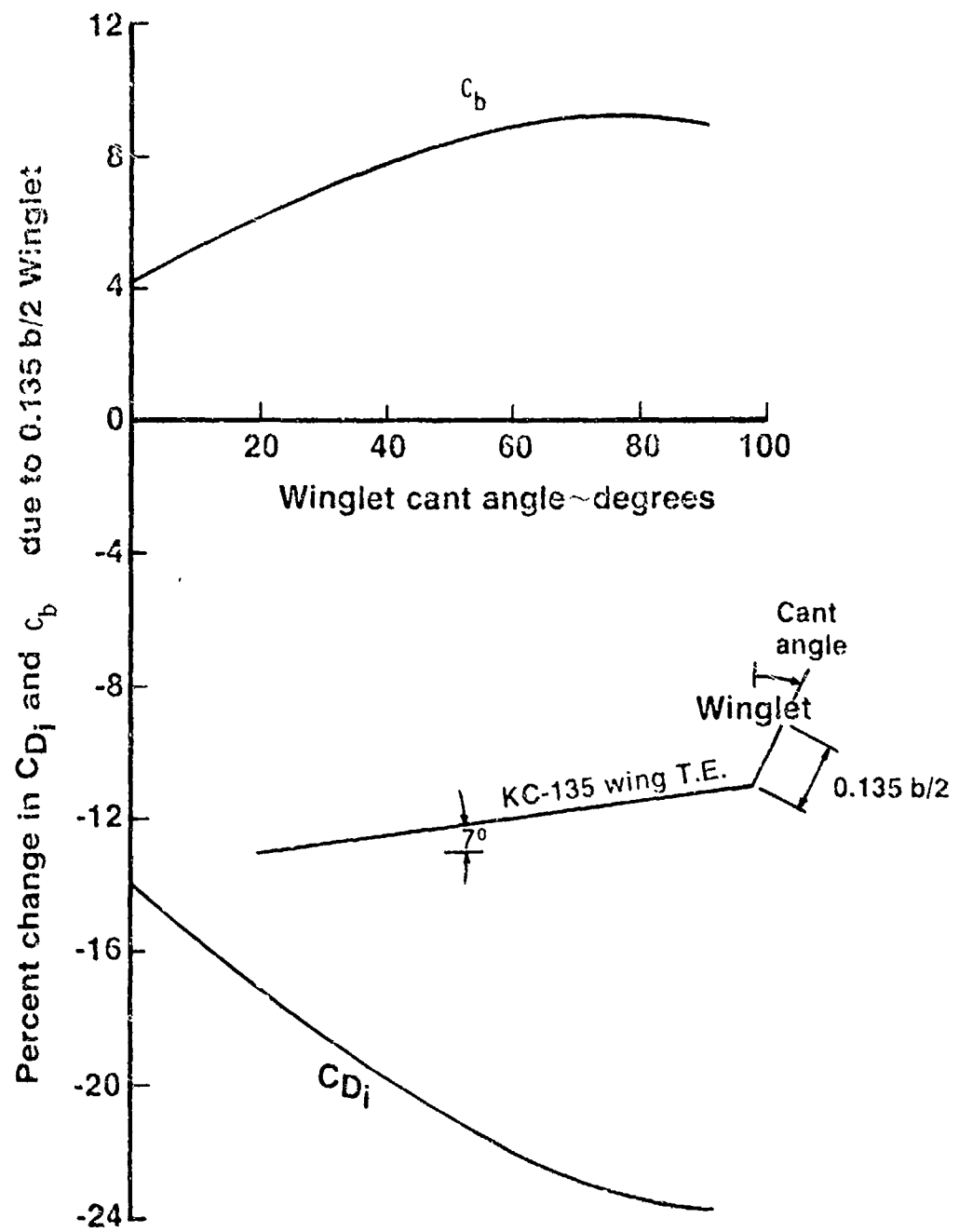
Figure 9.   Effect of Winglet Cant Angle - Variable Span
$C_{L_{CONFIG}}$ = 0.426 (Reference 1)
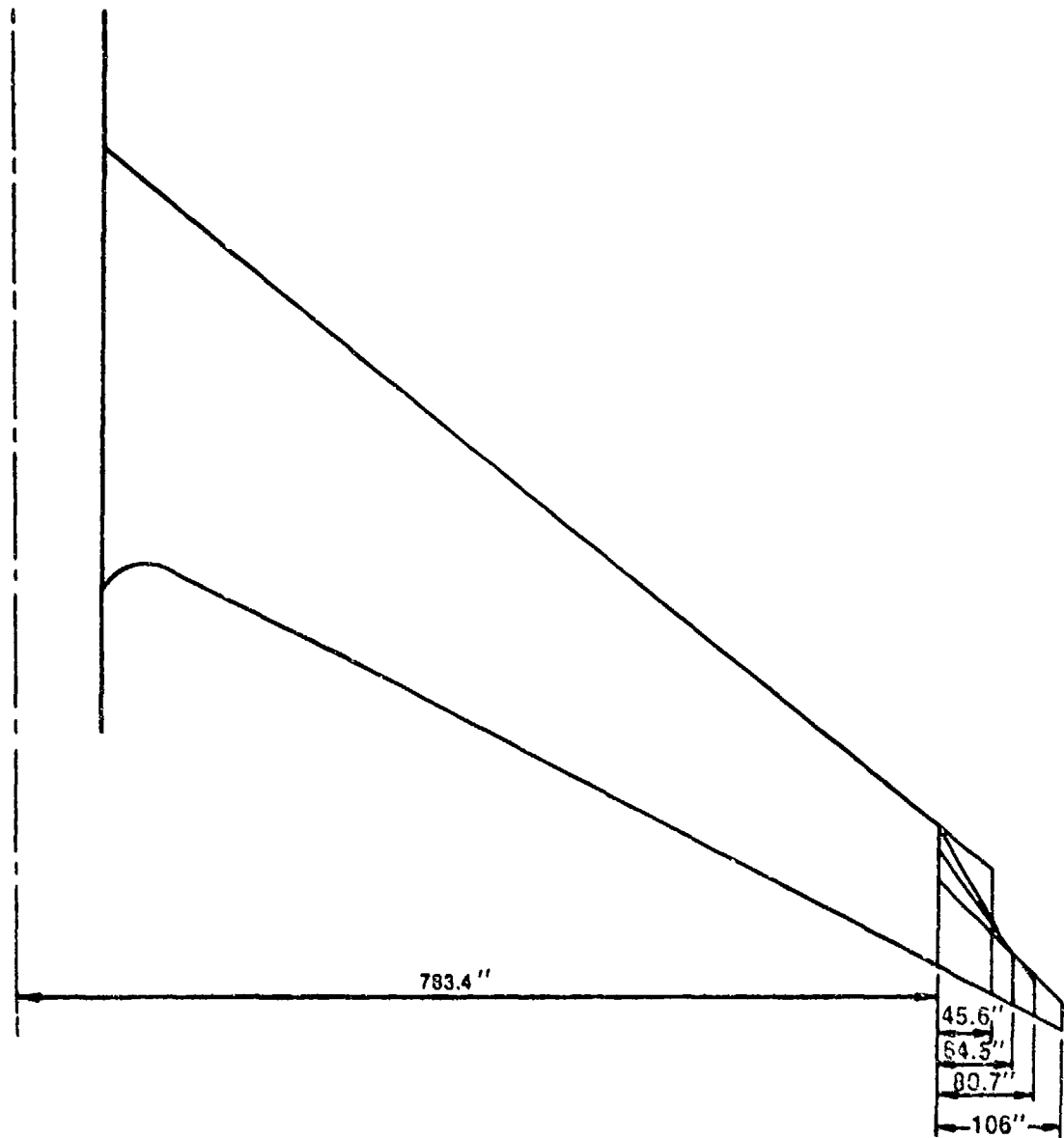
Figure 10. Equal Area Tip Extension Geometry Investigated in Reference 1
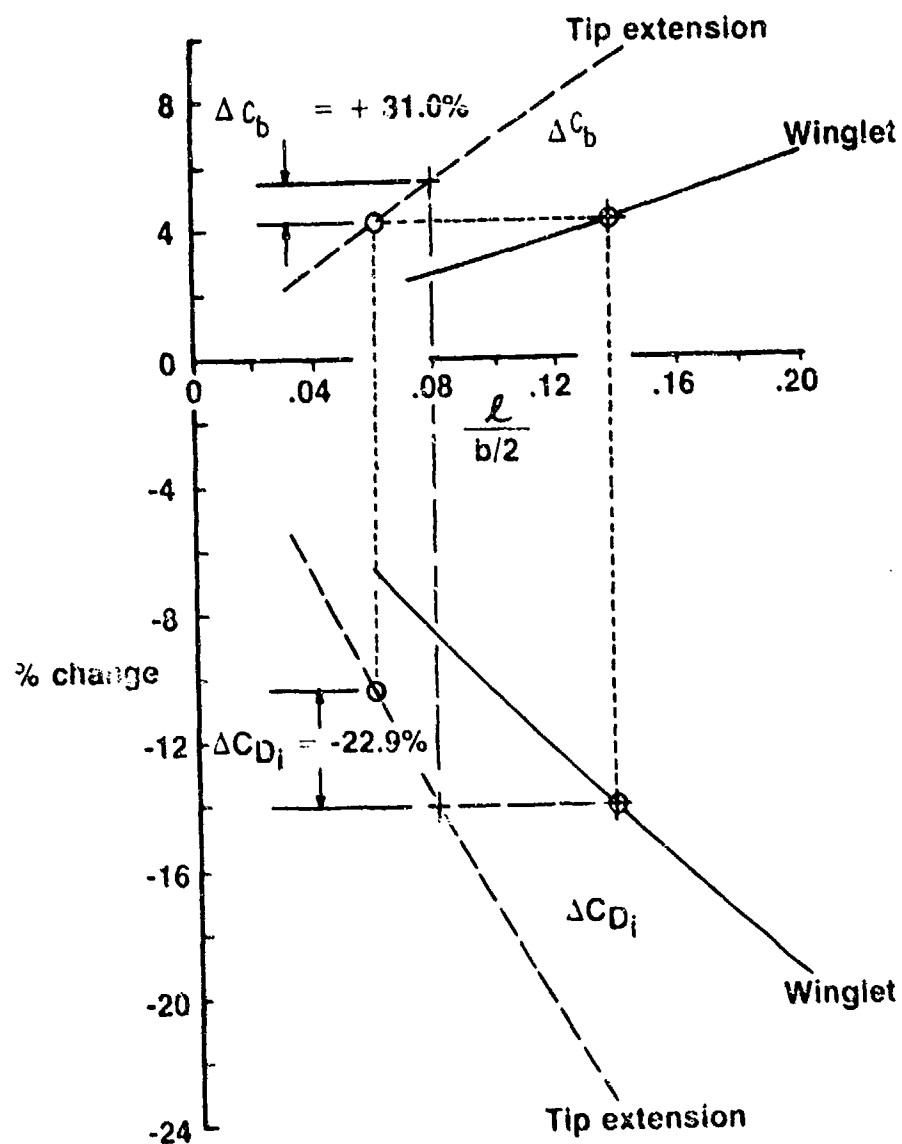
Figure 11.   Comparison of Induced Drag and Wing Root
             Bending Moment Increments Between Zero Cant
             Winglets and Tip Extensions (Reference 1)

42
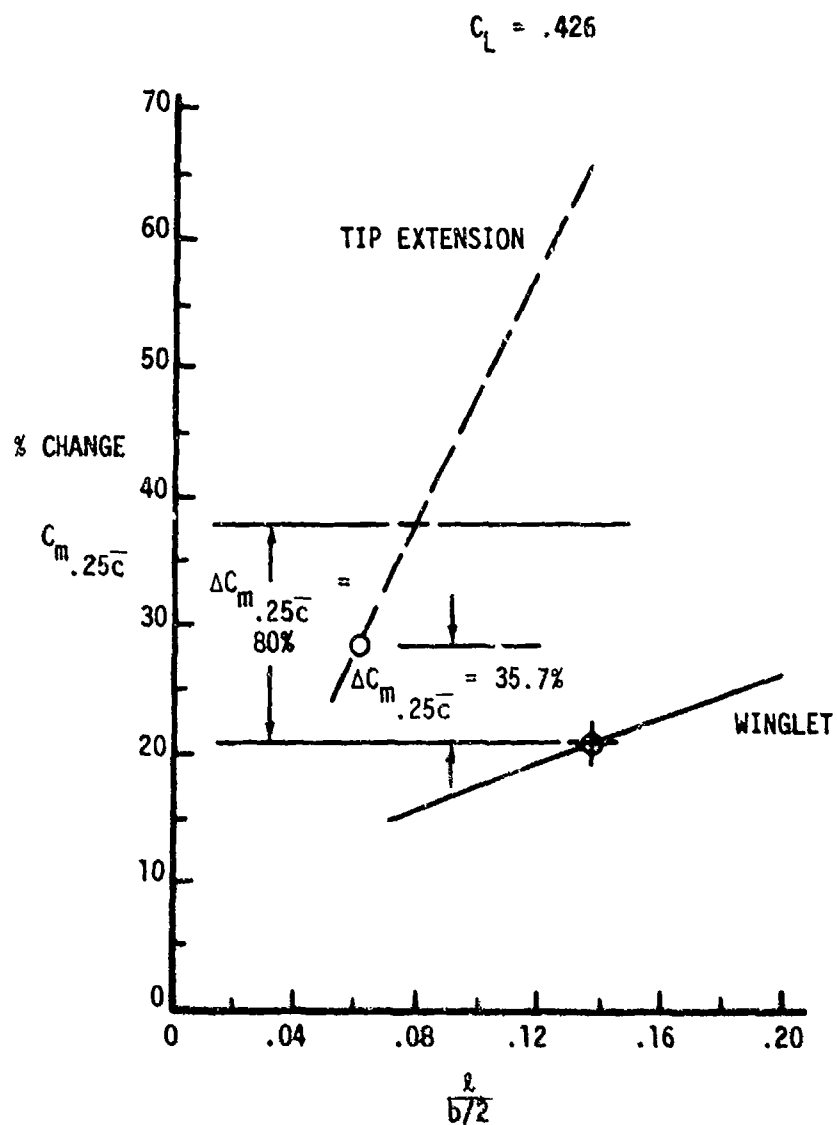
Figure 12. Comparison of Pitching Moment Increment Between Zero Cant Winglets and Tip Extensions (Reference 1)

SYMBOL	WINGLET CONFIG.	i_u	ϕ_U	i_L	ϕ_L
□	BOEING	-1	6	--	--
△	NASA UPPER	-4	15	--	--
○	NASA UPPER + LOWER	-4	15	-7	36

M = 0.78

$\delta_F = 0$
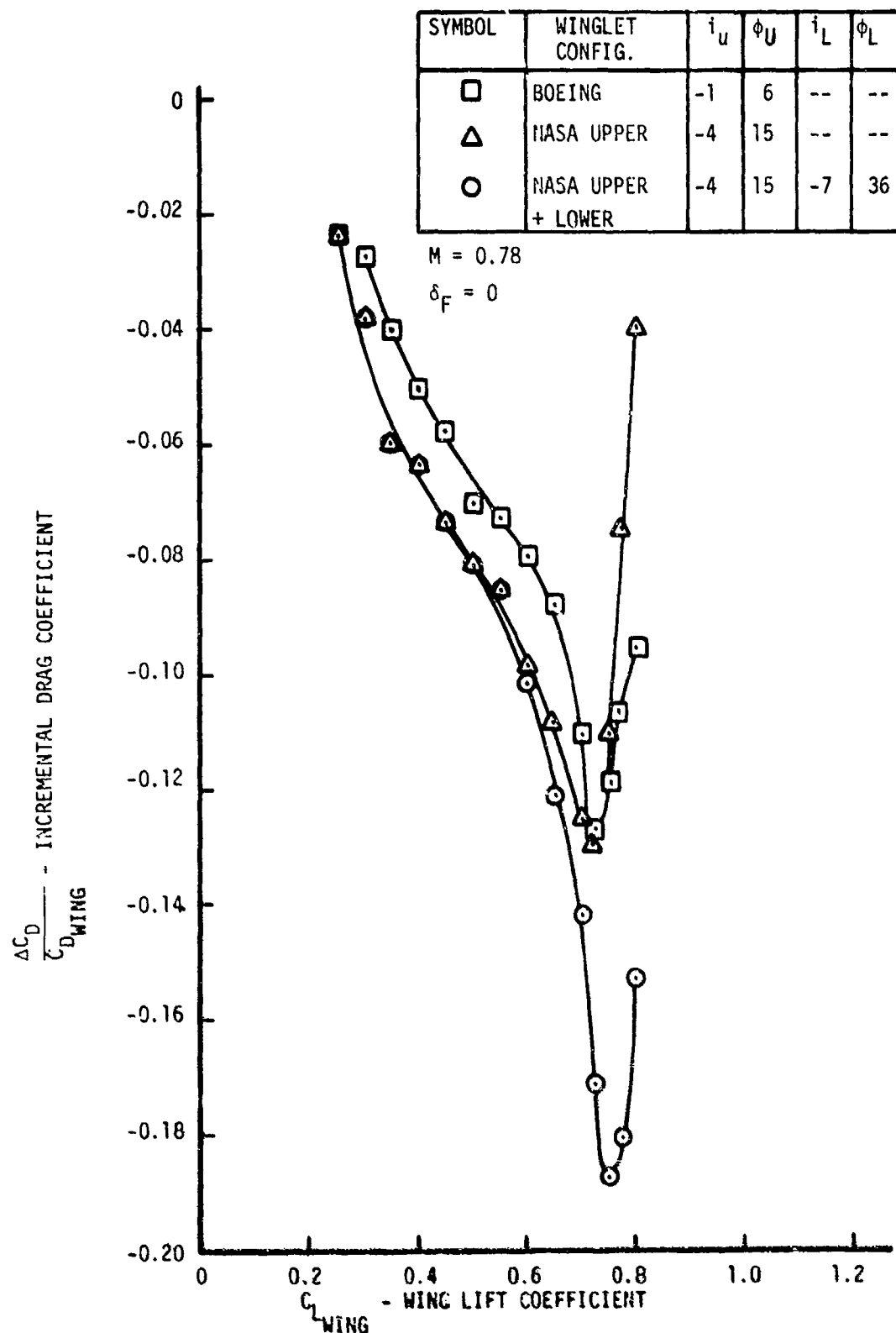
Figure 13. Effect of Winglet Configuration on Semispan
KC-135A Model Drag. M = 0.78. $\delta_F = 0$

44

SYMBOL	WINGLET CONFIG.	i_u	ϕ_U	i_L	ϕ_L
□	BOEING	-1	6	--	--
△	NASA UPPER	-4	15	--	--
○	NASA UPPER + LOWER	-4	15	-7	36
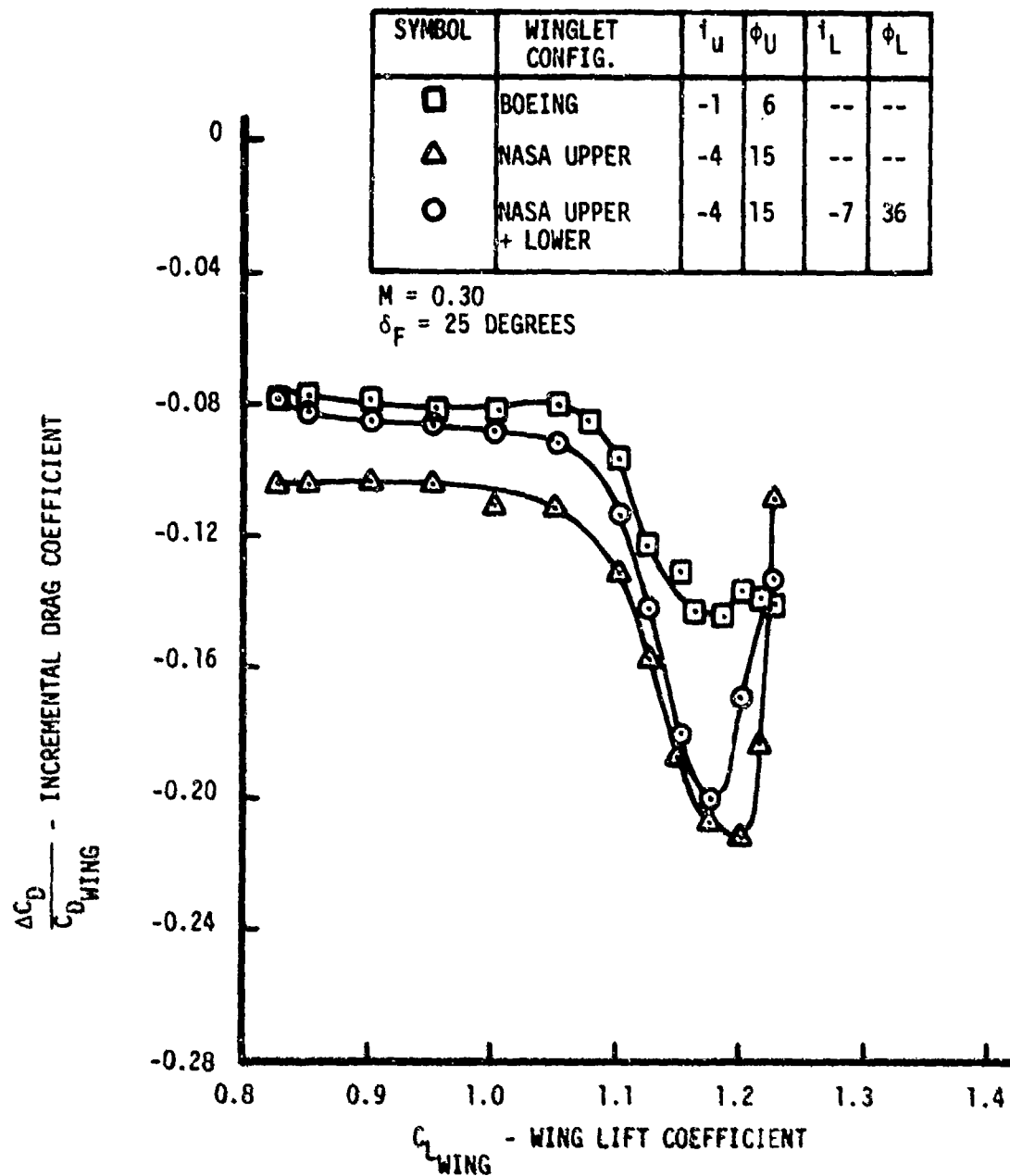
$M = 0.30$
$\delta_F = 25$ DEGREES

Figure 14. Effect of Winglet Configuration on Semispan
KC-135A Model Drag. $M = 0.30$. $\delta_F = 25$ Degrees

45

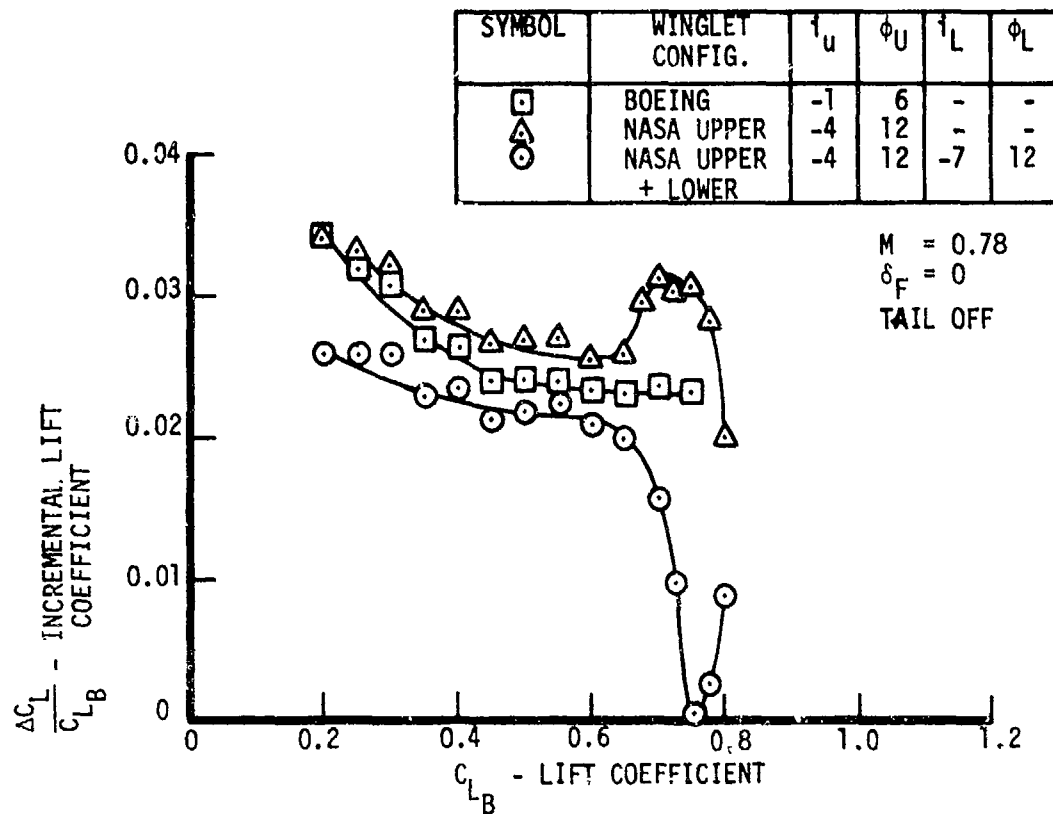| SYMBOL	WINGLET CONFIG.	i_u	ϕ_U
△	NASA UPPER	-4	12
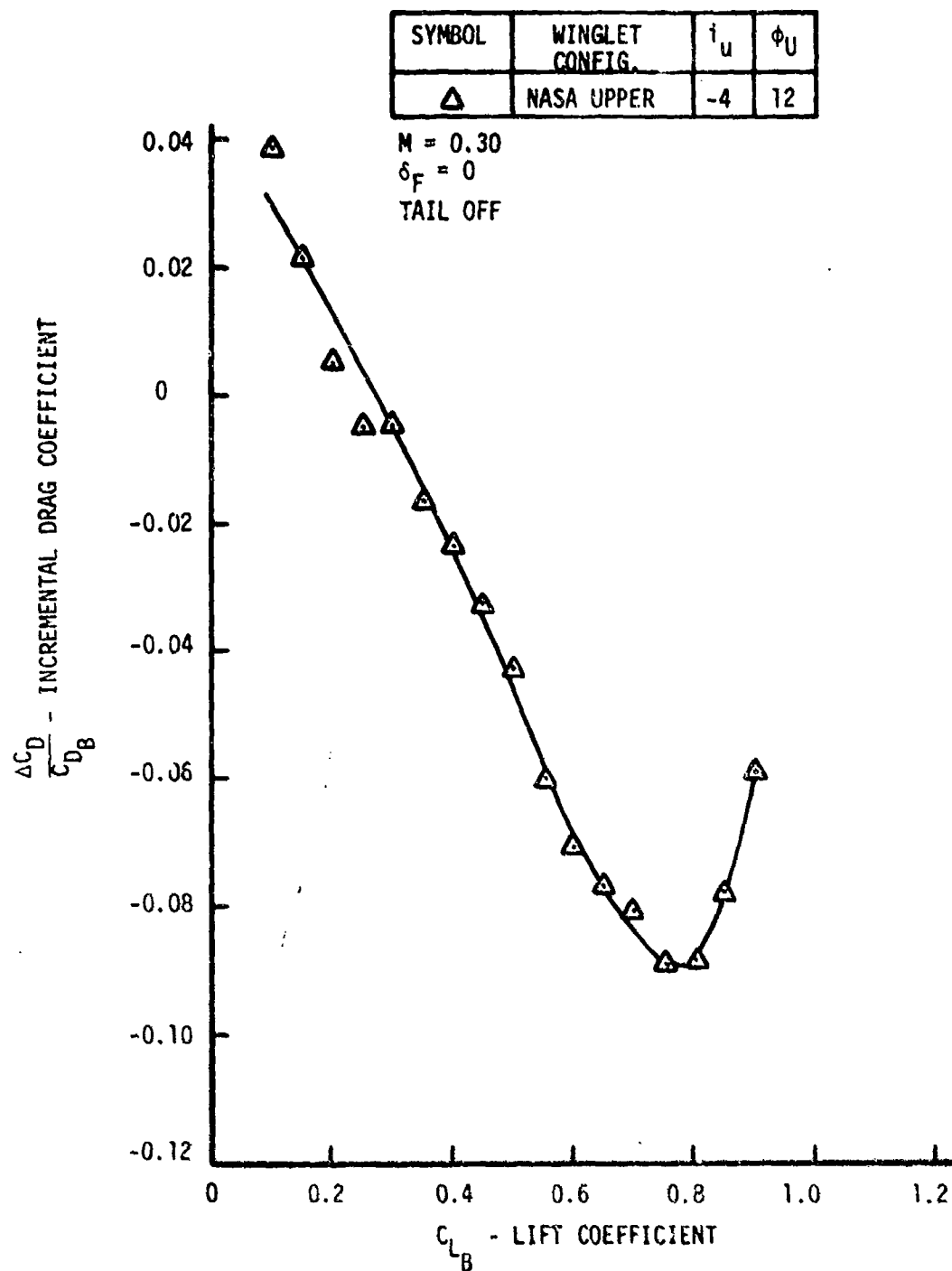
M = 0.30
δ_F = 0
TAIL OFF

Figure 15. Effect of Winglet Configuration on Full-Span KC-135A Model Drag. M = 0.30. δ_F = 0

46
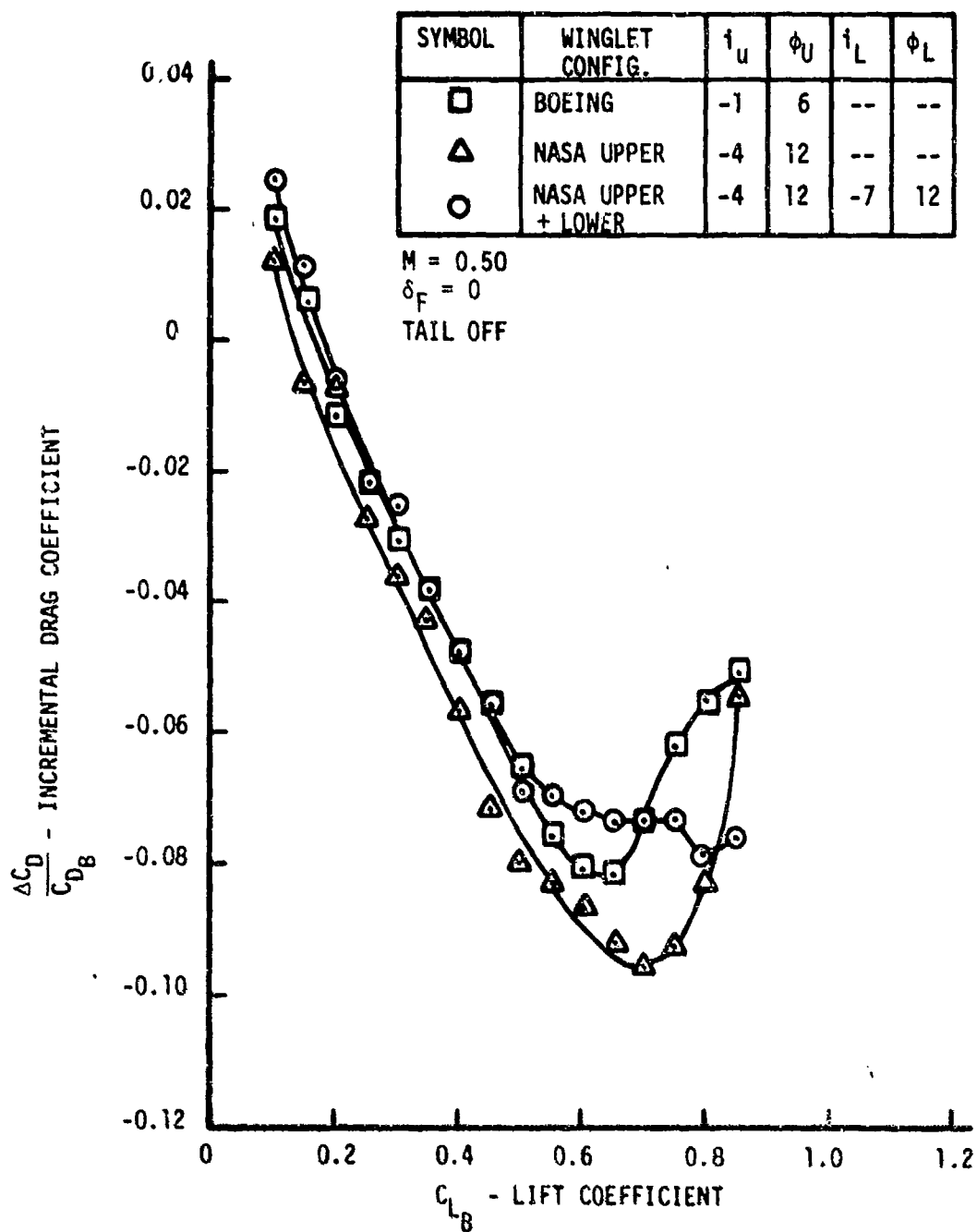
Figure 16. Effect of Winglet Configuration on Full-
Span KC-135A Model Drag. $M = 0.50$. $\delta_F = 0$

47

SYMBOL	WINGLET CONFIG.	i_U	ϕ_U	i_L	ϕ_L
□	BOEING	-1	6	--	--
△	NASA UPPER	-4	12	--	--
○	NASA UPPER + LOWER	-4	12	-7	12
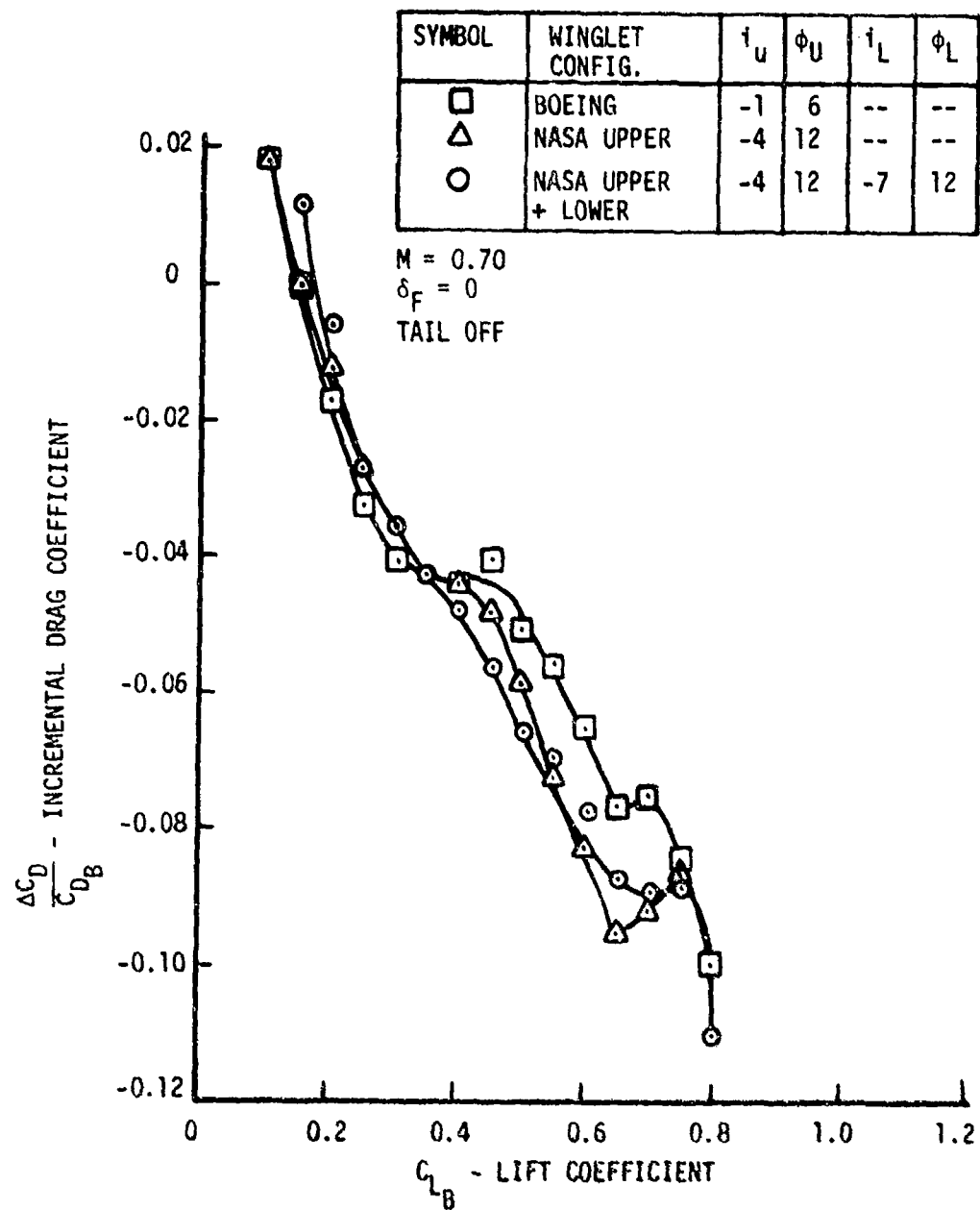
M = 0.70
δ_F = 0
TAIL OFF

Figure 17. Effect of Winglet Configuration on Full-Span KC-135A Model Drag. M = 0.70. δ_F = 0

SYMBOL	WINGLET CONFIG.	i_u	ϕ_U	i_L	ϕ_L
⊡	BOEING	-1	6	--	--
△	NASA UPPER	-4	12	--	--
⊙	NASA UPPER + LOWER	-4	12	-7	12
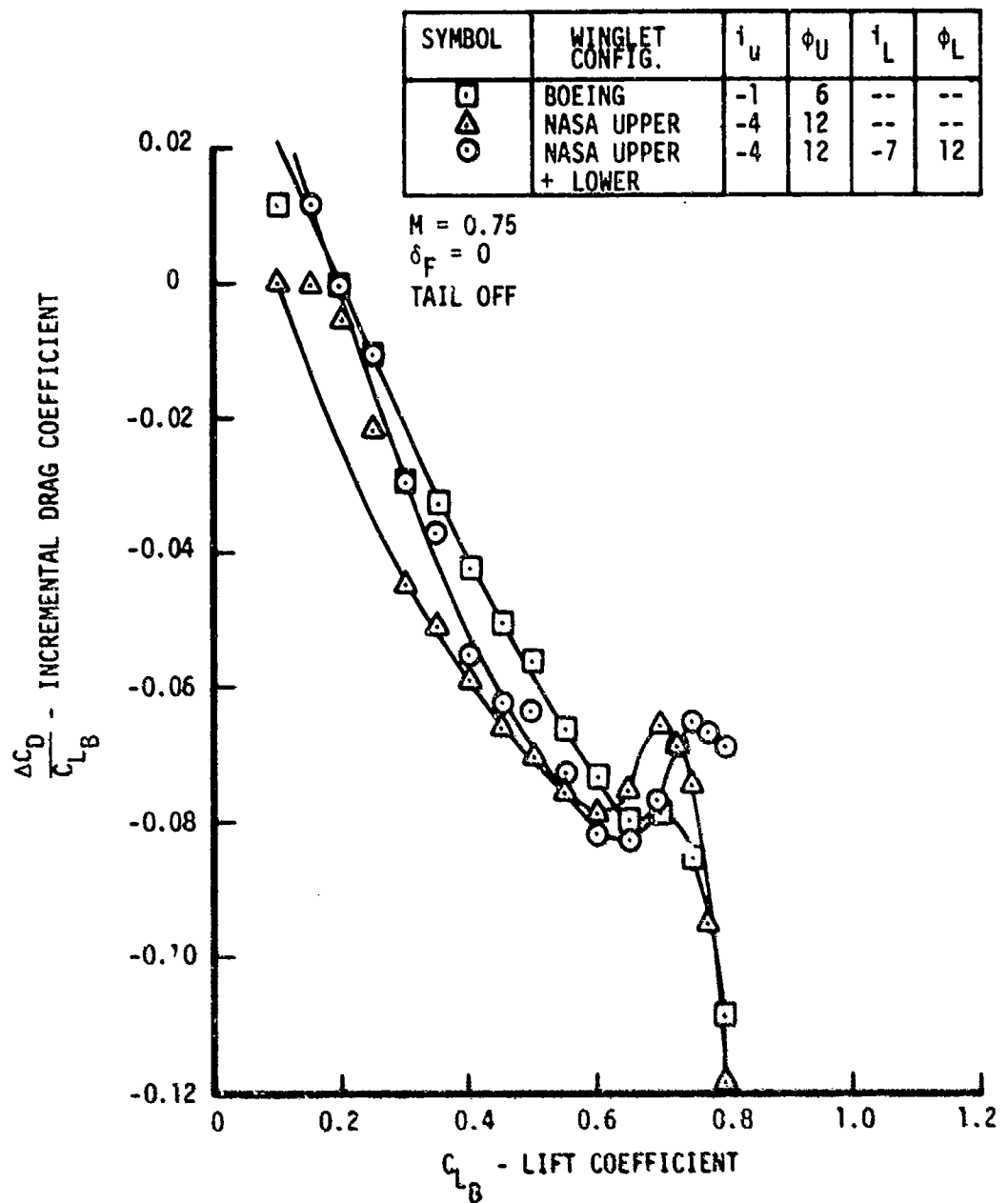
M = 0.75
δ_F = 0
TAIL OFF

Figure 18. Effect of Winglet Configuration on Full-Span KC-135A Model Drag. M = 0.75. δ_F = 0

SYMBOL	WINGLET CONFIG.	i_U	ϕ_U	i_L	ϕ_L
⊡	BOEING	-1	6	--	--
△	NASA UPPER	-4	12	--	--
⊙	NASA UPPER + LOWER	-4	12	-7	12
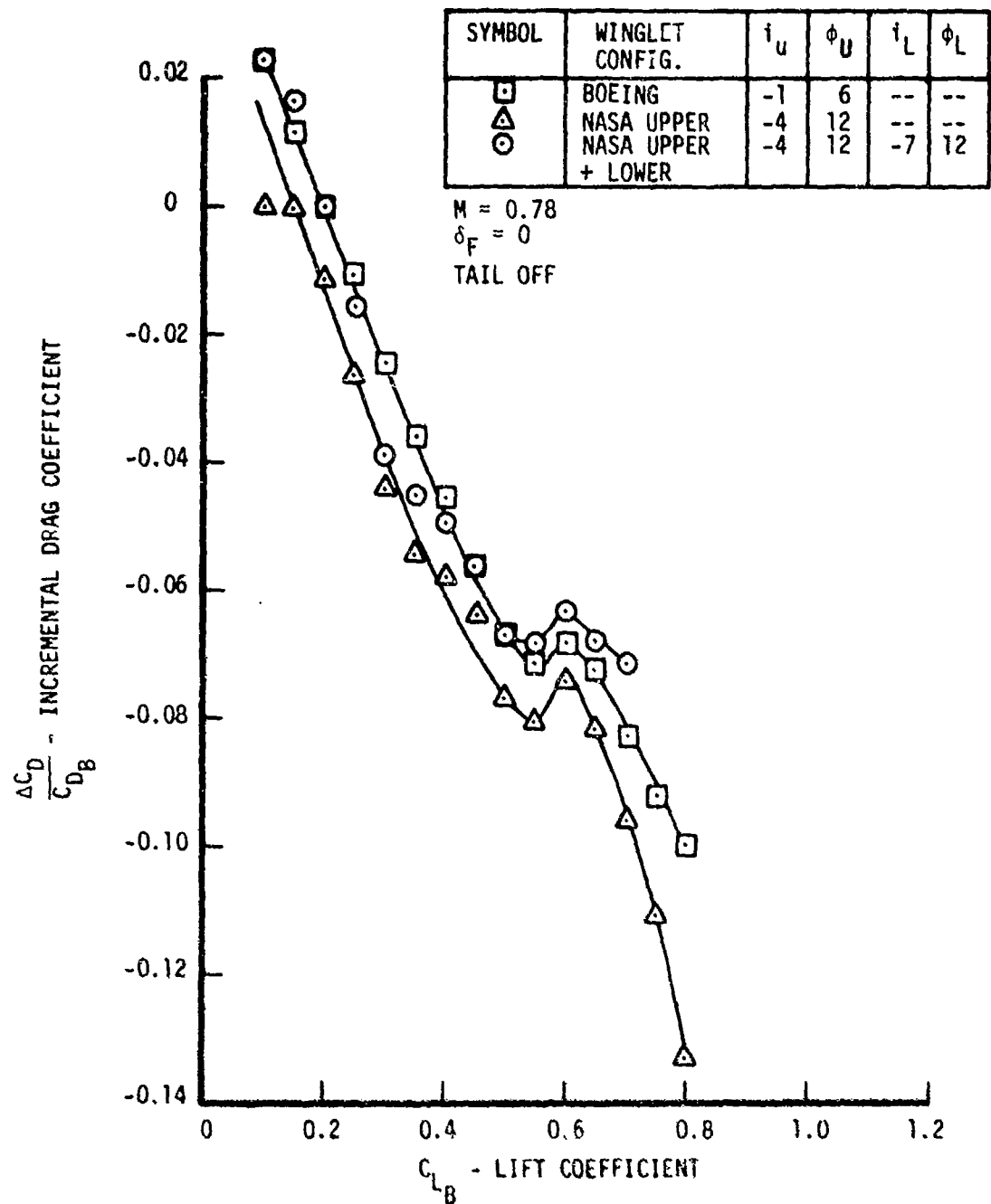
M = 0.78
$\delta_F = 0$
TAIL OFF

Figure 19. Effect of Winglet Configuration on Full-
Span KC-135A Model Drag. M = 0.78. $\delta_F = 0$

50

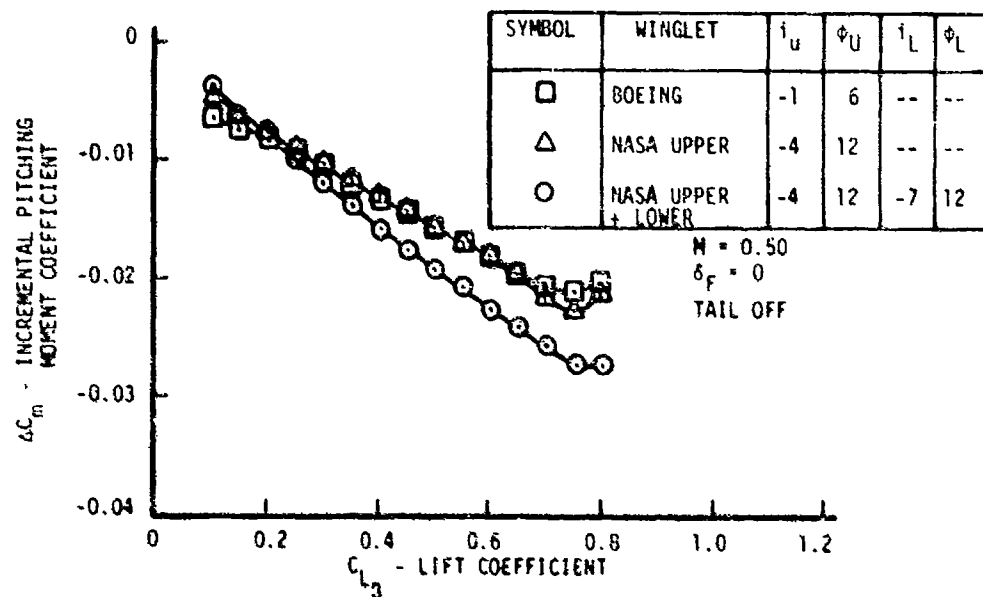| SYMBOL	WINGLET CONFIG.	i_u	ϕ_U	i_L	ϕ_L
⊡	BOEING	-1	6	--	--
△	NASA UPPER	-4	12	--	--
⊙	NASA UPPER + LOWER	-4	12	-7	12
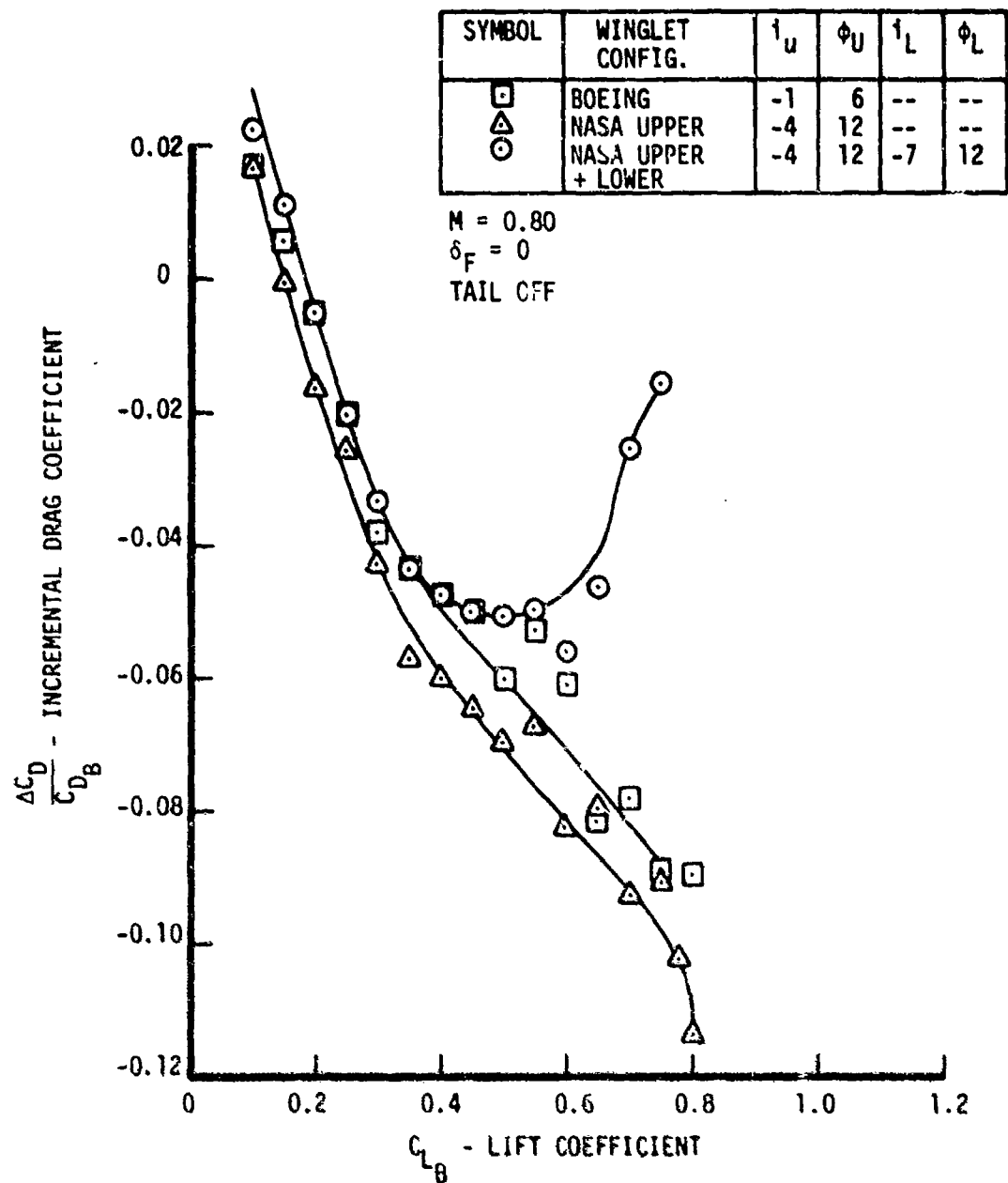
M = 0.80
$\delta_F = 0$
TAIL OFF
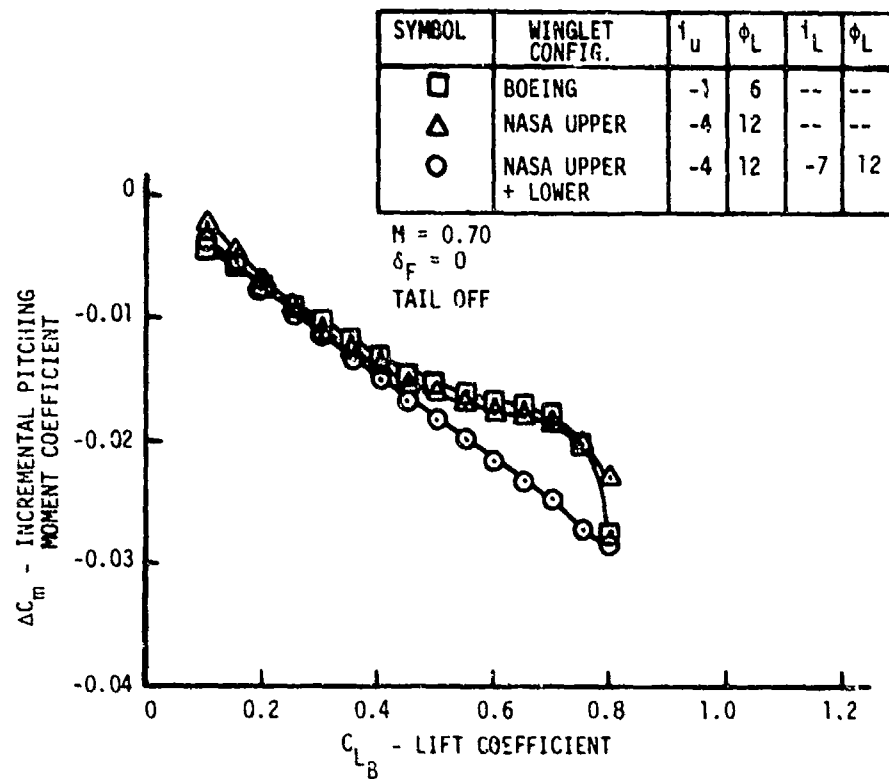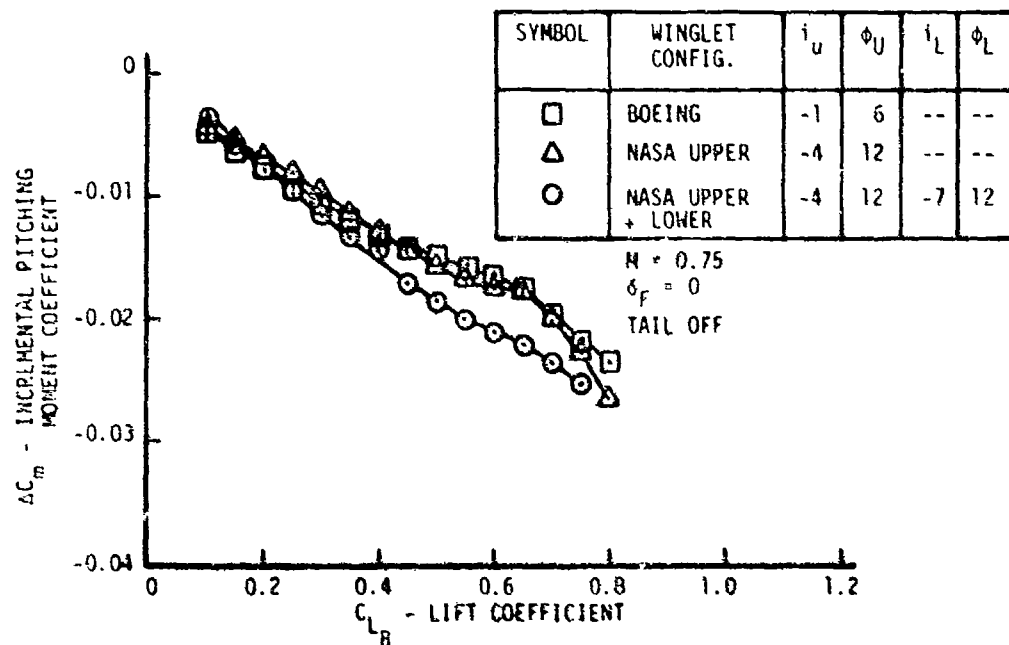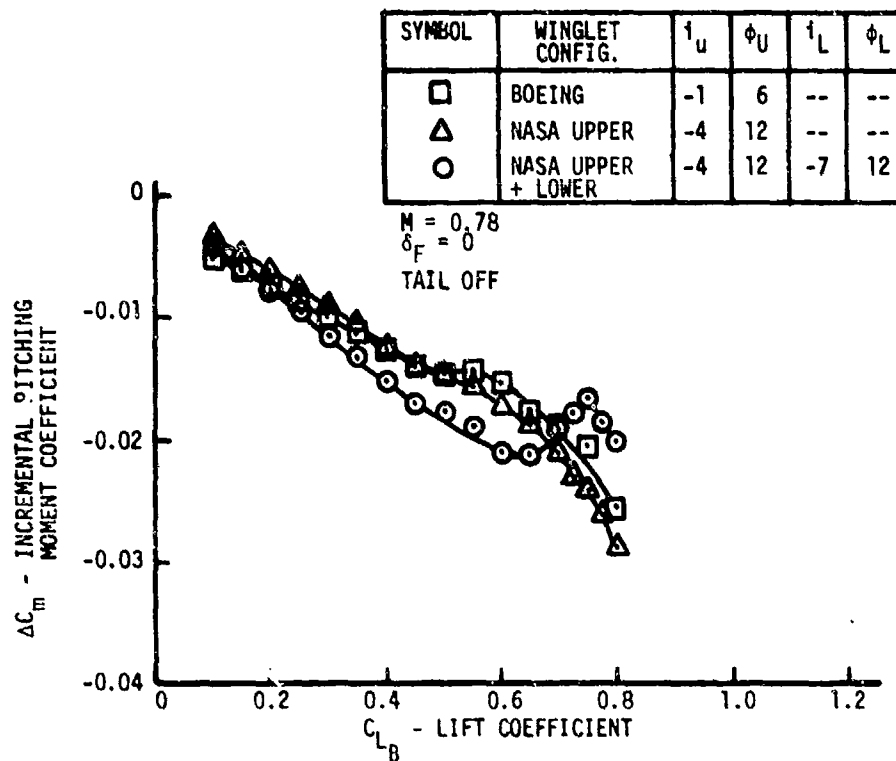
Figure 20.   Effect of Winglet Configuration on Full-
             Span KC-135A Model Drag.   M = 0.80. $\delta_F = 0$

51
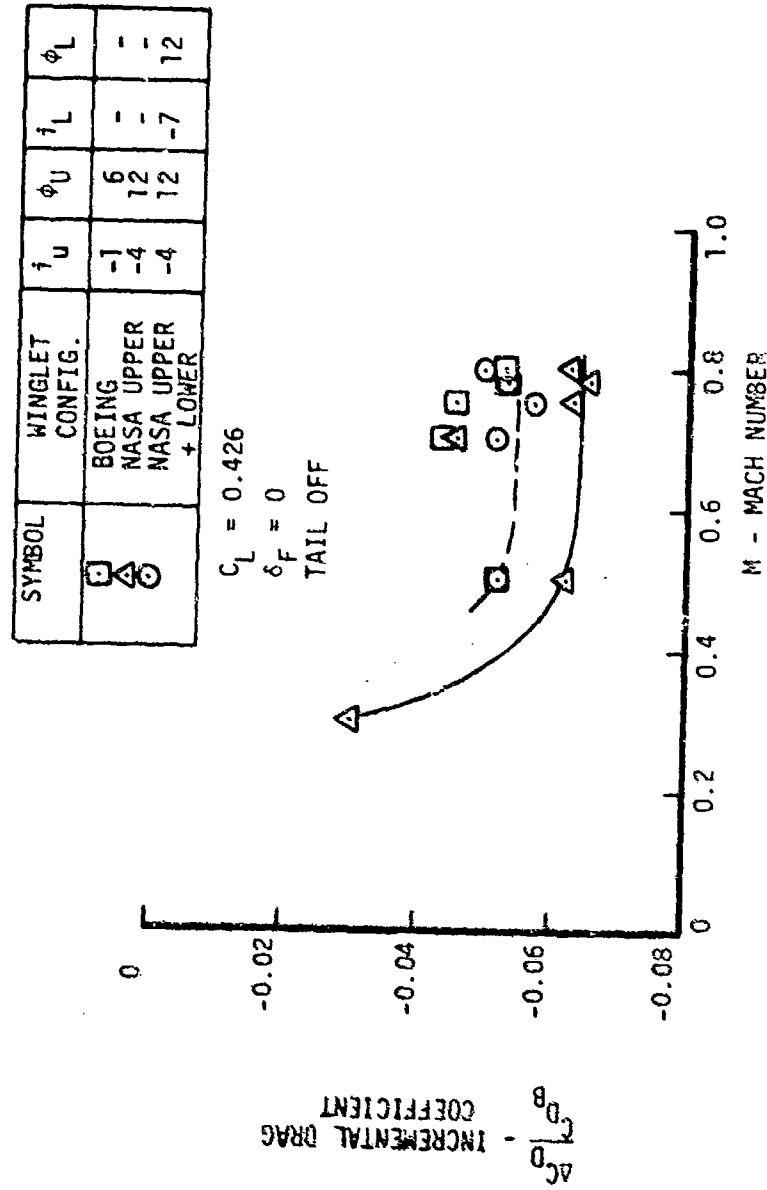
Figure 21. Effect of Winglet Configuration on Full-Span KC-135A Model Drag for Different Mach Numbers. $C_L = 0.426$

SYMBOL	WINGLET CONFIG.	i_u	ϕ_U
△	NASA UPPER	-4	12

M = 0.3
$\delta_F = 0$
TAIL OFF
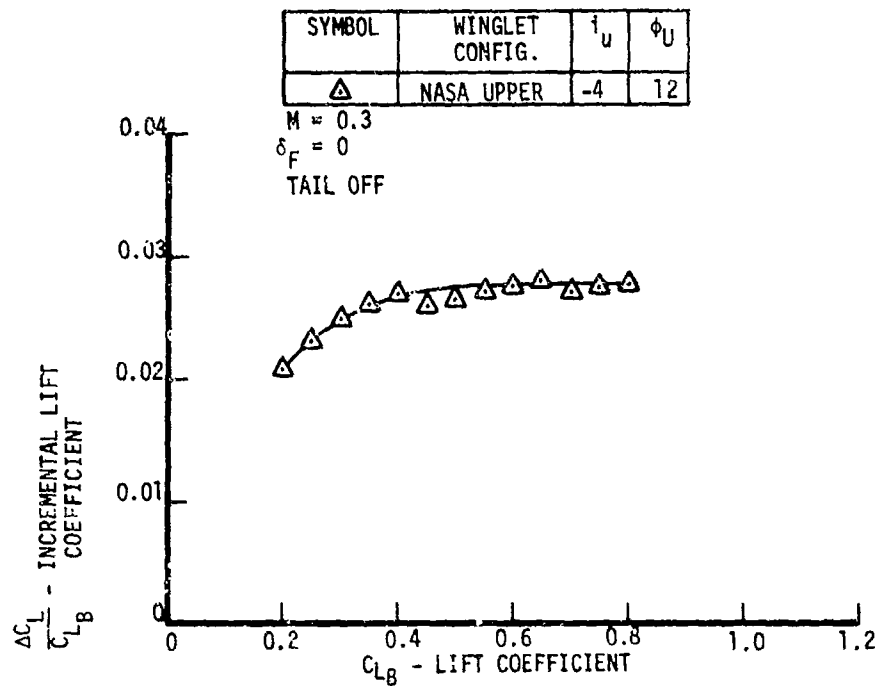
Figure 22. Effect of Winglet Configuration on Full-
Span KC-135A Model Lift. M = 0.30. $\delta_F = 0$

SYMBOL	WINGLET CONFIG.	i_u	ϕ_U	i_L	ϕ_L
▢	BOEING	-1	6	-	-
△	NASA UPPER	-4	12	-	-
⊙	NASA UPPER + LOWER	-4	12	-7	12
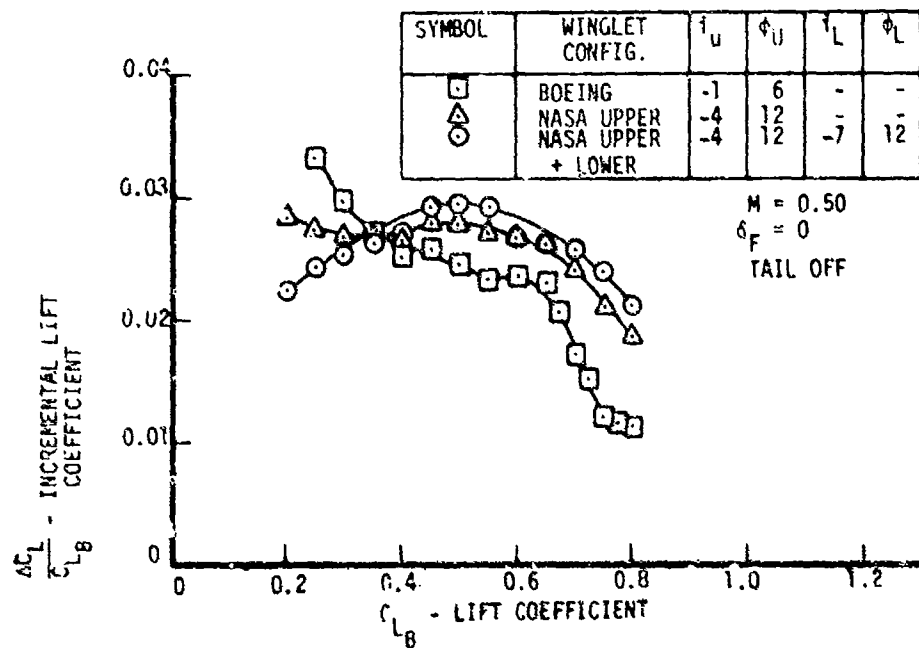
M = 0.50
$\delta_F = 0$
TAIL OFF

Figure 23. Effect of Winglet Configuration on Full-
Span KC-135A Model Lift. M = 0.50. $\delta_F = 0$

53

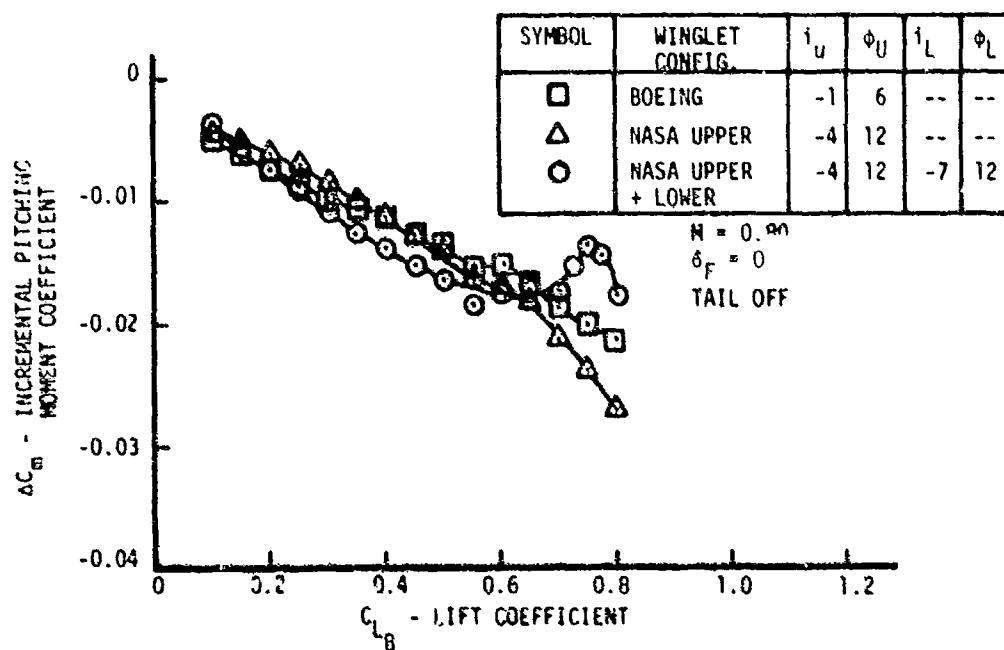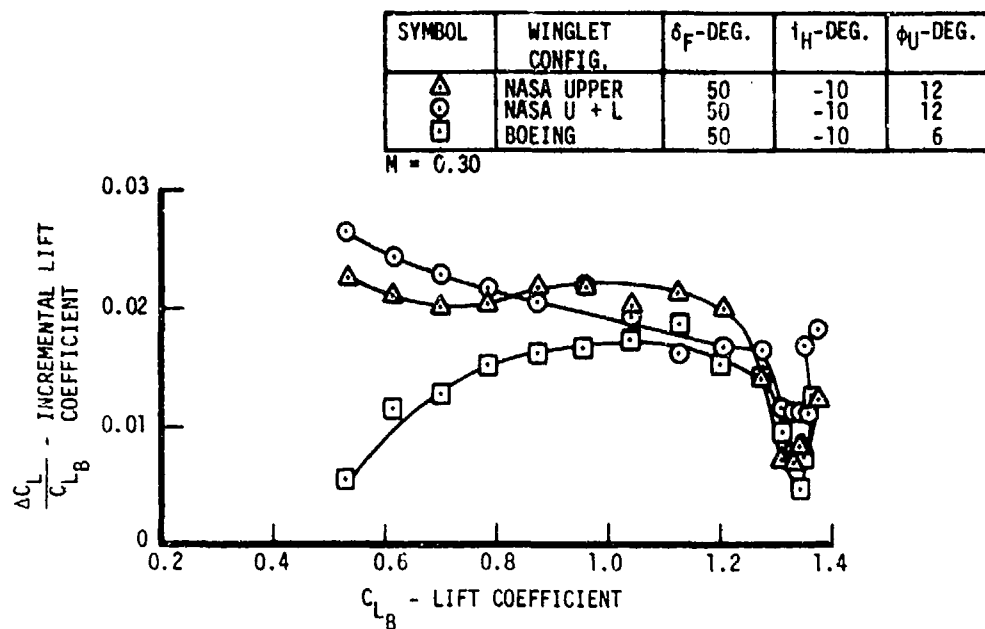| SYMBOL	WINGLET CONFIG.	i_u	ϕ_U	i_L	ϕ_L
▣	BOEING	-1	6	-	-
△	NASA UPPER	-4	12	-	-
⊙	NASA UPPER + LOWER	-4	12	-7	12
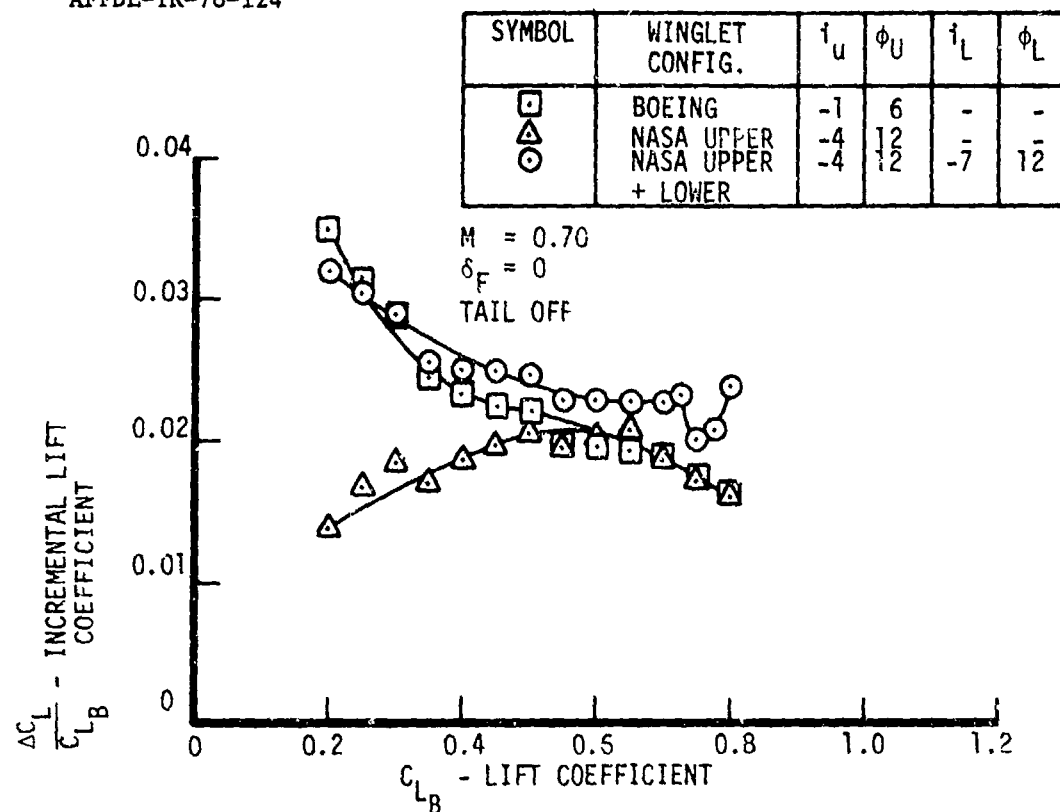
Figure 24. Effect of Winglet Configuration on Full-Span KC-135A Model Lift. M = 0.70. δ_F = 0
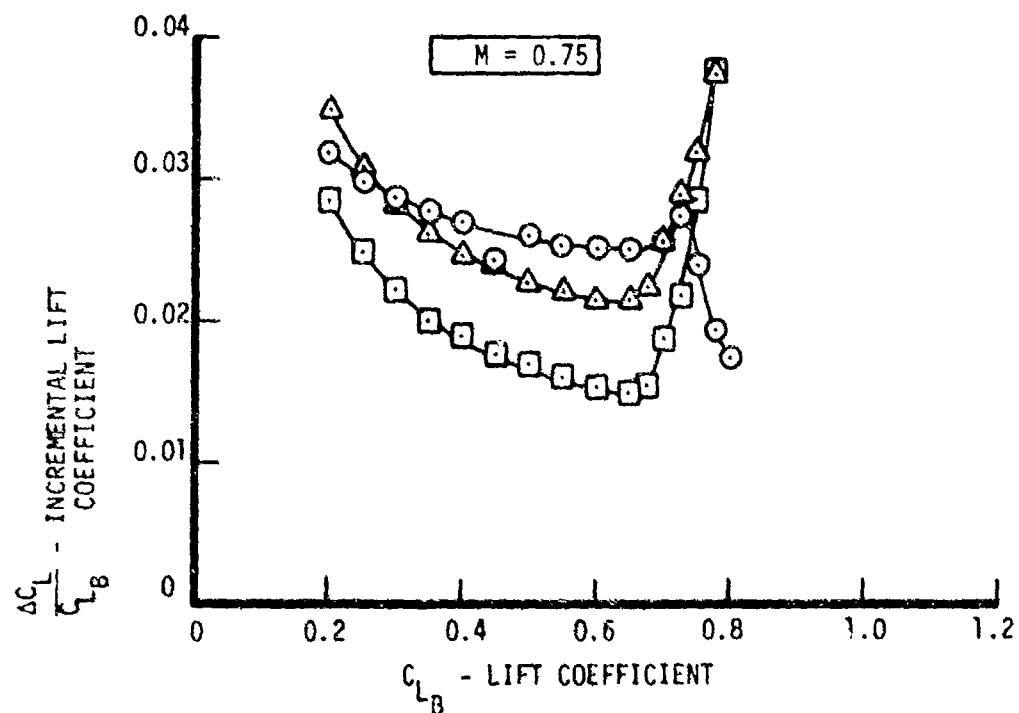
Figure 25. Effect of Winglet Configuration on Full-Span KC-135A Model Lift. M = 0.75. δ_F = 0

54

SYMBOL	WINGLET CONFIG.	i_u	ϕ_U	i_L	ϕ_L
⊡	BOEING	-1	6	-	-
△	NASA UPPER	-4	12	-	-
⊙	NASA UPPER + LOWER	-4	12	-7	12

M = 0.78
δ_F = 0
TAIL OFF

Figure 26. Effect of Winglet Configuration on Full-
Span KC-135A Model Lift. M = 0.78. δ_F = 0
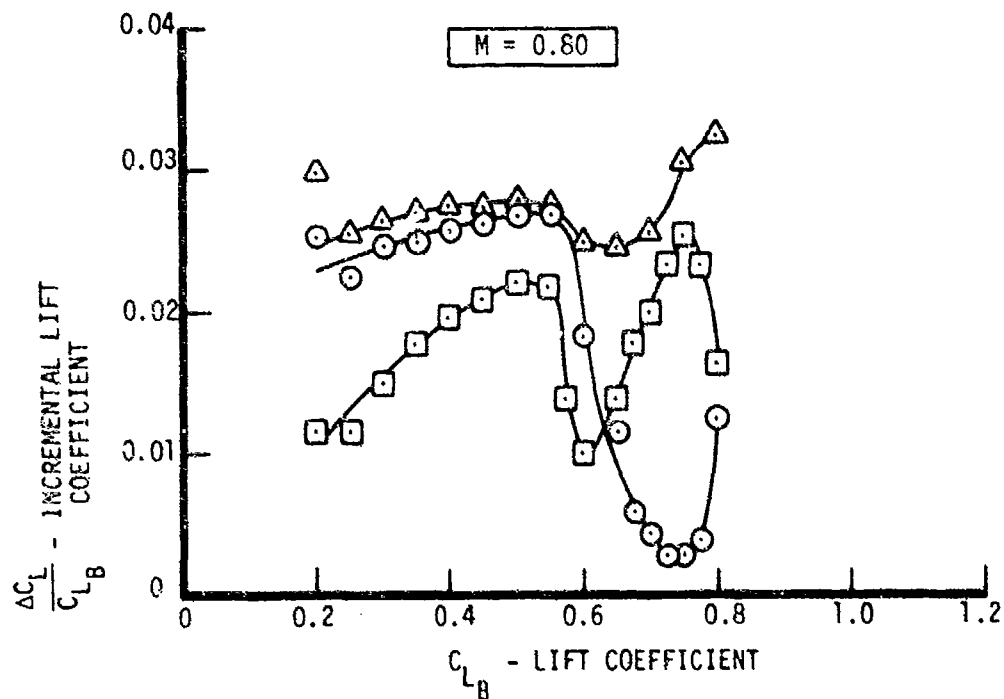
M = 0.80

Figure 27. Effect of Winglet Configuration on Full-
Span KC-135A Model Lift. M = 0.80. δ_F = 0

55
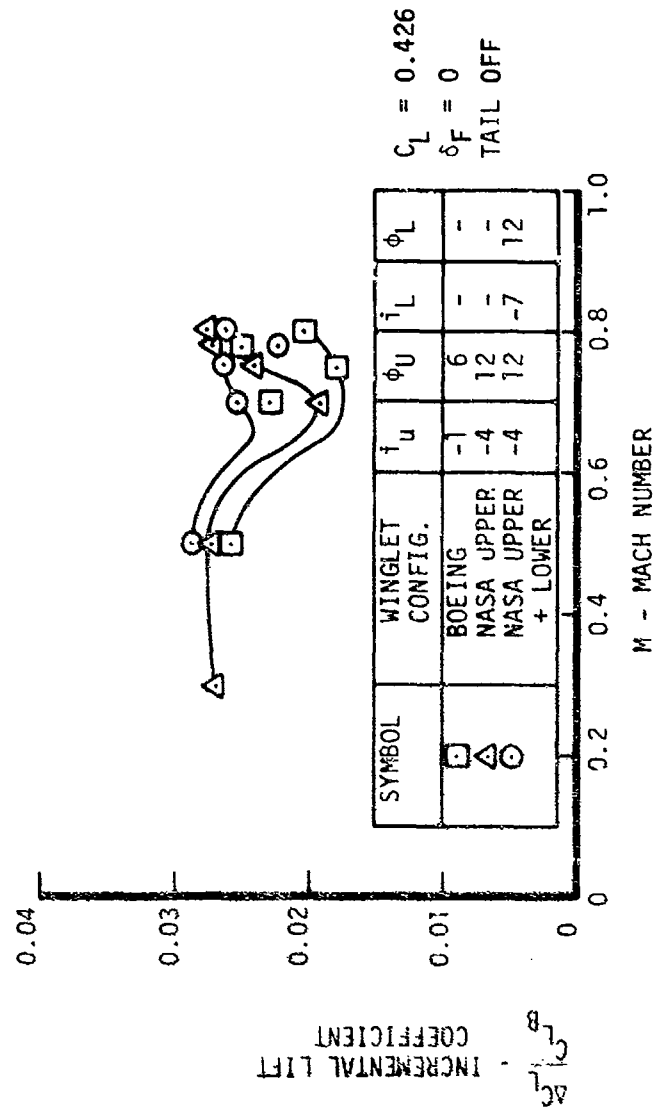
Figure 28. Effect of Winglet Configuration on Full-Span KC-135A Model Lift for Different Mach Numbers. $C_L = 0.426$

SYMBOL	WINGLET CONFIG.	i_u	ϕ_U	i_L	ϕ_L
⊡	BOEING	-1	6	-	-
△	NASA UPPER	-4	12	-	-
⊙	NASA UPPER + LOWER	-4	12	-7	12

$C_L = 0.426$

$\delta_F = 0$

TAIL OFF
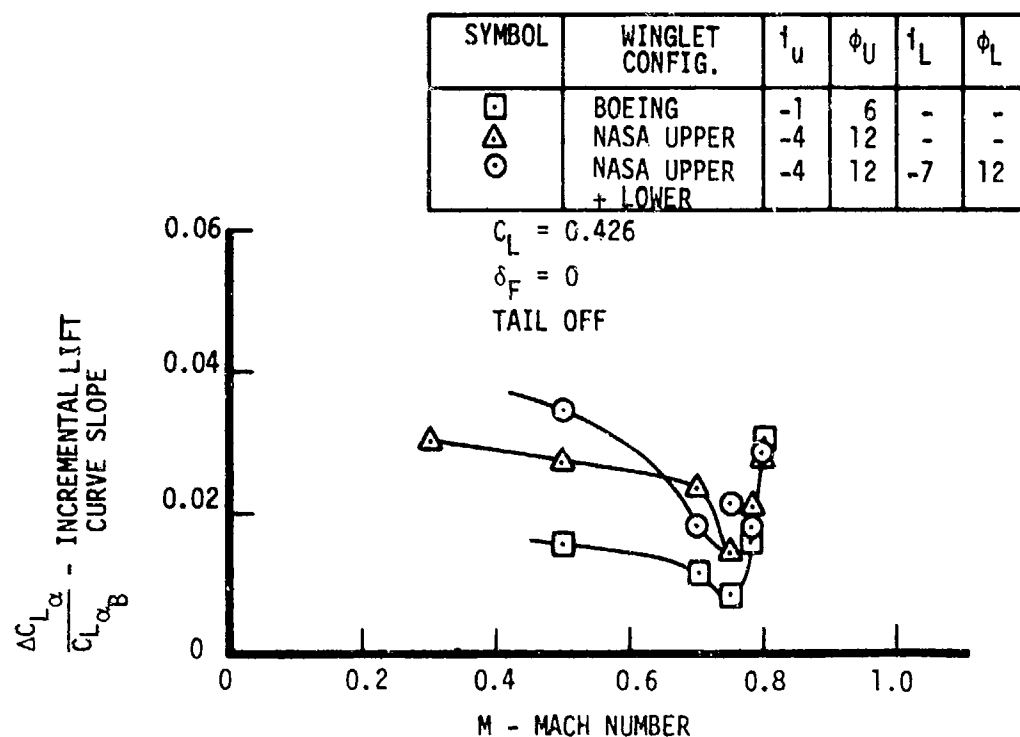
Figure 29. Effect of Winglet Configuration on Full-Span KC-135A Model Lift Curve Slope for Different Mach Numbers

SYMBOL	WINGLET CONFIG.
⊡	BOEING
△	NASA UPPER
⊙	NASA UPPER + LOWER

SYMBOL	i_u	ϕ_U	i_L	ϕ_L
⊡	-1	6	-	-
△	-4	12	-	-
⊙	-4	12	-7	12

$M = 0.78$

$\delta_F = 0$

TAIL OFF
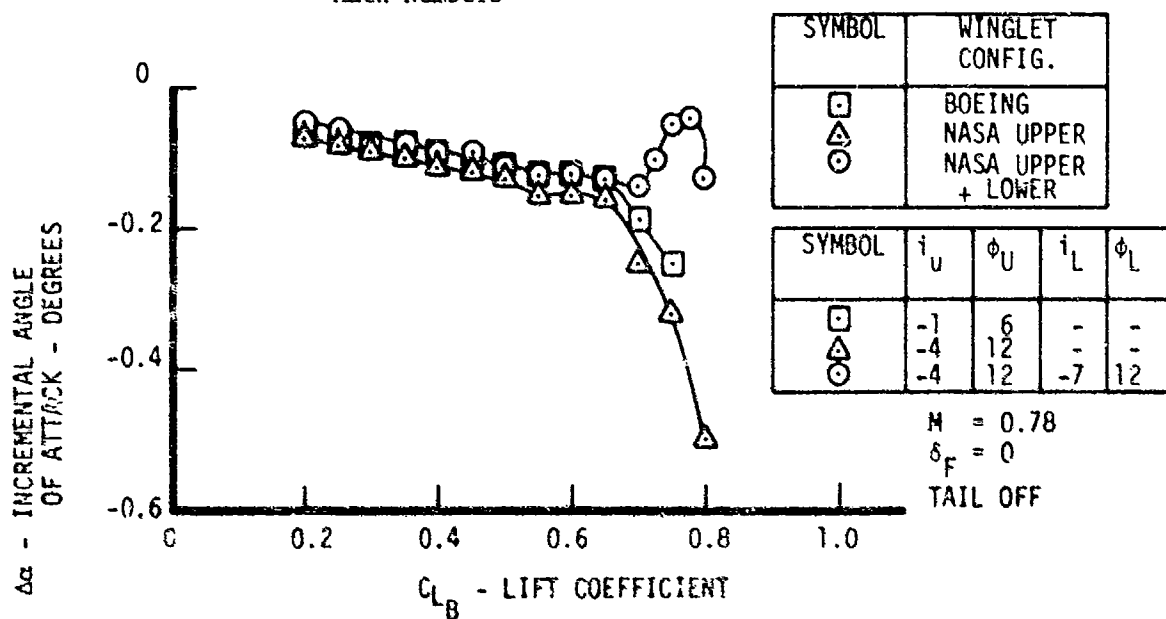
Figure 30. Effect of Winglet Configuration on Full-Span KC-135A Model Angle of Attack Near Cruise Conditions

SYMBOL	WINGLET CONFIG.	i_u	ϕ_U	i_L	ϕ_L
▣	BOEING	-1	6	--	--
△	NASA UPPER	-4	12	--	--
⊙	NASA UPPER + LOWER	-4	12	-7	12

$\delta_F = 0$

TAIL OFF
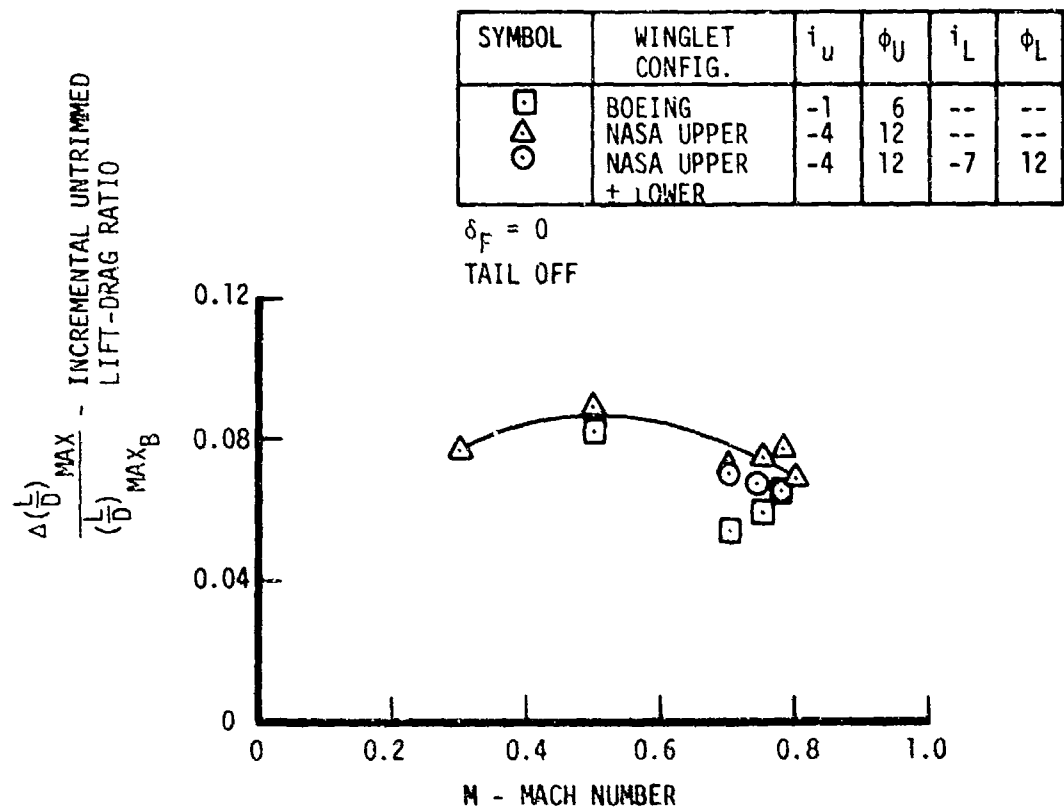
Figure 31. Effect of Winglet Configuration on Full-Span KC-135A Model Untrimmed Maximum Lift-Drag Ratio for Different Mach Numbers

58

SYMBOL	WINGLET CONFIG.	i_u	ϕ_U	i_L	ϕ_L
□	BOEING	-1	6	--	--
△	NASA UPPER	-4	12	--	--
○	NASA UPPER + LOWER	-4	12	-7	12
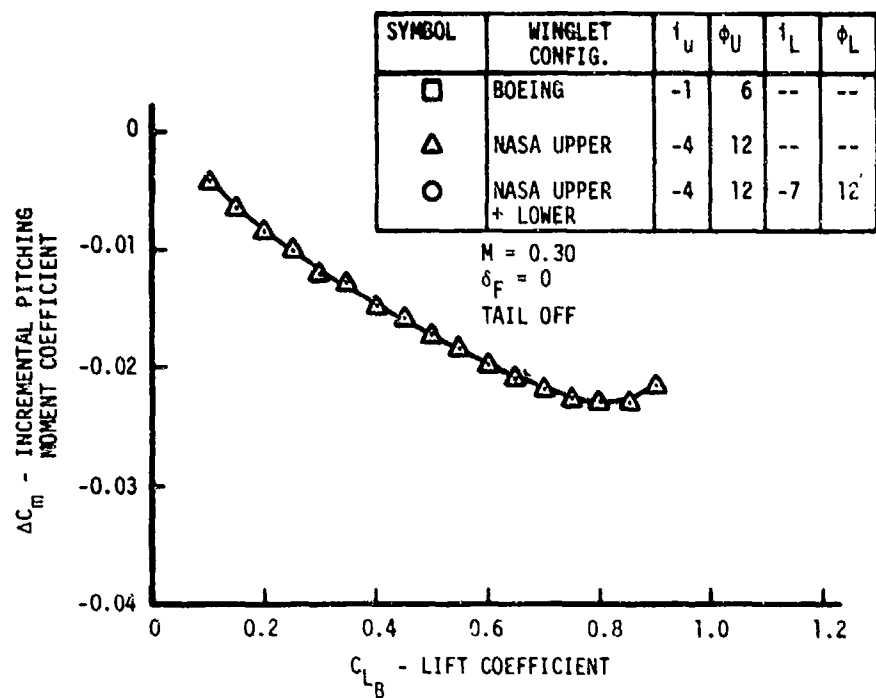
M = 0.30
δ_F = 0
TAIL OFF

Figure 32. Effect of Winglet Configuration on Full-Span
KC-135A Model Pitching Moment. M = 0.30.
δ_F = 0

SYMBOL	WINGLET	i_u	ϕ_U	i_L	ϕ_L
□	BOEING	-1	6	--	--
△	NASA UPPER	-4	12	--	--
○	NASA UPPER + LOWER	-4	12	-7	12

M = 0.50
δ_F = 0
TAIL OFF

Figure 33. Effect of Winglet Configuration on Full-Span
KC-135A Model Pitching Moment. M = 0.50.
δ_F = 0

59

SYMBOL	WINGLET CONFIG.	i_u	ϕ_L	i_L	ϕ_L
□	BOEING	-1	6	--	--
△	NASA UPPER	-4	12	--	--
○	NASA UPPER + LOWER	-4	12	-7	12

M = 0.70
δ_F = 0
TAIL OFF

Figure 34. Effect of Winglet Configuration on Full-Span KC-135A Model Pitching Moment. M = 0.70. δ_F = 0

SYMBOL	WINGLET CONFIG.	i_u	ϕ_U	i_L	ϕ_L
□	BOEING	-1	6	--	--
△	NASA UPPER	-4	12	--	--
○	NASA UPPER + LOWER	-4	12	-7	12

M = 0.75
δ_F = 0
TAIL OFF

Figure 35. Effect of Winglet Configuration on Full-Span KC-135A Model Pitching Moment. M = 0.75. δ_F = 0

SYMBOL	WINGLET CONFIG.	i_u	ϕ_U	i_L	ϕ_L
□	BOEING	-1	6	--	--
△	NASA UPPER	-4	12	--	--
○	NASA UPPER + LOWER	-4	12	-7	12

M = 0.78
$\delta_F = 0$
TAIL OFF

Figure 36. Effect of Winglet Configuration on Full-Span
KC-135A Model Pitching Moment. M = 0.78.
$\delta_F = 0$

SYMBOL	WINGLET CONFIG.	i_u	ϕ_U	i_L	ϕ_L
□	BOEING	-1	6	--	--
△	NASA UPPER	-4	12	--	--
○	NASA UPPER + LOWER	-4	12	-7	12

M = 0.80
$\delta_F = 0$
TAIL OFF

Figure 37. Effect of Winglet Configuration on Full-Span
KC-135A Model Pitching Moment. M = 0.80.
$\delta_F = 0$
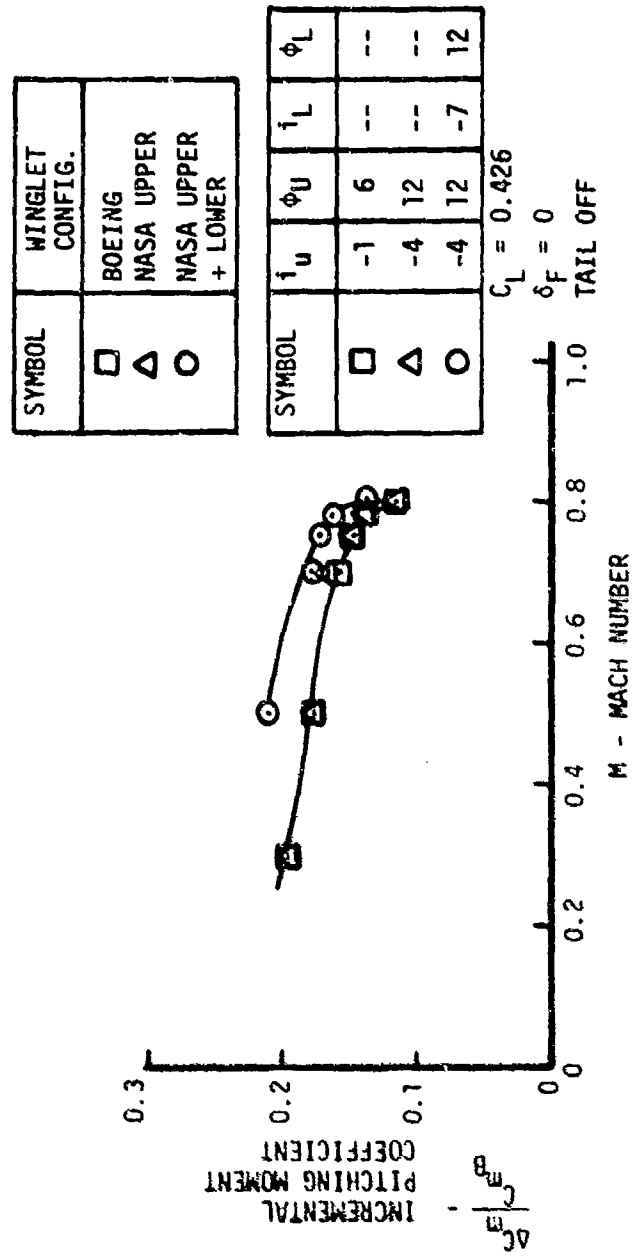
Figure 38. Effect of Winglet Configuration on Full-Span KC-135A Model Pitching Moment for Different Mach Numbers. $C_L = 0.426$

SYMBOL	WINGLET CONFIG.	δ_F-DEG.	i_H-DEG.	ϕ_U-DEG.
△	NASA UPPER	50	-10	12
○	NASA U + L	50	-10	12
□	BOEING	50	-10	6
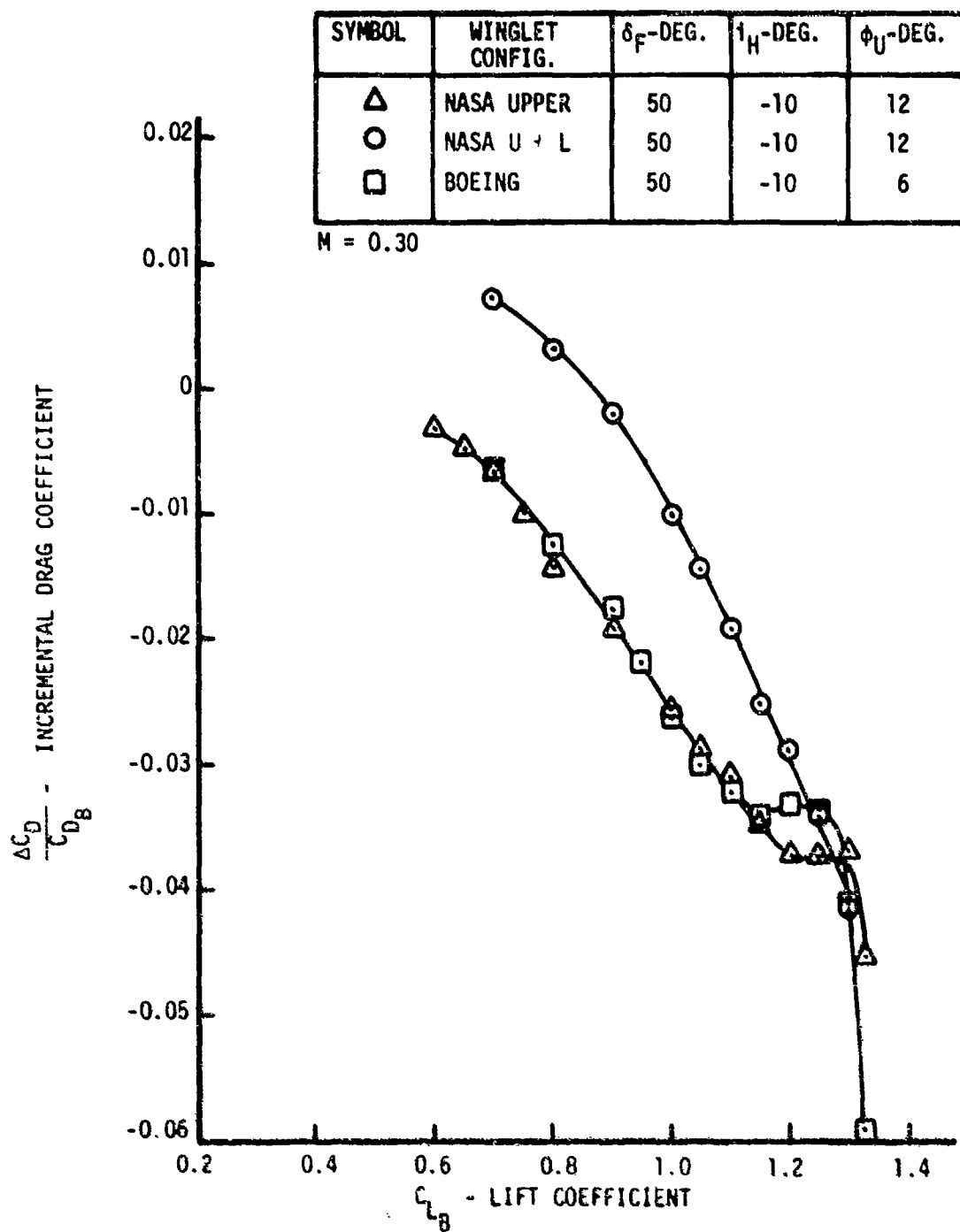
M = 0.30

Figure 39. Effect of Winglet Configuration on Full-Span KC-135A Model Drag. M = 0.30. δ_F = 50 Degrees. i_H = -10 Degrees

SYMBOL	WINGLET CONFIG.	δ_F-DEG.	i_H-DEG.	ϕ_U-DEG.
△	NASA UPPER	50	-10	12
⊙	NASA U + L	50	-10	12
☐	BOEING	50	-10	6

M = 0.30
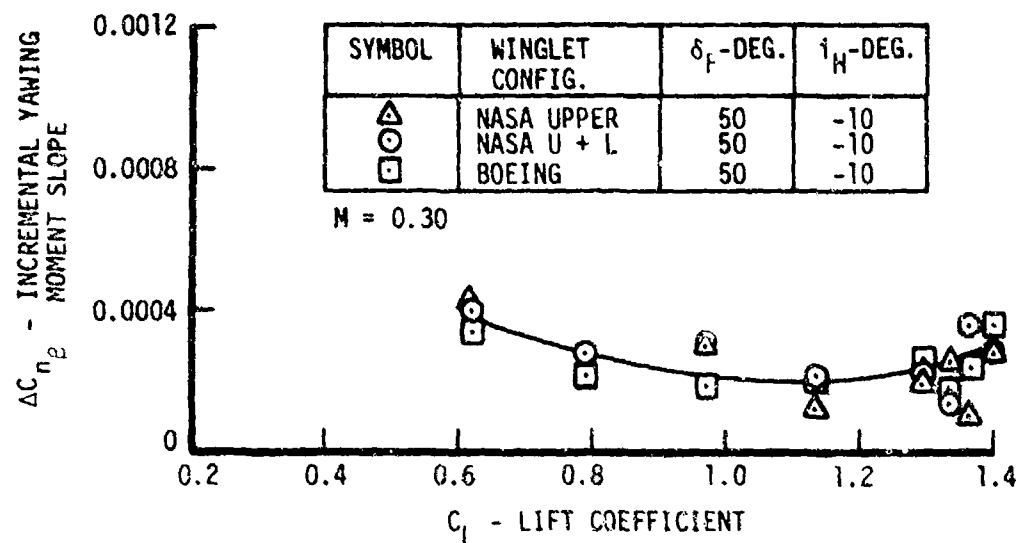

Figure 40. Effect of Winglet Configuration on Full-Span KC-135A Model Lift. M = 0.30. δ_F = 50 Degrees i_H = -10 Degrees

SYMBOL	WINGLET CONFIG.	δ_F-DEG.	i_H-DEG.	ϕ_U-DEG.
△	NASA UPPER	50	-10	12
⊙	NASA U + L	50	-10	12
☐	BOEING	50	-10	6
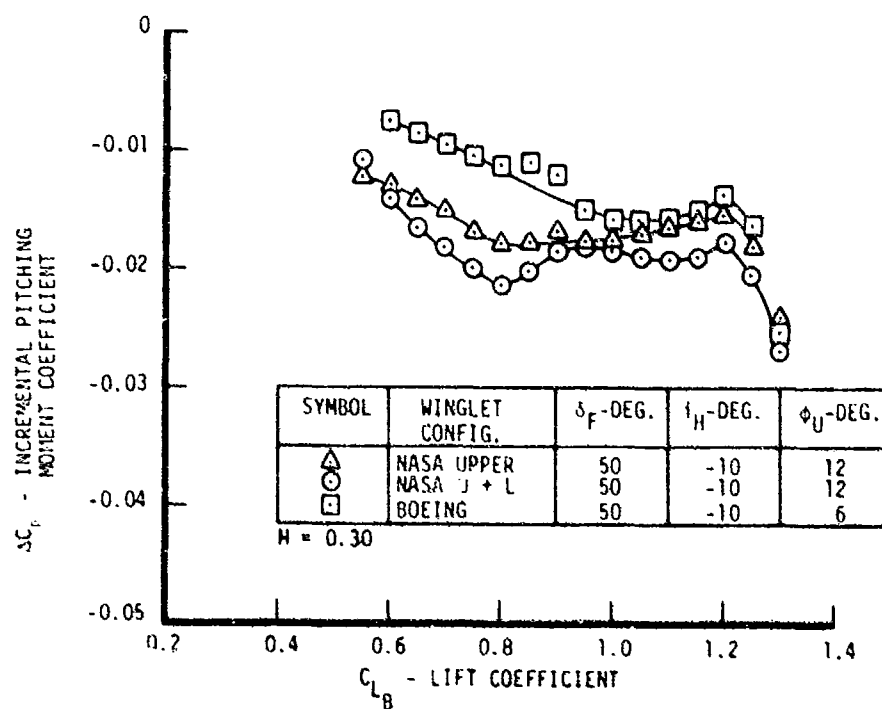
M = 0.30

Figure 41. Effect of Winglet Configuration on Full-Span KC-135A Model Pitching Moment. M = 0.30. δ_F = 50 Degrees. i_H = -10 Degrees
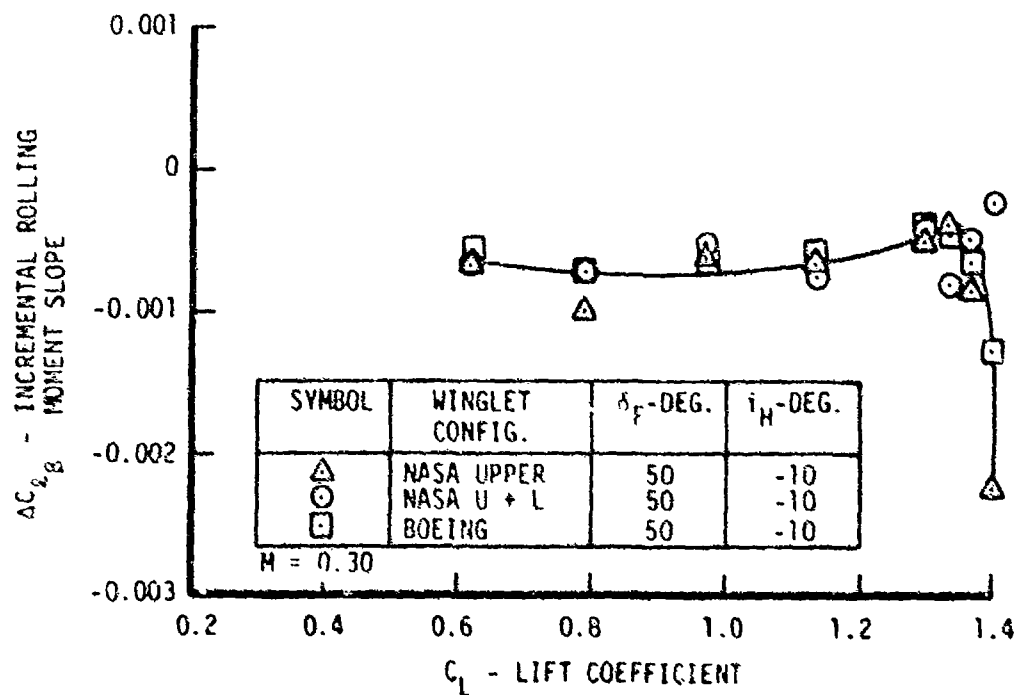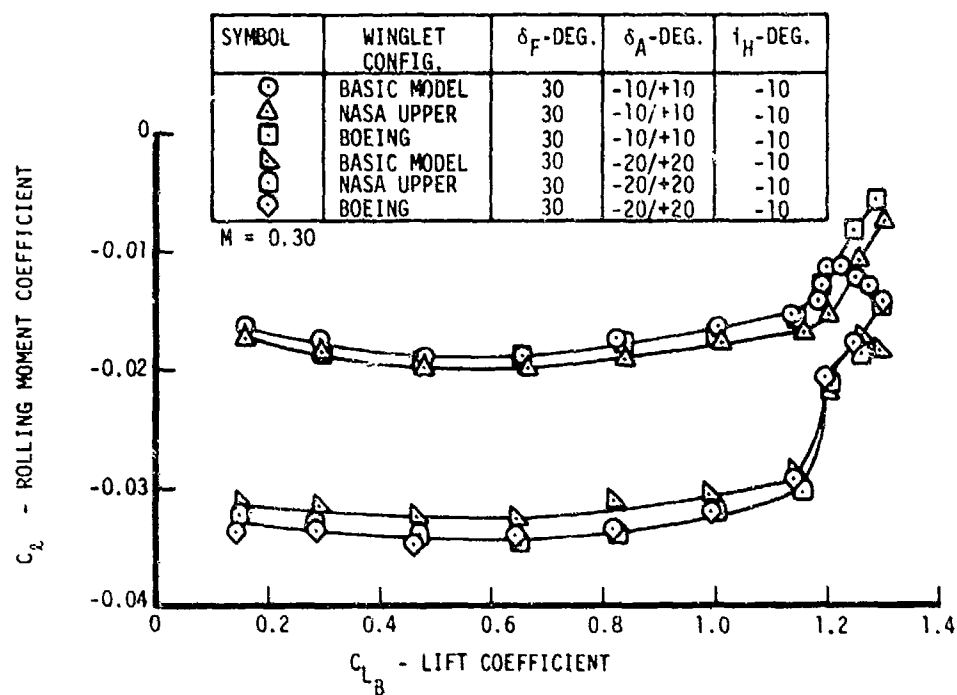
64

SYMBOL	WINGLET CONFIG.	i_u	ϕ_U	i_L	ϕ_L
▢	BOEING	-1	6	--	--
△	NASA UPPER	-4	15	--	--
⊙	NASA UPPER + LOWER	-4	15	-7	30
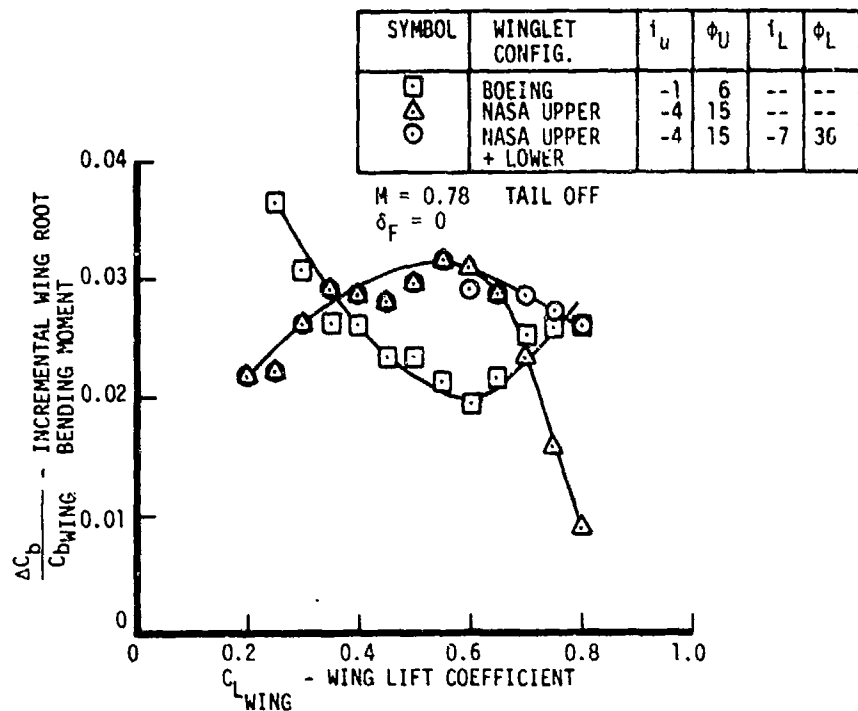
Figure 42. Effect of Winglet Configuration on Semispan KC-135A Model Wing Root Bending Moment. M = 0.78. δ_F = 0
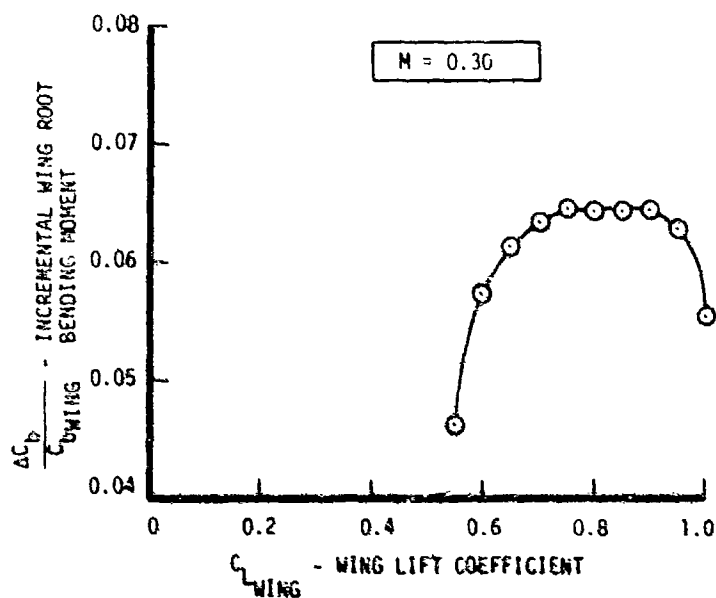
Figure 43. Effect of NASA Upper Plus Lower Winglet Configuration on Semispan KC-135A Model Wing Root Bending Moment. M = 0.30. δ_F = 0

65
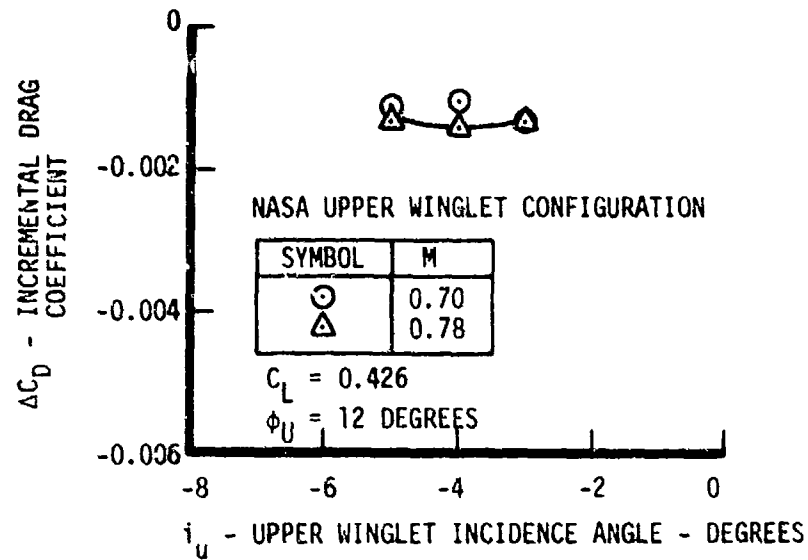
Figure 44. Effect of Upper Winglet Incidence on KC-135A Model Drag Near Cruise Conditions. NASA Upper Winglet Configuration. $C_L = 0.426$
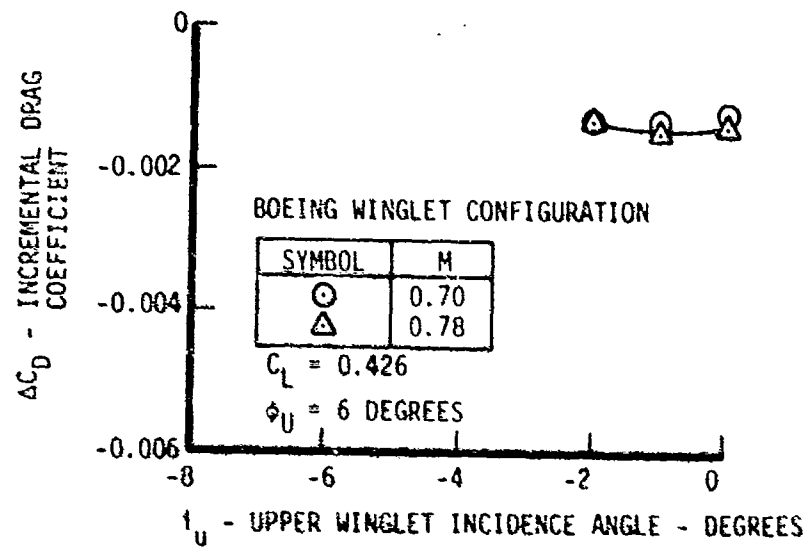
Figure 45. Effect of Upper Winglet Incidence on KC-135A Model Drag Near Cruise Conditions. Boeing Winglet Configuration. $C_L = 0.426$
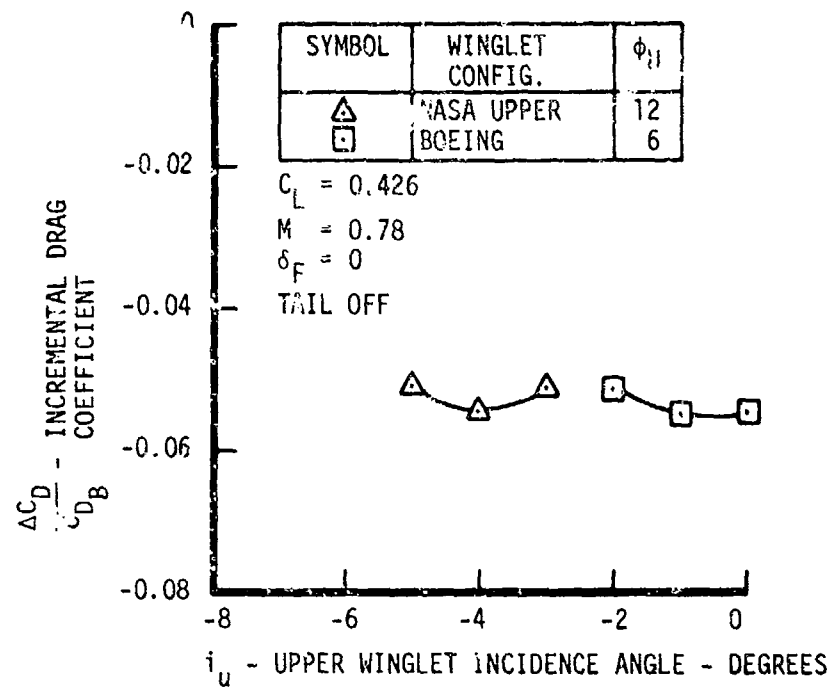
Figure 46. Effect of Upper ... et Incidence on KC-135A
Model Drag Near Cruise Conditions. $C_L = 0.426$
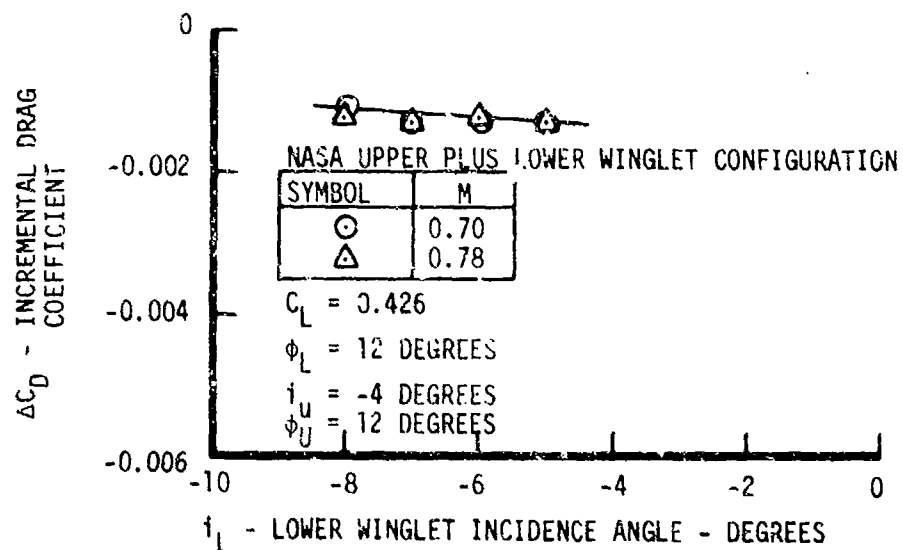
Figure 47. Effect of Lower Winglet Incidence on KC-135A
Model Drag Near Cruise Conditions. NASA Upper
Plus Lower Winglet Configuration. $C_L = 0.426$
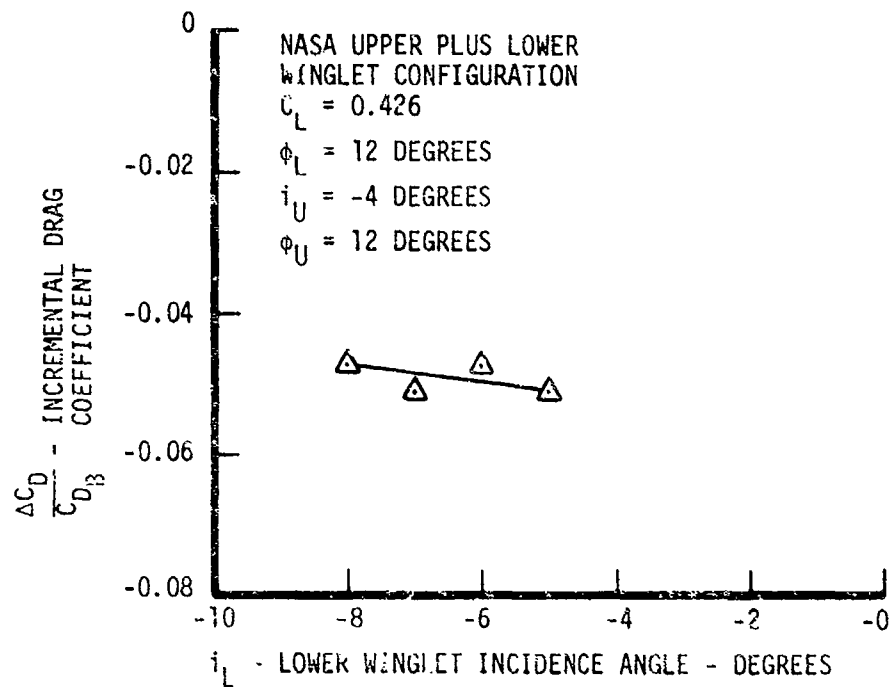
Figure 48.   Effect of Lower Winglet Incidence on KC-135A
Model Drag Near Cruise Conditions. C_L = 0.426
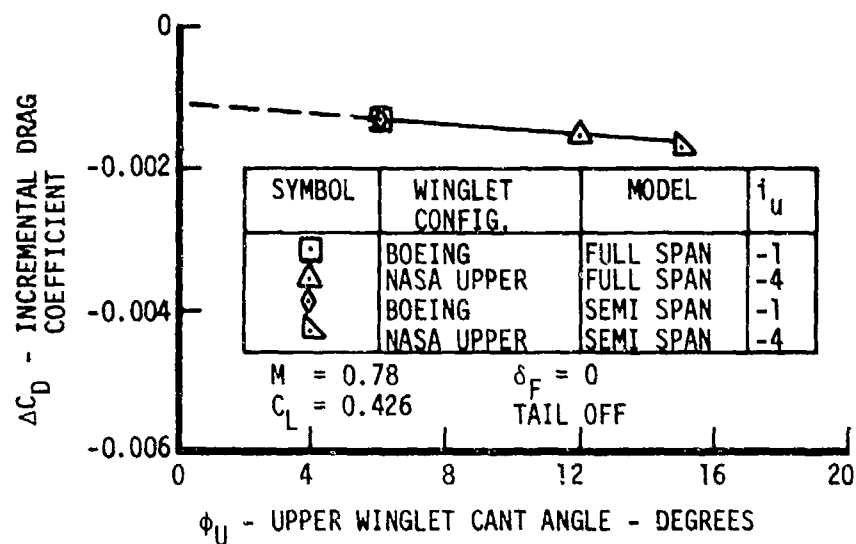
Figure 49. Effect of Upper Winglet Cant on KC-135A
Model Drag. $M = 0.78$. $C_L = 0.426$. $\delta_F = 0$
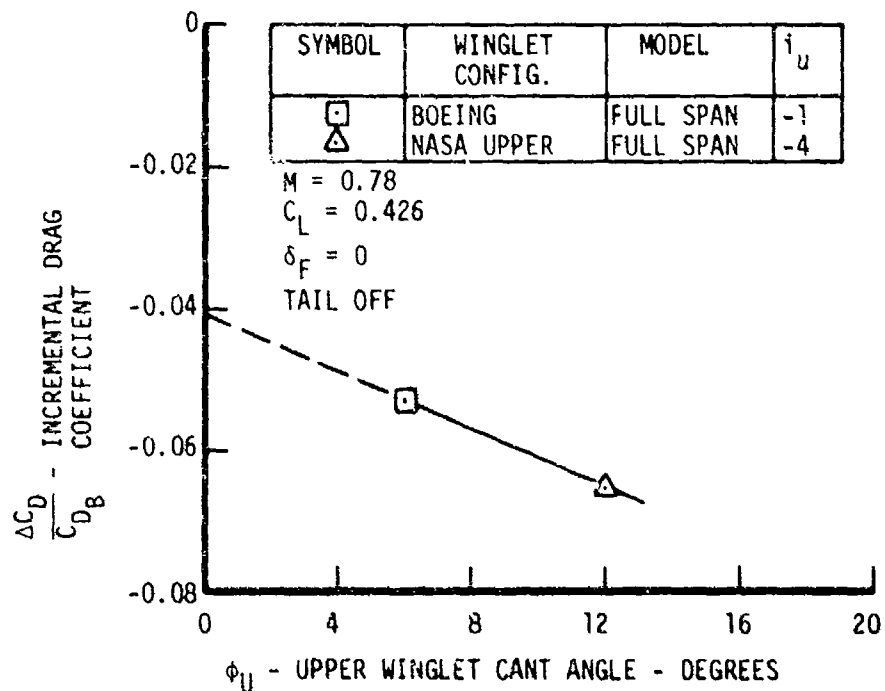
Figure 50. Effect of Upper Winglet Cant on KC-135A Model
Drag. $M = 0.78$. $C_L = 0.426$. $\delta_F = 0$
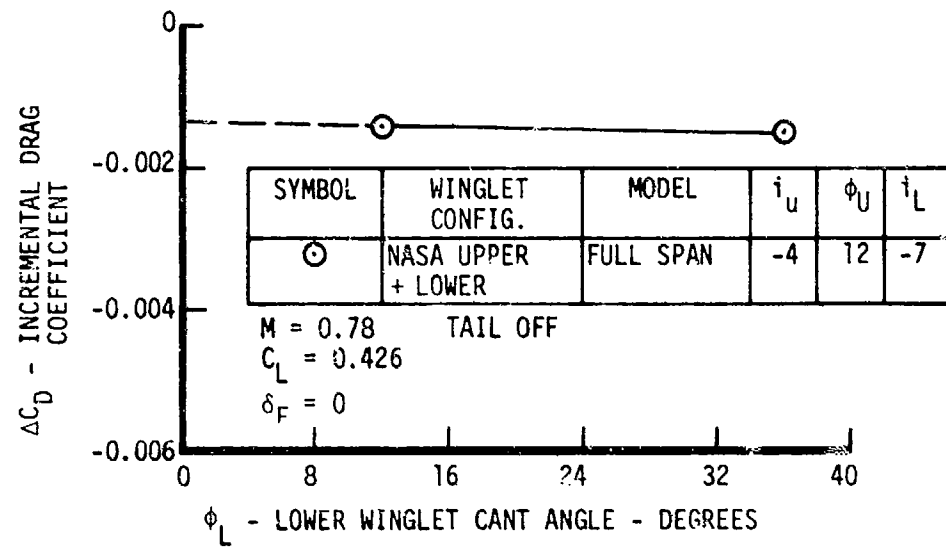
Figure 51. Effect of Lower Winglet Cant on KC-135A Model
Drag. M = 0.78. C_L = 0.426. δ_F = 0
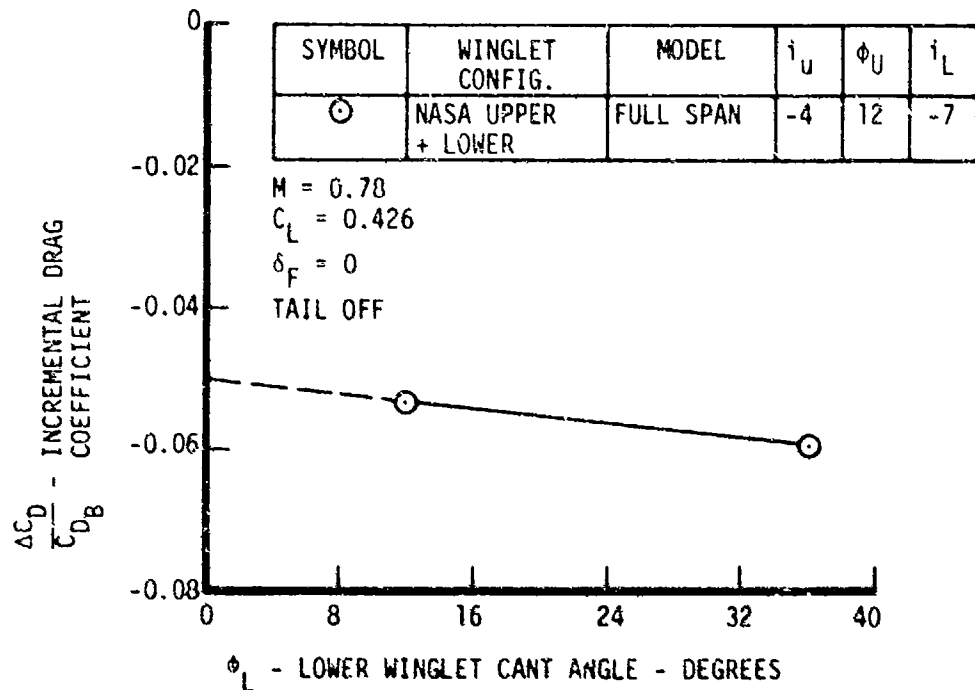
Figure 52. Effect of Lower Winglet Cant on KC-135A Model
Drag. M = 0.78. C_L = 0.426 δ_F = 0

70
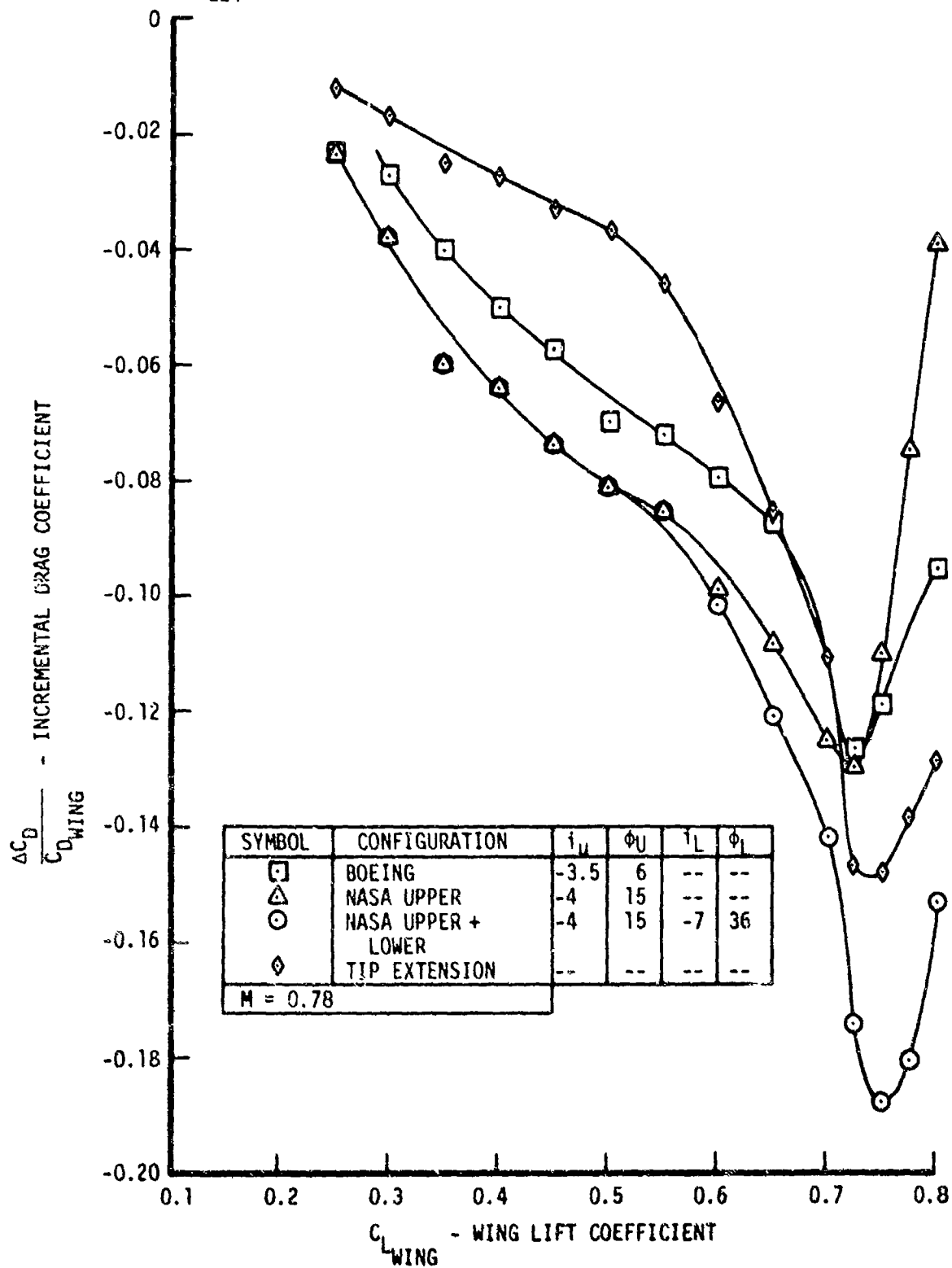
Figure 53. Comparison of Semispan KC-135A Model Drag with Winglets and Tip Extension. $M = 0.78$. $\delta_F = 0$
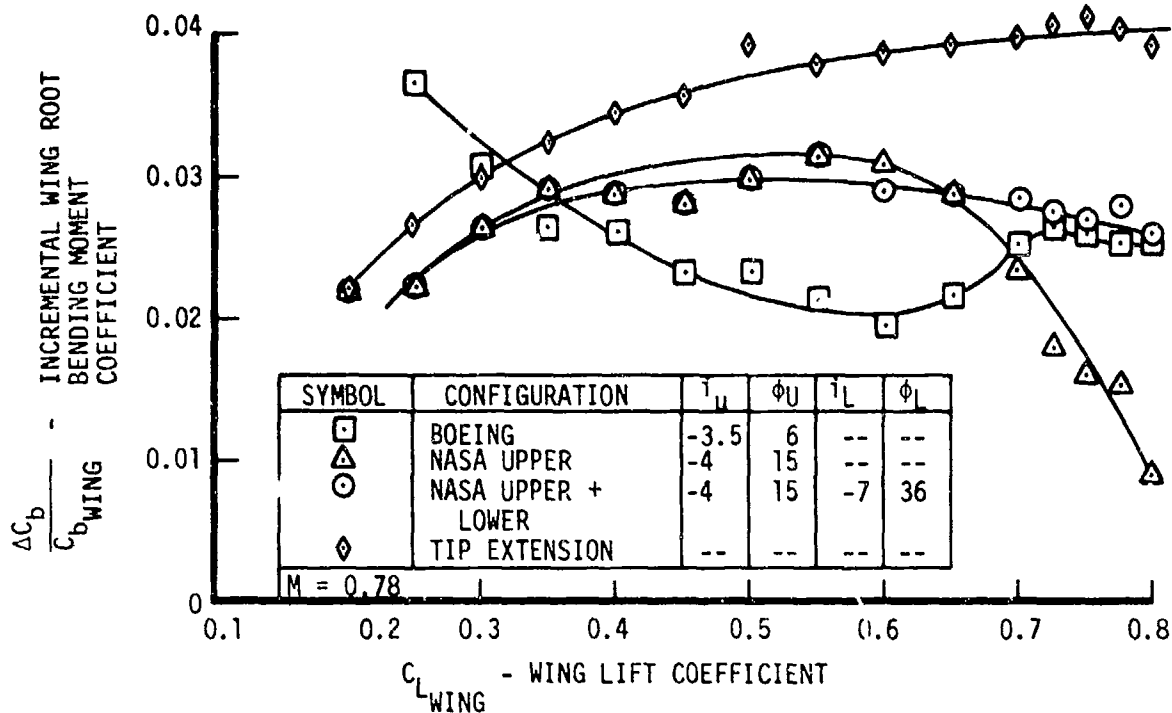
Figure 54. Comparison of Semispan KC-135A Model Wing Root
Bending Moment with Winglets and Tip Extension
$M = 0.78$. $\delta_F = 0$
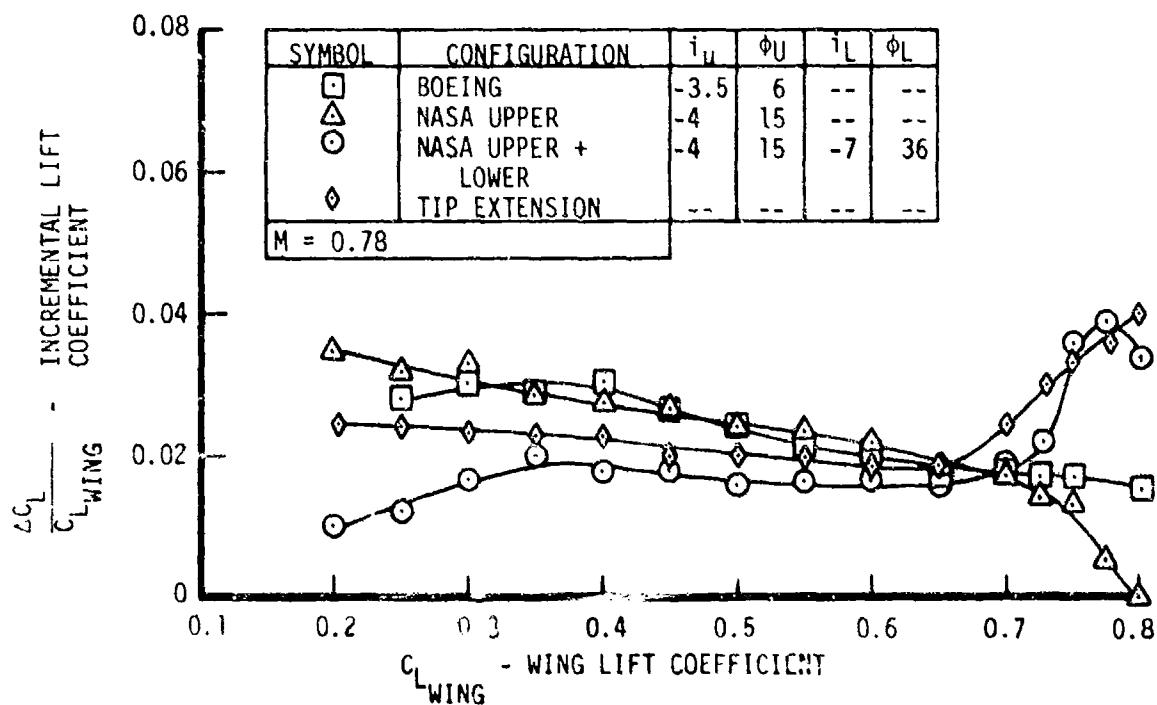
Figure 55. Comparison of Semispan KC-135A Model Lift
with Winglets and Tip Extension. $M = 0.78$.
$\delta_F = 0$

72
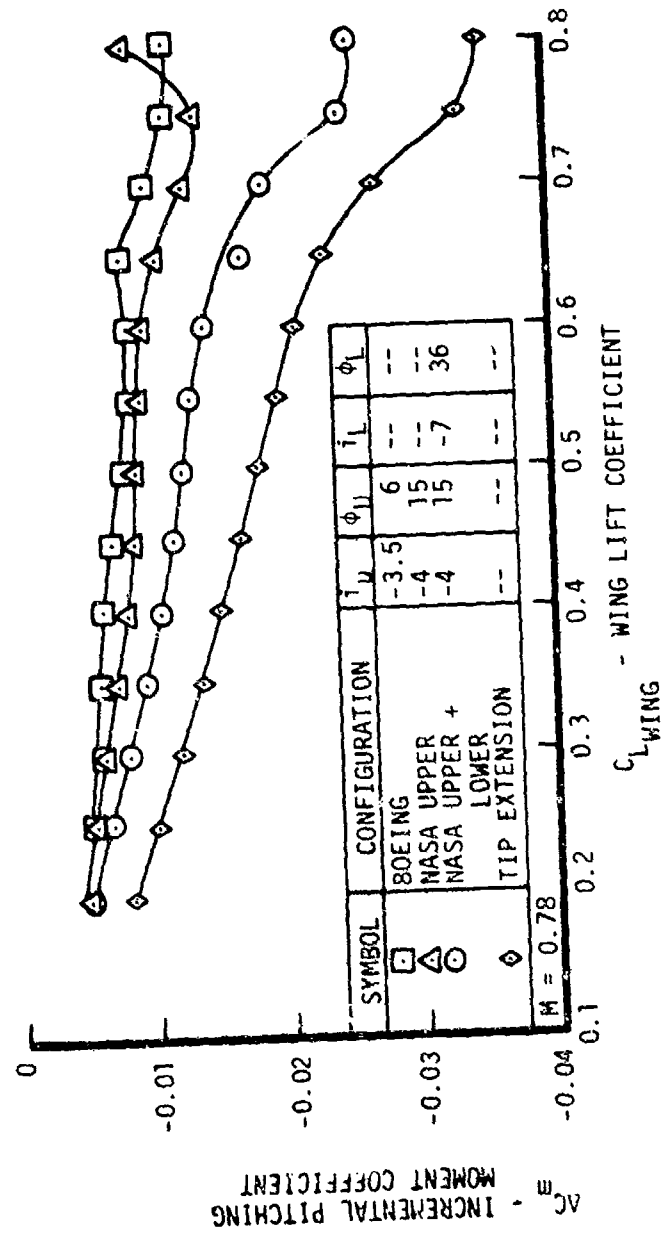
Figure 56. Comparison of Semispan KC-135A Model Pitching Moment with Winglets and Tip Extension. M = 0.78.

73
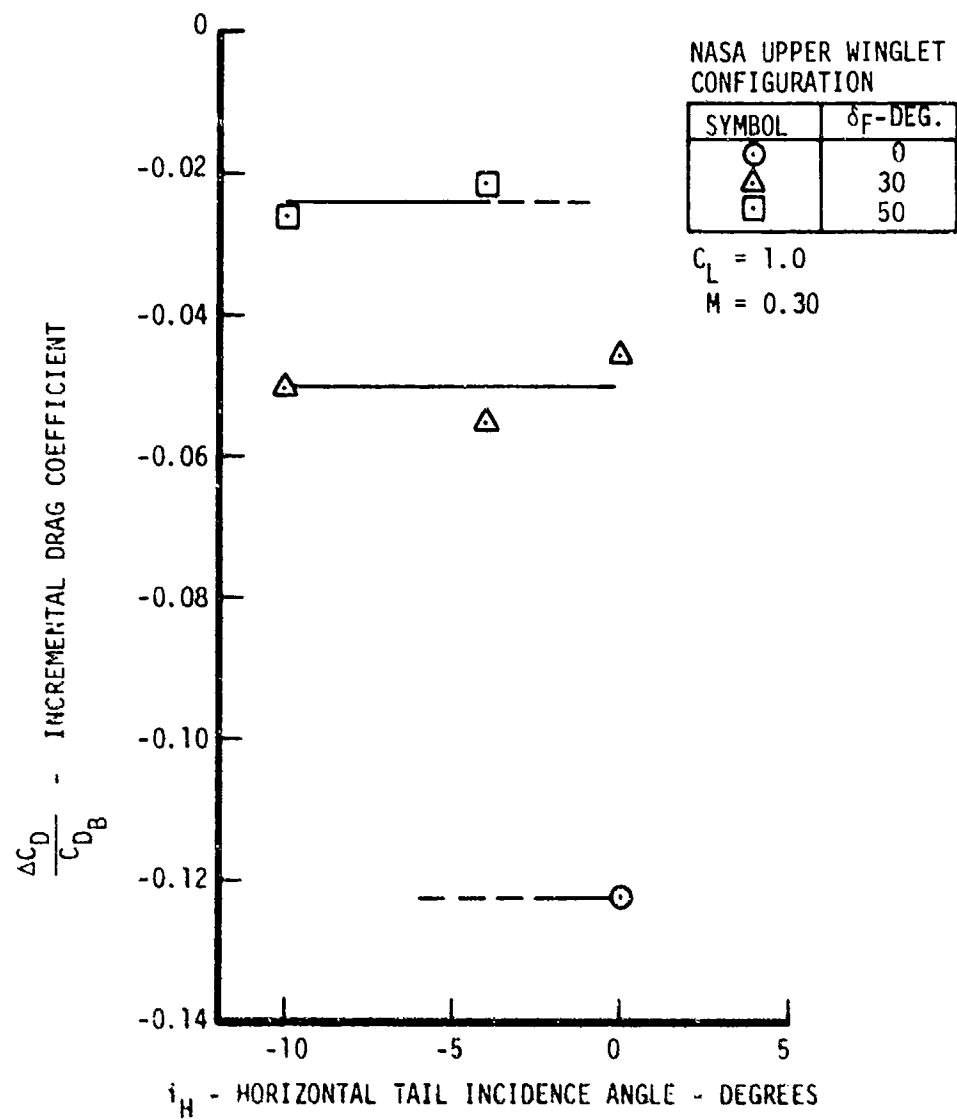
Figure 57.   Effect of Flap and Horizontal Tail Deflection on
KC-135A Model Drag.   M = 0.30. C_L = 1.0
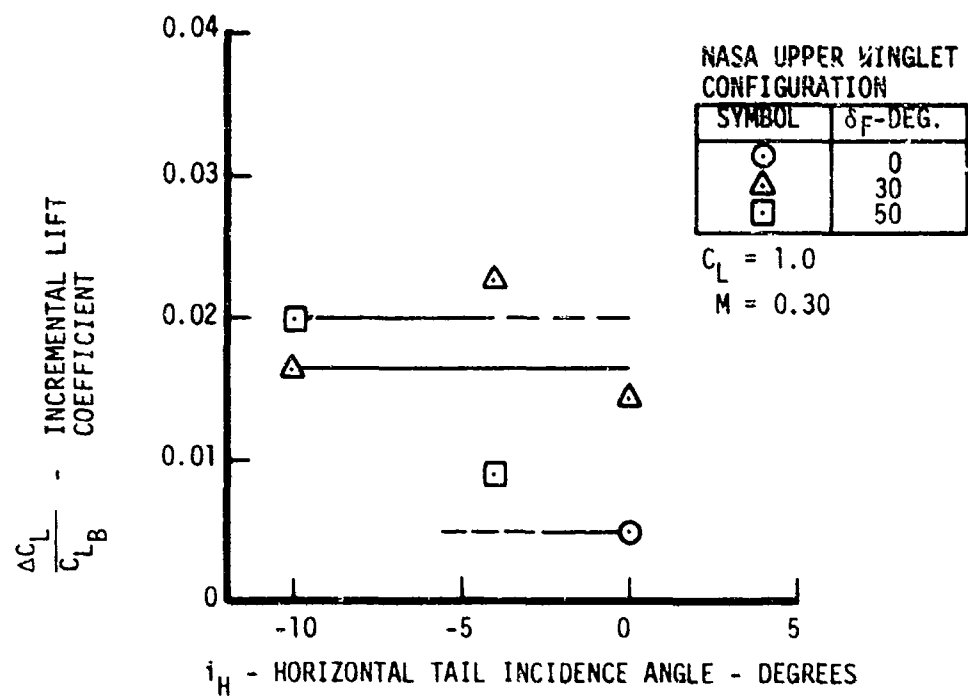
Figure 58. Effect of Flap and Horizontal Tail Deflection on
KC-135A Model Lift. M = 0.30. C_L = 1.0
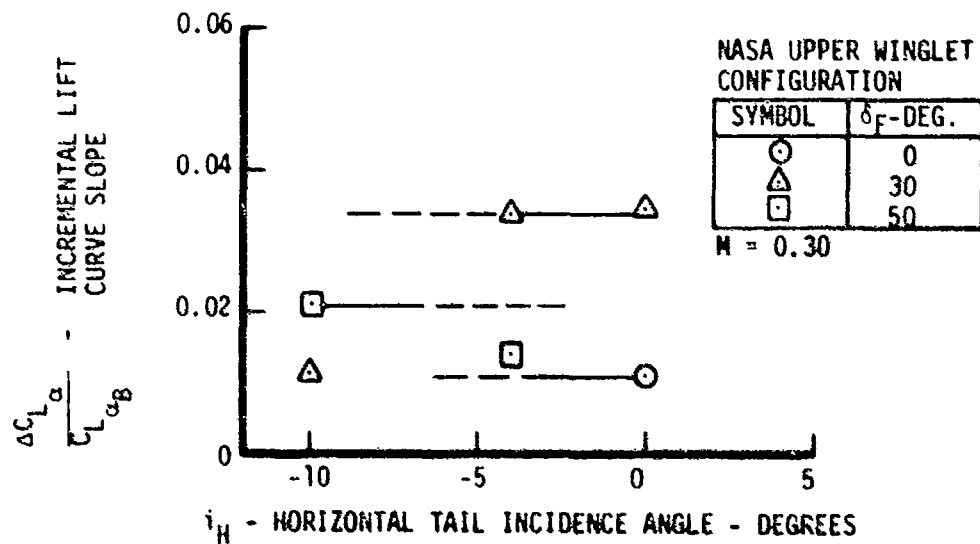
Figure 59. Effect of Flap and Horizontal Tail Deflection
on KC-135A Model Lift Curve Slope. M = 0.30
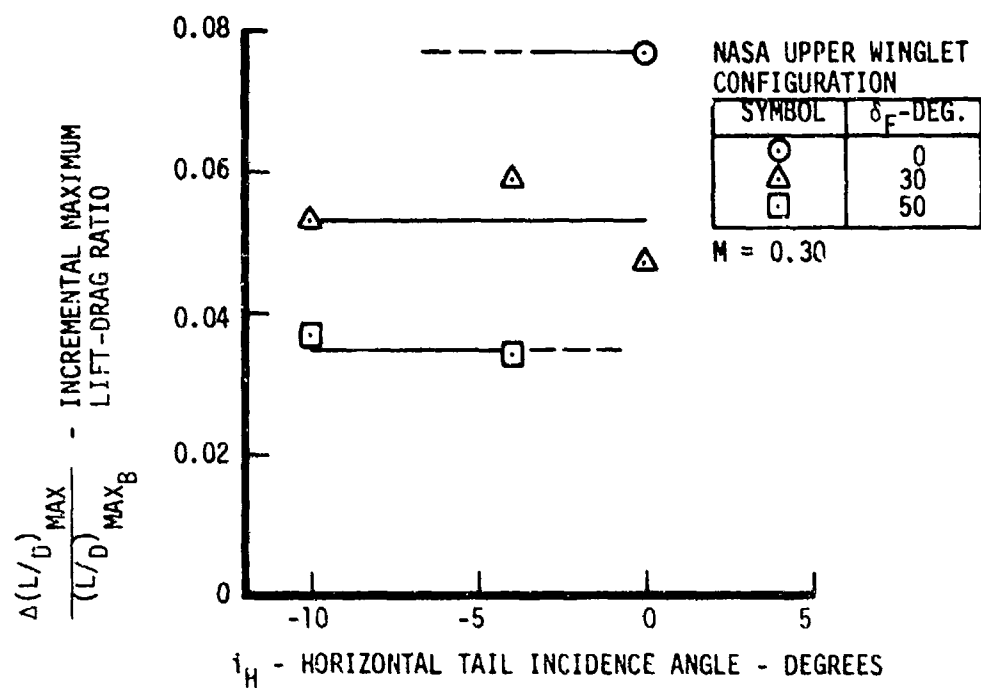
Figure 60.   Effect of Flap and Horizontal Tail Deflection
on KC-135A Model Lift-Drag Ratio.   M = 0.30
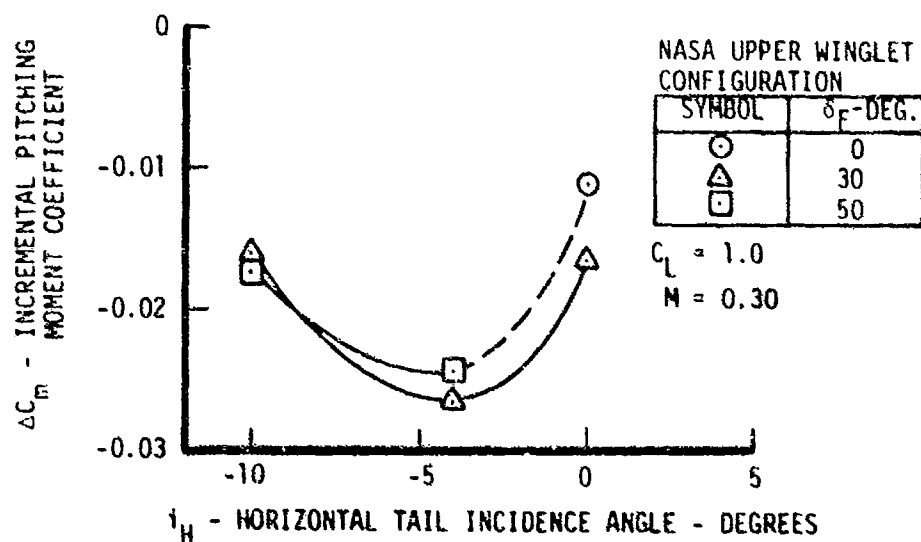
Figure 61.   Effect of Flap and Horizontal Tail Deflection
on KC-135A Model Pitching Moment.   M = 0.30.
C_L = 1.0

Figure 62. Effect of Winglet Configuration on Full-Span
KC-135A Model Yawing Moment. M = 0.30.
δ_F = 50 Degrees. i_H = -10 Degrees

Figure 63. Effect of Winglet Configuration on Full-Span
KC-135A Model Rolling Moment. M = 0.30.
δ_F = 50 Degrees. i_H = -10 Degrees

Figure 64. Effect of Aileron Deflection on Rolling Moment
M = 0.30. δ_F = 30 Degrees. i_H = -10 Degrees
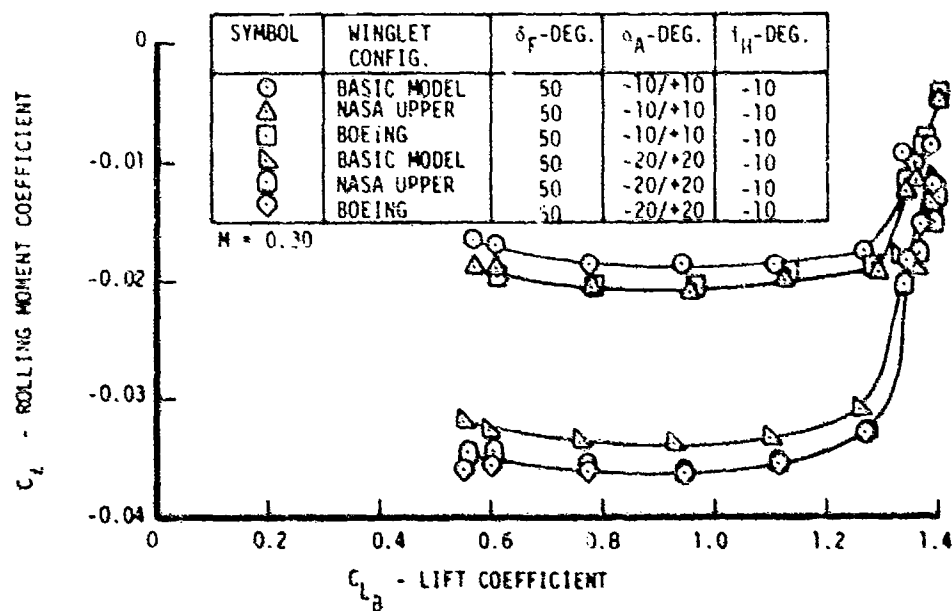
Figure 65. Effect of Aileron Deflection on Rolling Moment
M = 0.30. δ_F = 50 Degrees. i_H = -10 Degrees

SYMBOL	WINGLET CONFIG.	δ_F-DEG.	δ_A-DEG.	i_H-DEG.
⊙	BASIC MODEL	30	-10/+10	-10
△	NASA UPPER	30	-10/+10	-10
◻	BOEING	30	-10/+10	-10

M = 0.30

Figure 66. Effect of Aileron Deflection on Yawing Moment
M = 0.30. δ_F = 30 Degrees. i_H = -10 Degrees
δ_A = -10/+10 Degrees

SYMBOL	WINGLET CONFIG.	δ_F-DEG.	δ_A-DEG.	i_H-DEG.
⊙	BASIC MODEL	30	-20/+20	-10
△	NASA UPPER	30	-20/+20	-10
◻	BOEING	30	-20/+20	-10
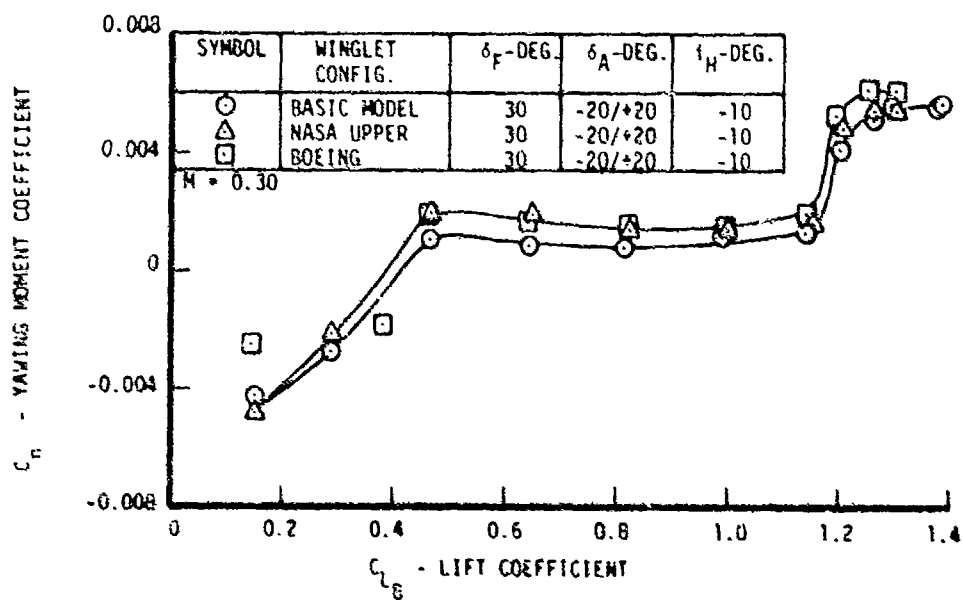
M = 0.30

Figure 67. Effect of Aileron Deflection on Yawing Moment.
M = 0.30. δ_F = 30 Degrees. i_H = -10 Degrees.
δ_A = -20/20 Degrees

79
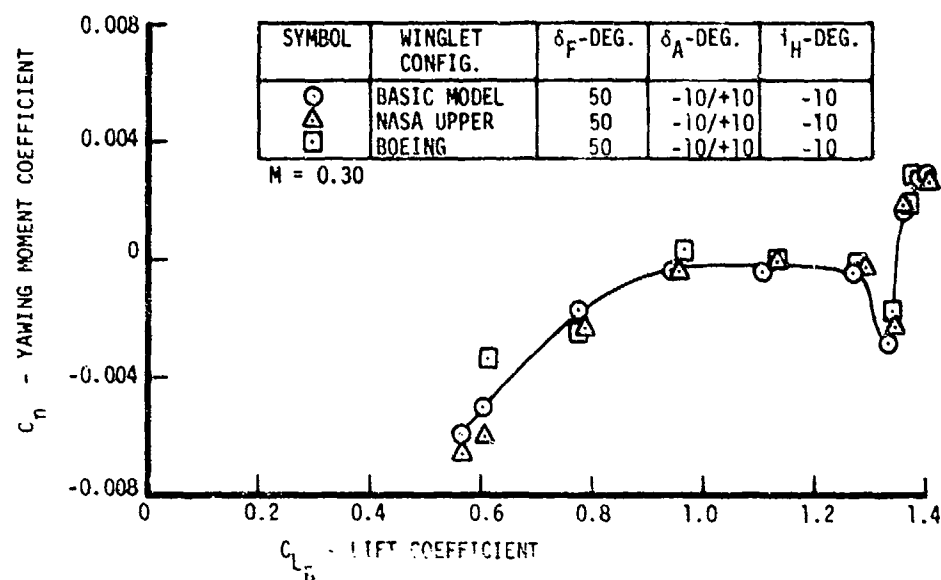
Figure 68. Effect of Aileron Deflection on Yawing Moment.
M = 0.30. δ_F = 50 Degrees. i_H = -10 Degrees.
δ_A = -10/10 Degrees

Figure 69. Effect of Aileron Deflection on Yawing Moment.
M = 0.30. δ_F = 50 Degrees. i_H = -10 Degrees.
δ_A = -20/+20 Degrees

Figure 70. Effect of Winglet Loss on KC-135A Model Yawing Moment. $M = 0.30$. $\delta_F = 50$ Degrees. $i_H = -10$ Degrees
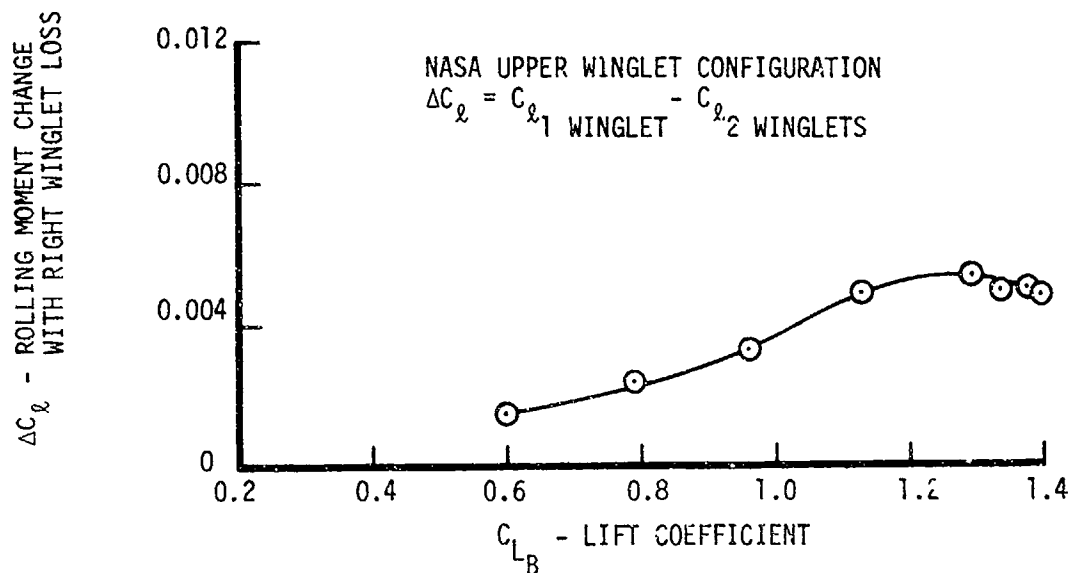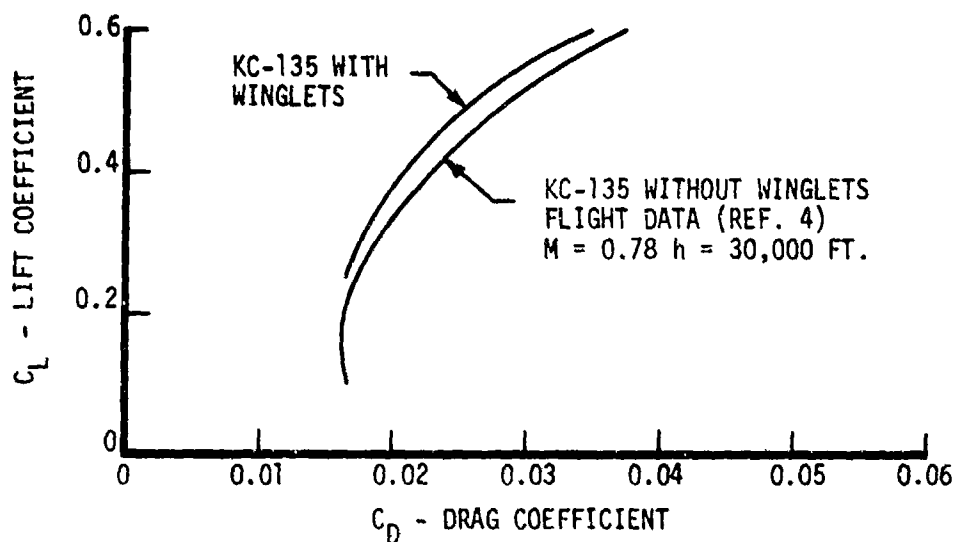
Figure 71. Effect of Winglet Loss on KC-135A Model Rolling
Moment. M = 0.30. δ_F = 50 Degrees. i_H = -10
Degrees
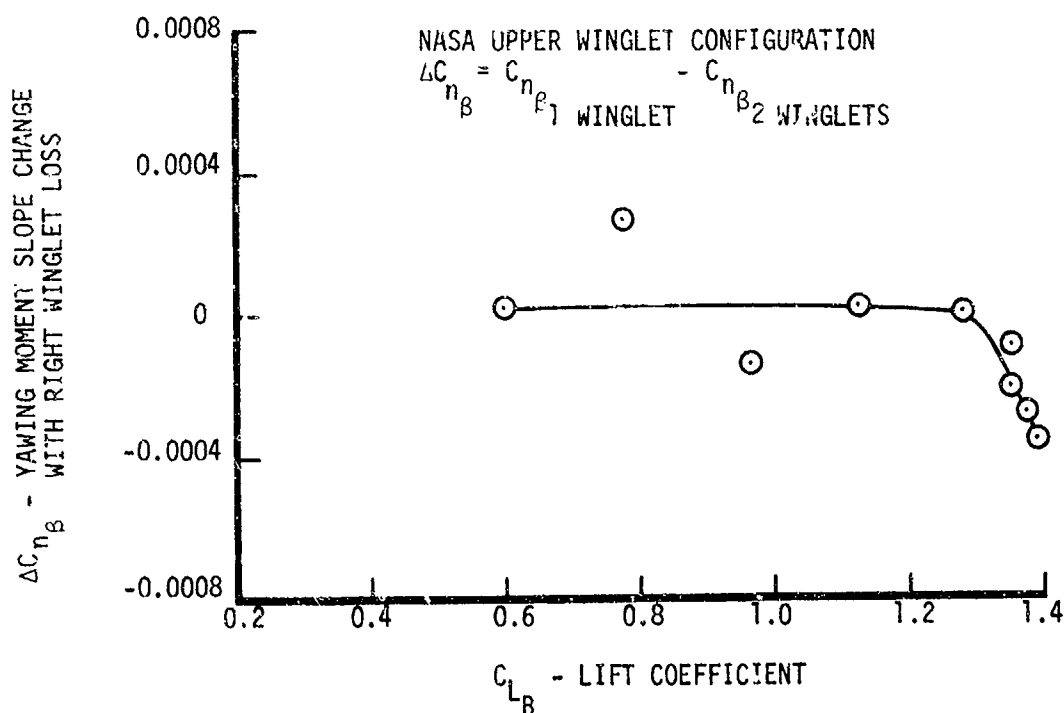
Figure 72. Effect of Winglet Loss on KC-135A Model Yawing
Moment Slope. M = 0.30. δ_F = 50 Degrees.
i_H = -10 Degrees
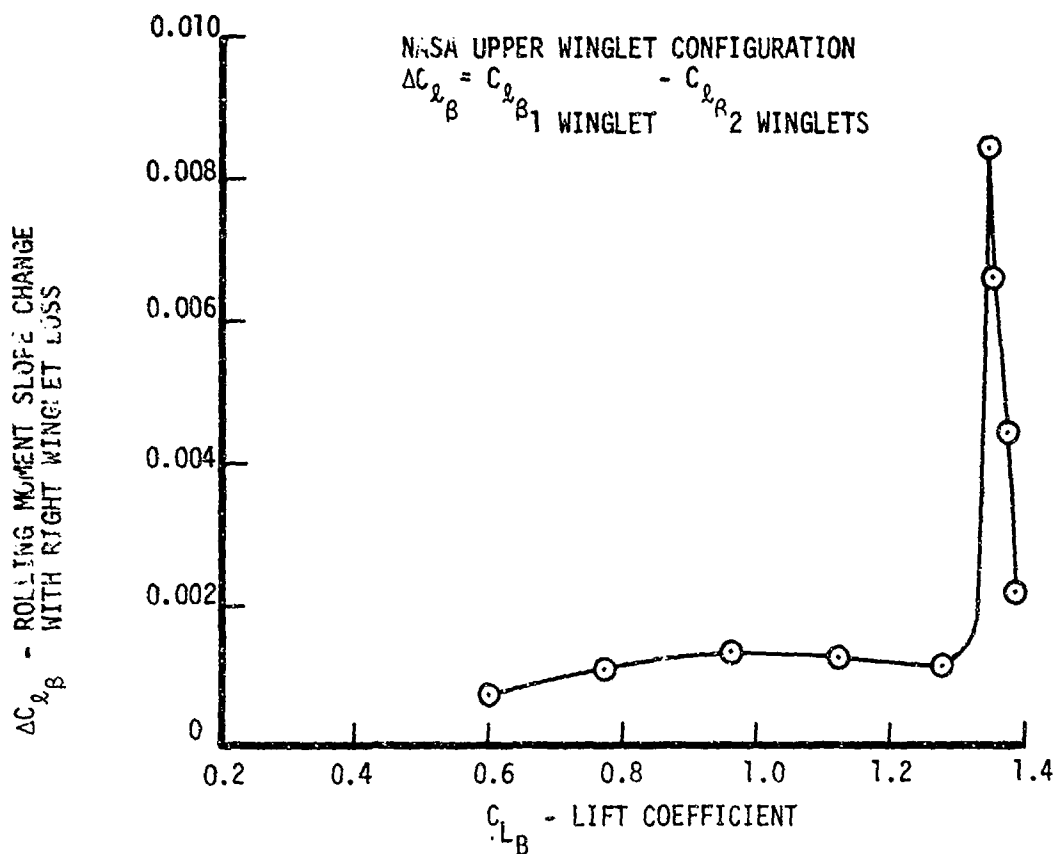
Figure 73. Effect of Winglet Loss on KC-135A Model Rolling Moment Slope. M = 0.30. δ_F = 50 Degrees. i_H = -10 Degrees
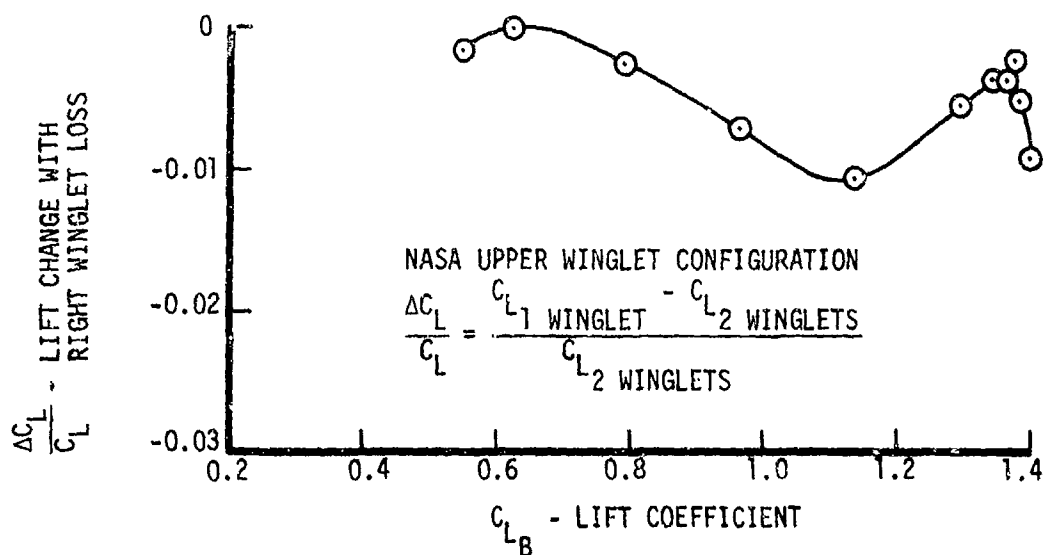
Figure 74. Effect of Winglet Loss on KC-135A Model Lift M = 0.30. δ_F = 50 Degrees. i_H = -10 Degrees
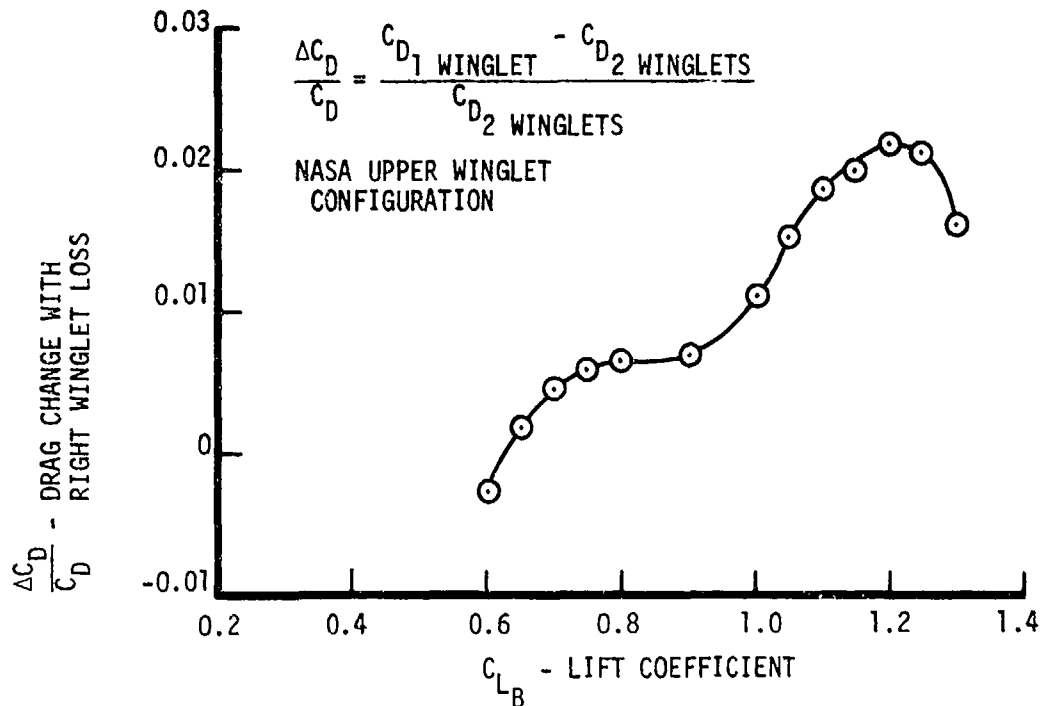
Figure 75. Effect of Winglet Loss on KC-135A Model Drag
M = 0.30. δ_F = 50 Degrees. i_H = -10 Degrees
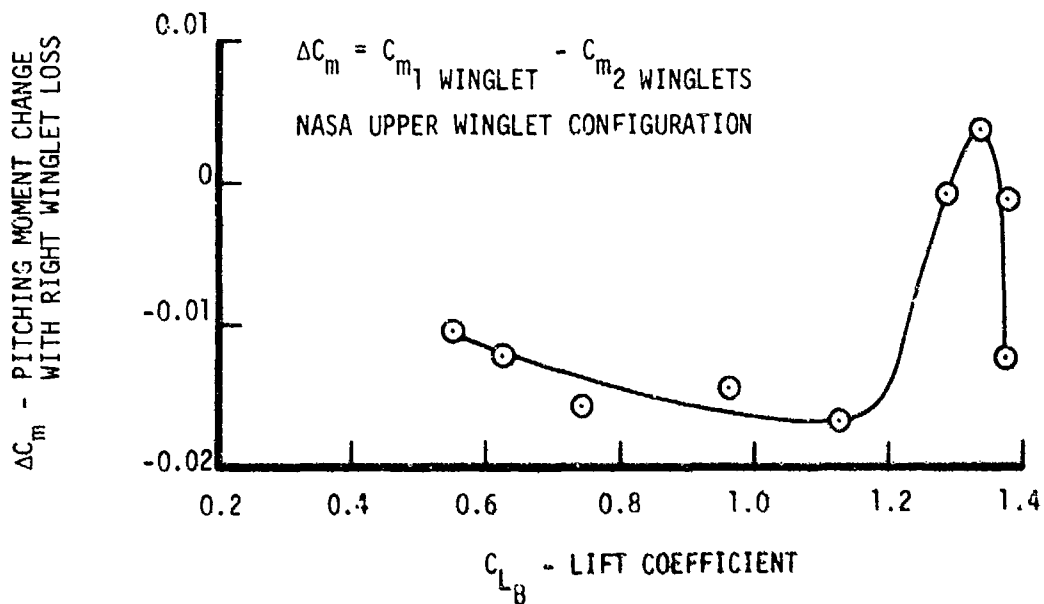
Figure 76. Effect of Winglet Loss on KC-135A Model
Pitching Moment. M = 0.30. δ_F = 50 Degrees.
i_H = -10 Degrees

Figure 77. Effect of Winglets on KC-135A Aircraft Drag
at Cruise Flight Conditions
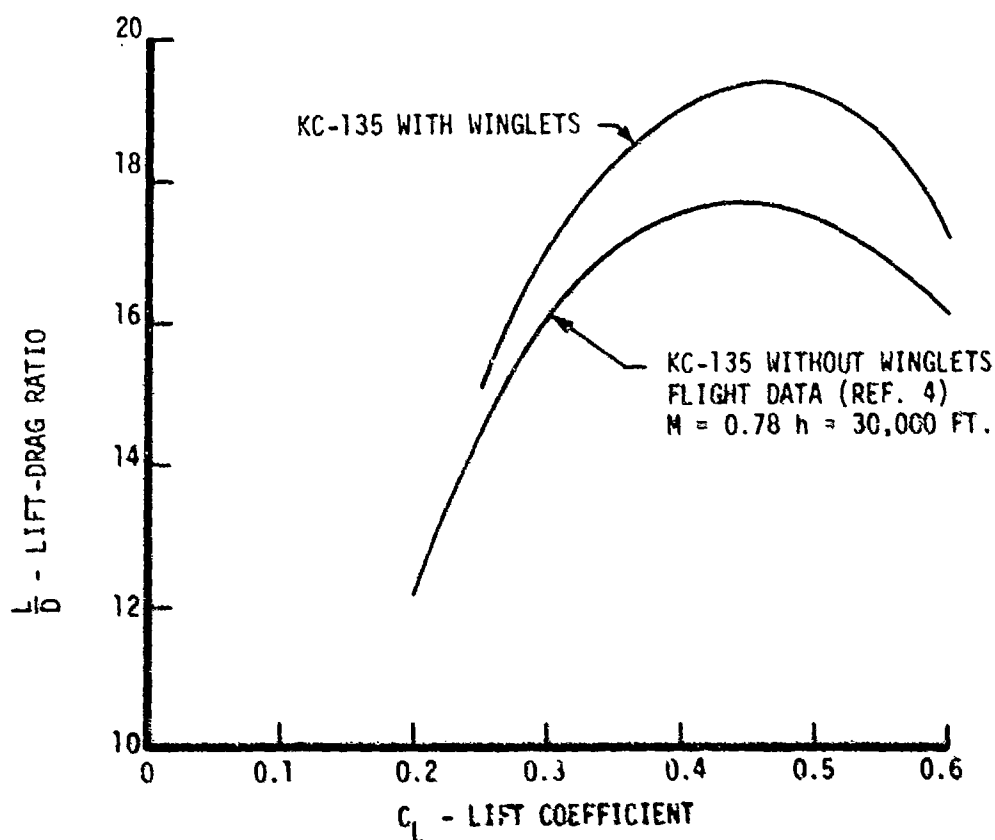
Figure 78. Effect of Winglets on KC-135A Aircraft Lift-
Drag Ratio at Cruise Flight Conditions
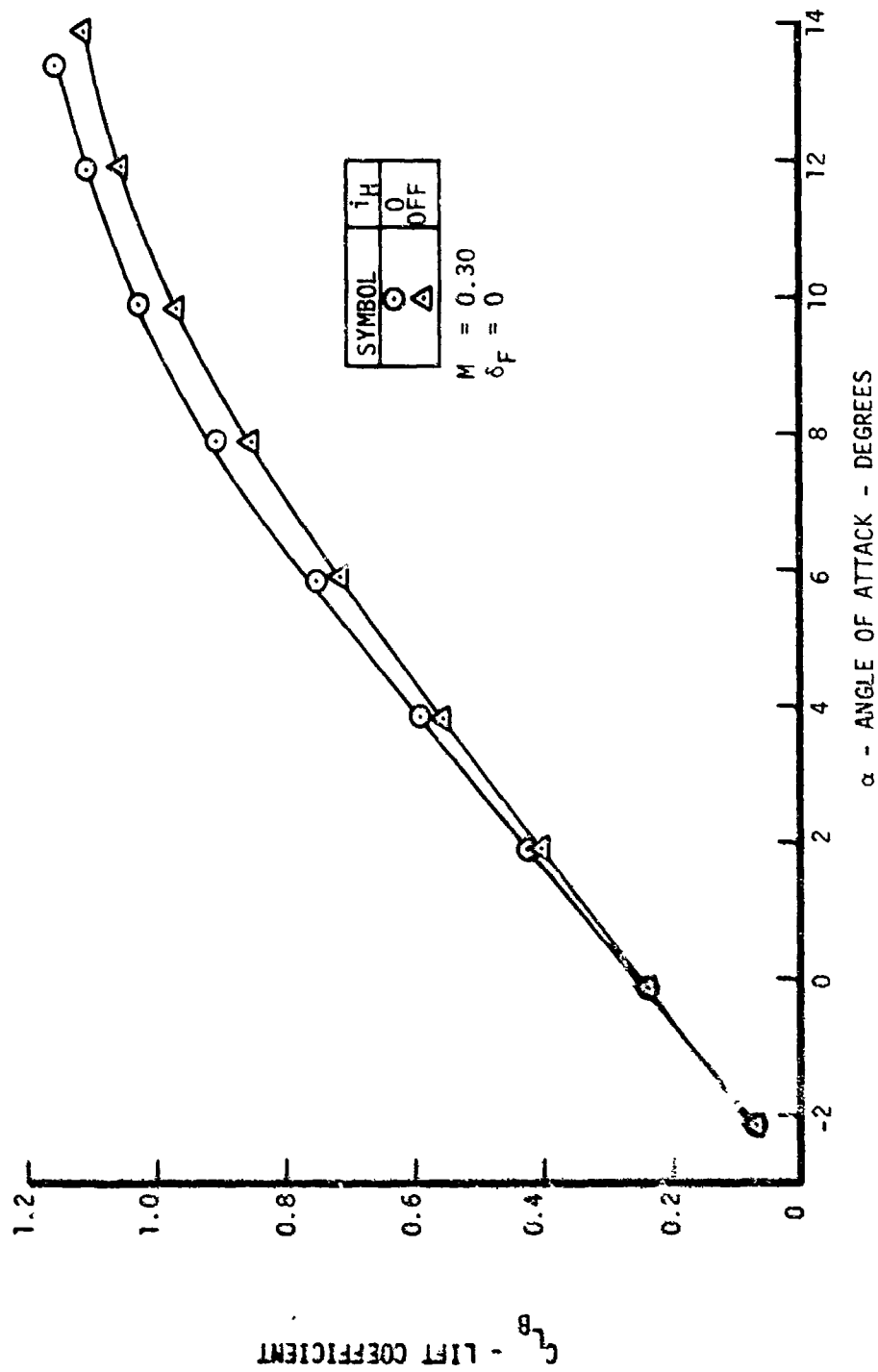
Figure 79. Variation of Lift of Basic KC-135A Model with Angle of Attack. M = 0.30. $\delta_F = 0$
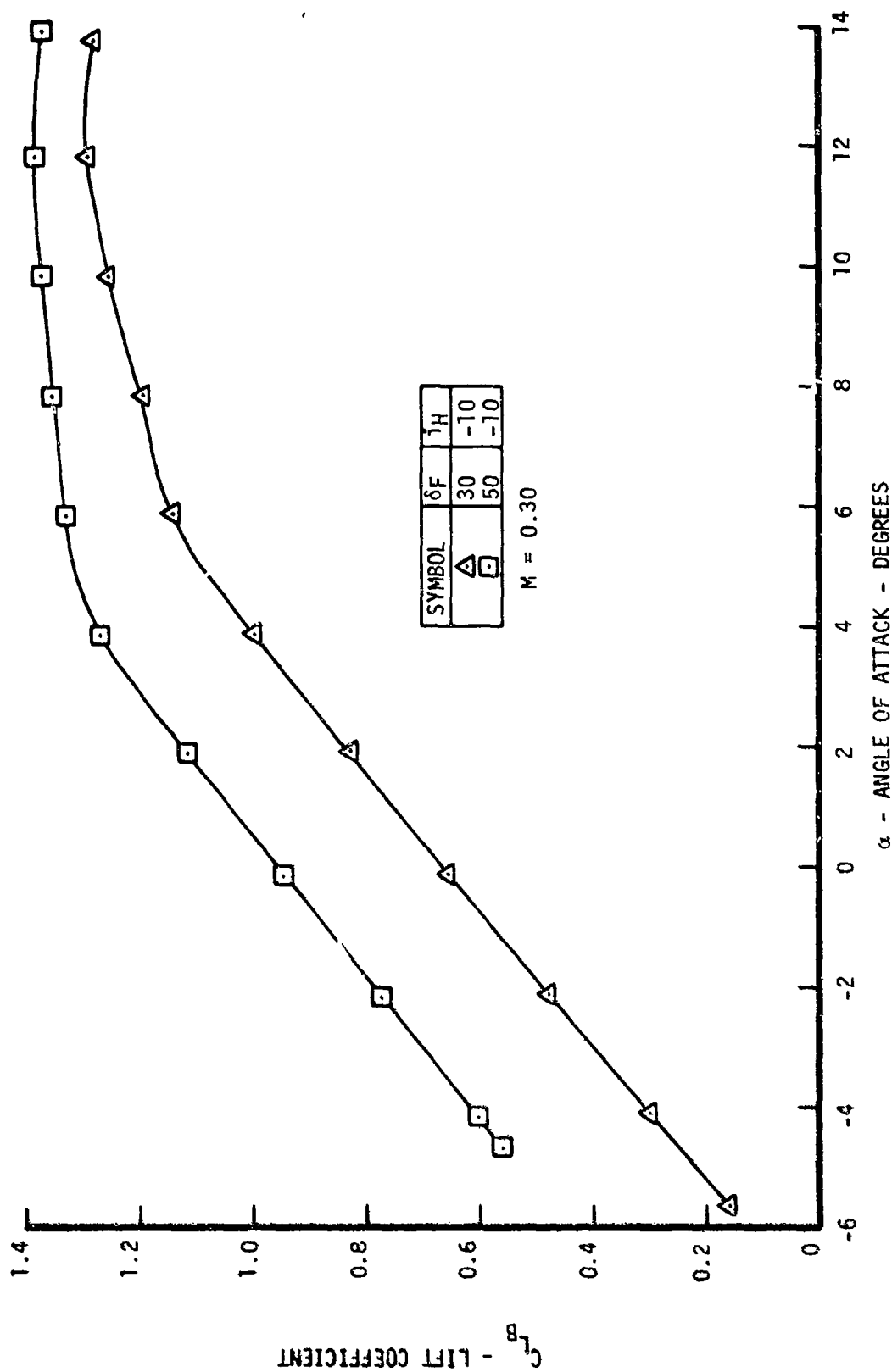
Figure 80. Variation of Lift of Basic KC-135A Model with Angle of Attack and Flap Deflection. M = 0.30. i_H = -10 Degrees
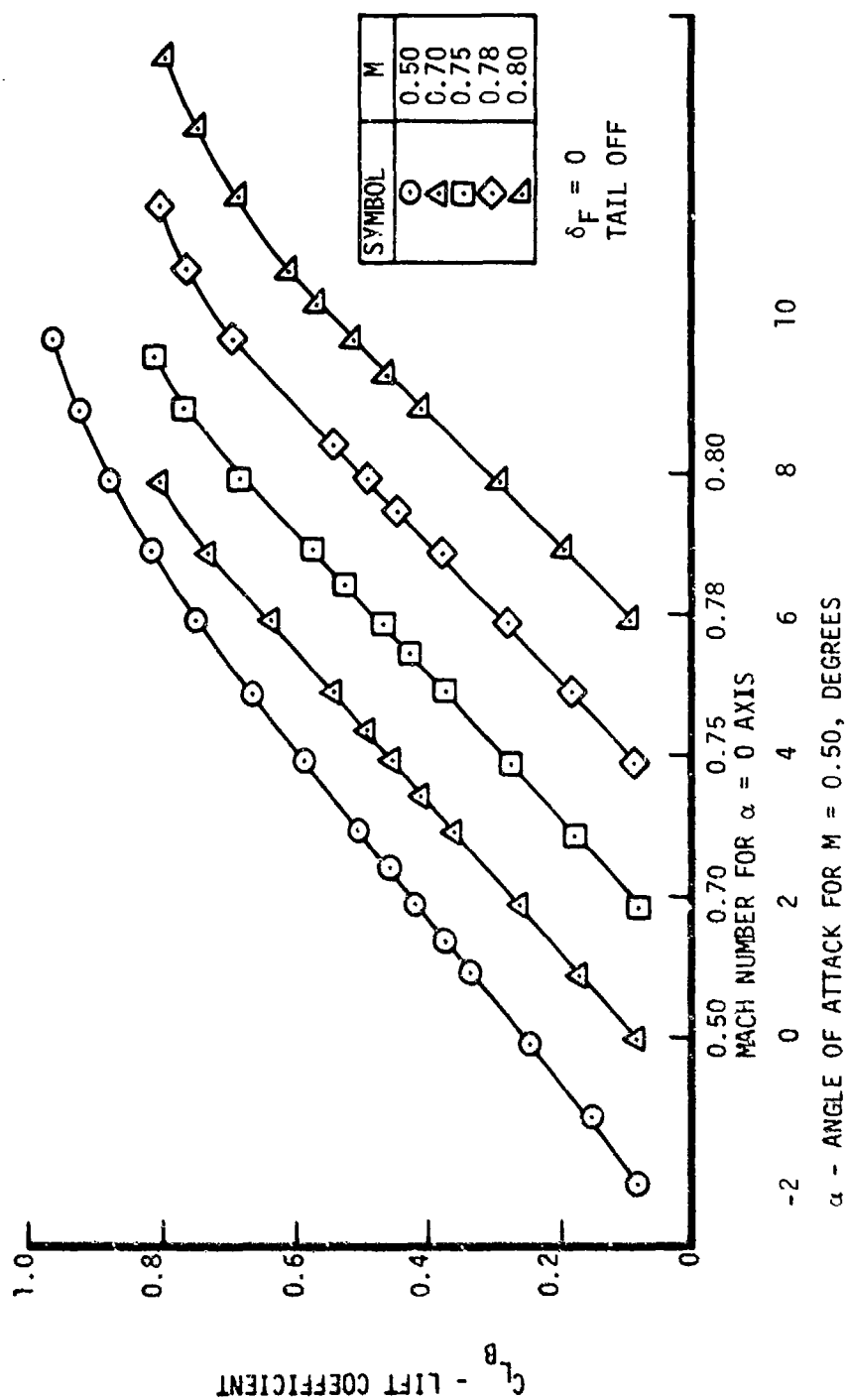
Figure 81. Variation of Lift of Basic KC-135A Model with Angle of Attack Near Cruise Conditions. $\delta_F = 0$
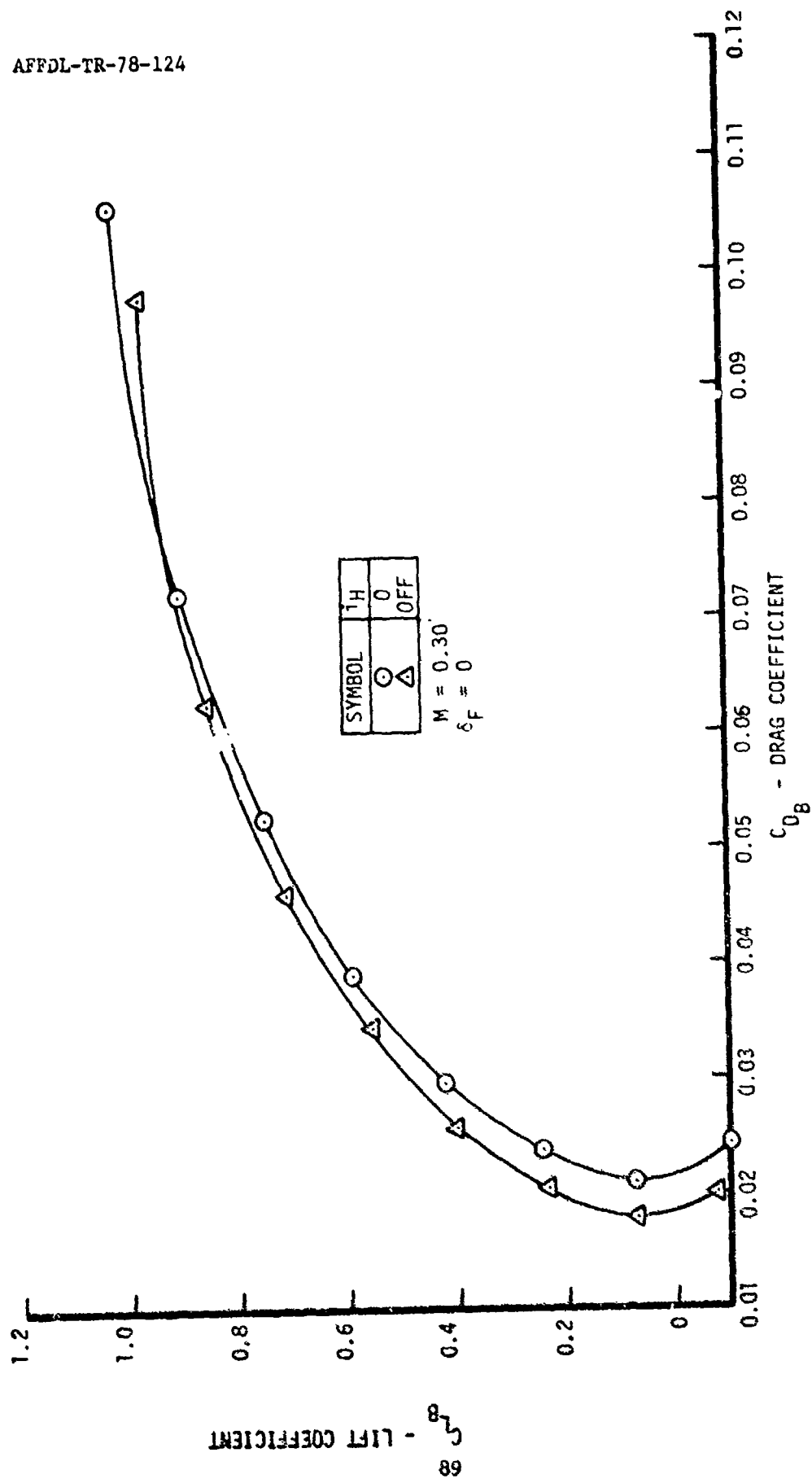
Figure 82. Variation of Drag of Basic KC-135A Model
with Lift. $M = 0.30$. $\delta_F = 0$

C_{D_B} - DRAG COEFFICIENT

M = 0.30

SYMBOL	δ_F	i_H
△	30	-10
⊡	50	-10
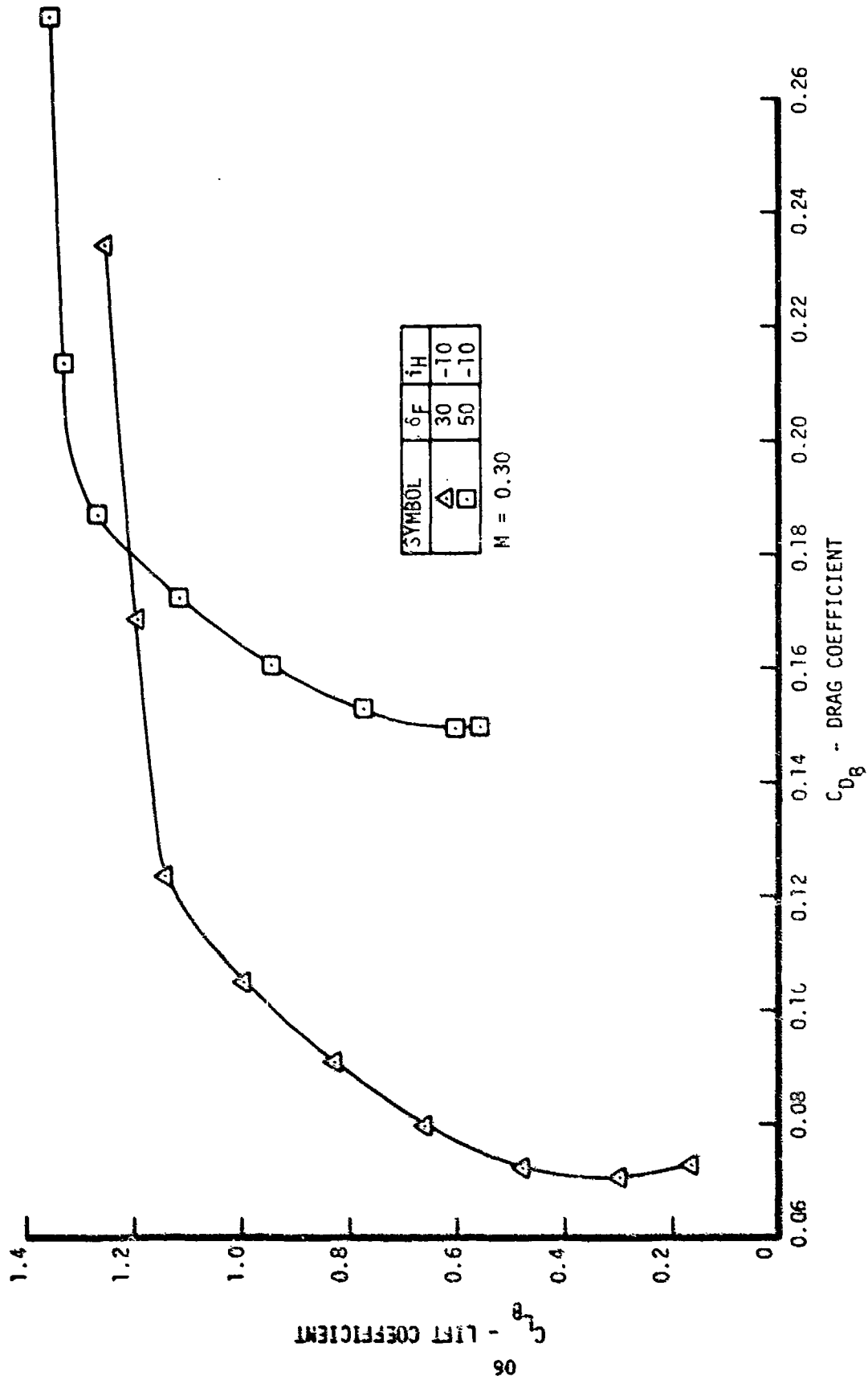
Figure 83. Variation of Drag of Basic KC-135A Model with
Lift and Flap Deflection. M = 0.30.
i_H = -10 Degrees

C_{L_B} - LIFT COEFFICIENT
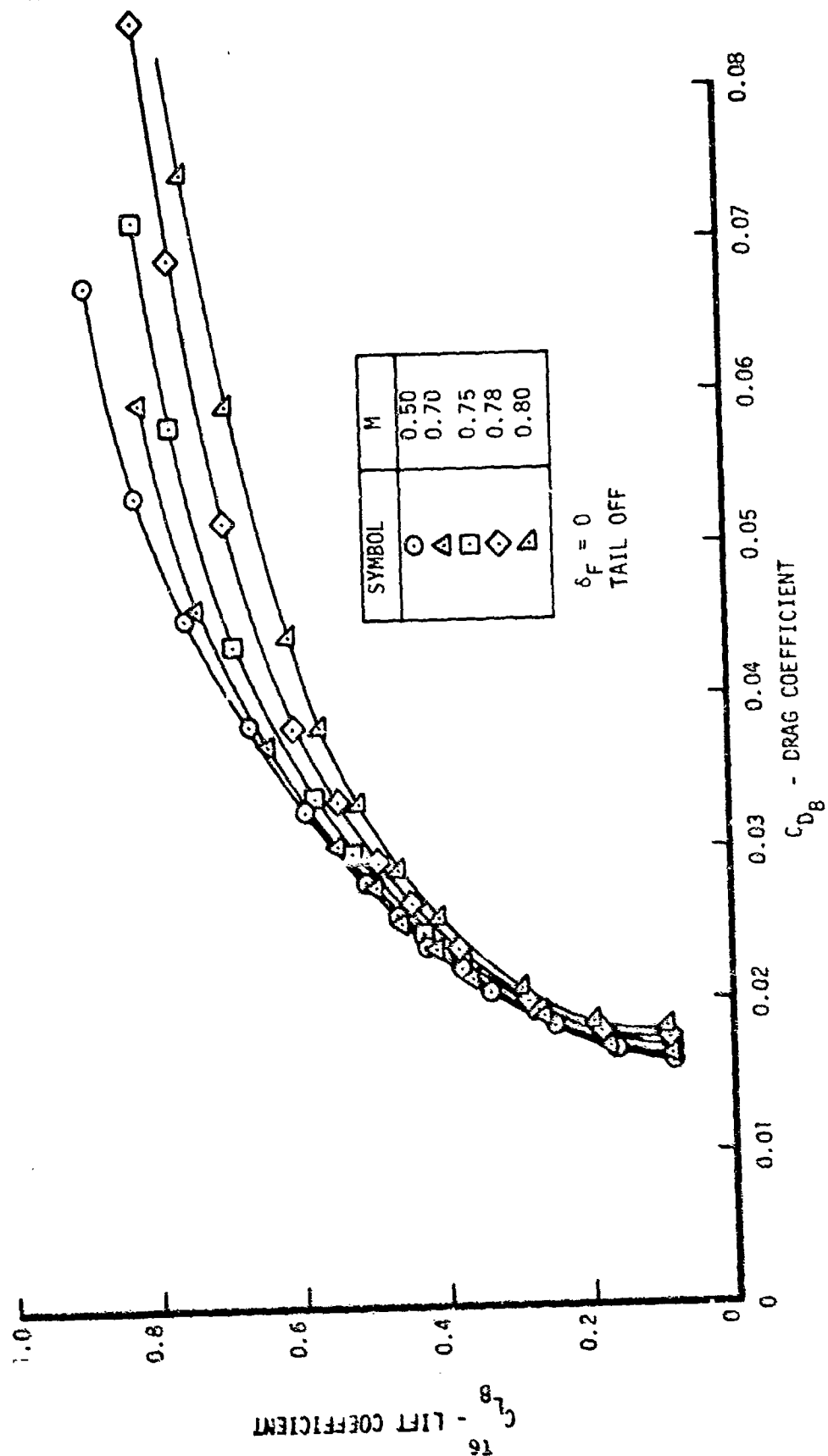
Figure 84. Variation of Drag of Basic KC-135A Model with Lift Near Cruise Condition. $\delta_F = 0$

SYMBOL	M
⊙	0.50
△	0.70
⊡	0.75
◇	0.78
△	0.80

$\delta_F = 0$
TAIL OFF

C_{D_B} - DRAG COEFFICIENT

C_{L_B} - LIFT COEFFICIENT
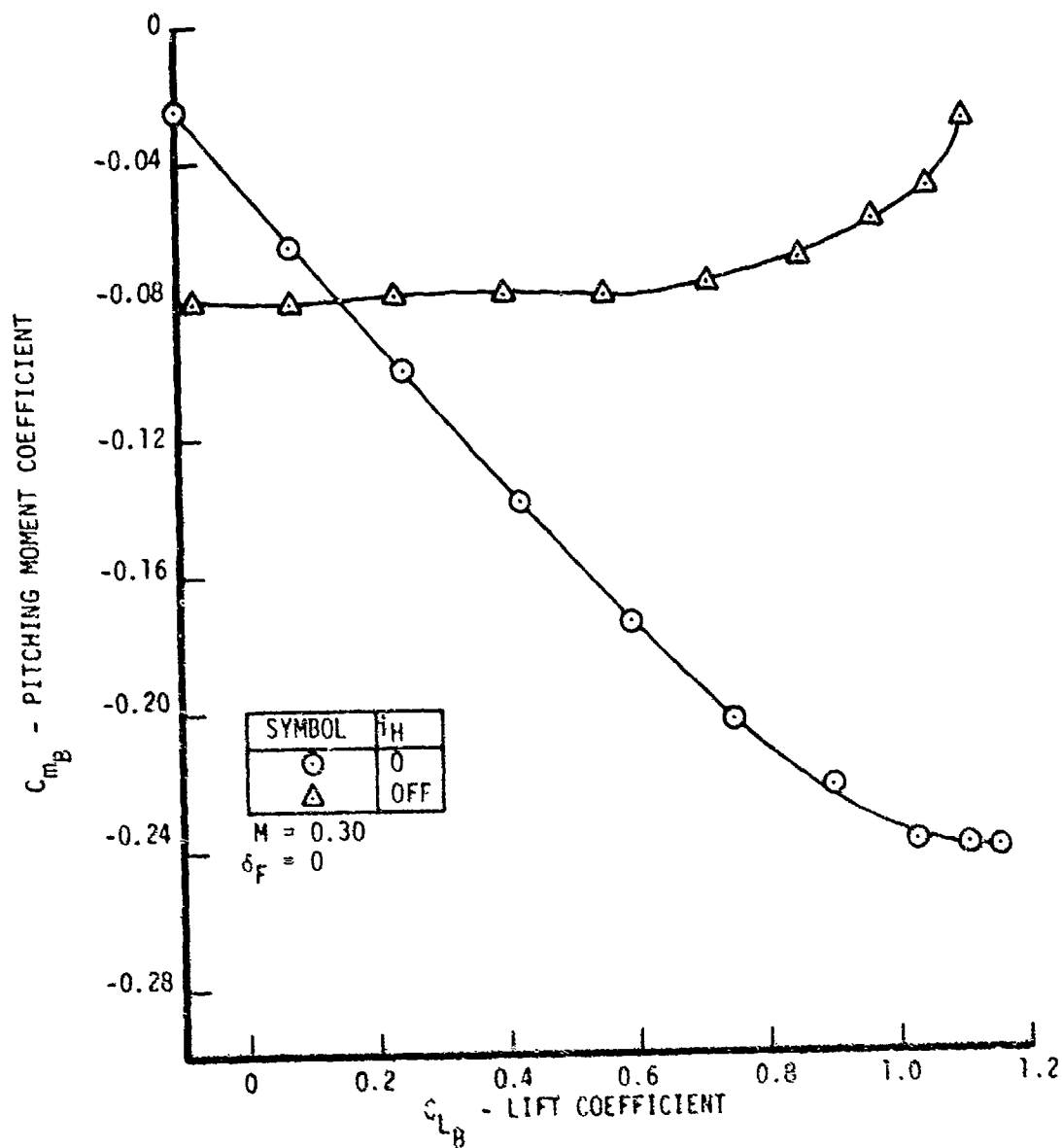
Figure 85. Variation of Pitching Moment of Basic KC-135A
Model with Lift. $M = 0.30$. $\delta_F = 0$
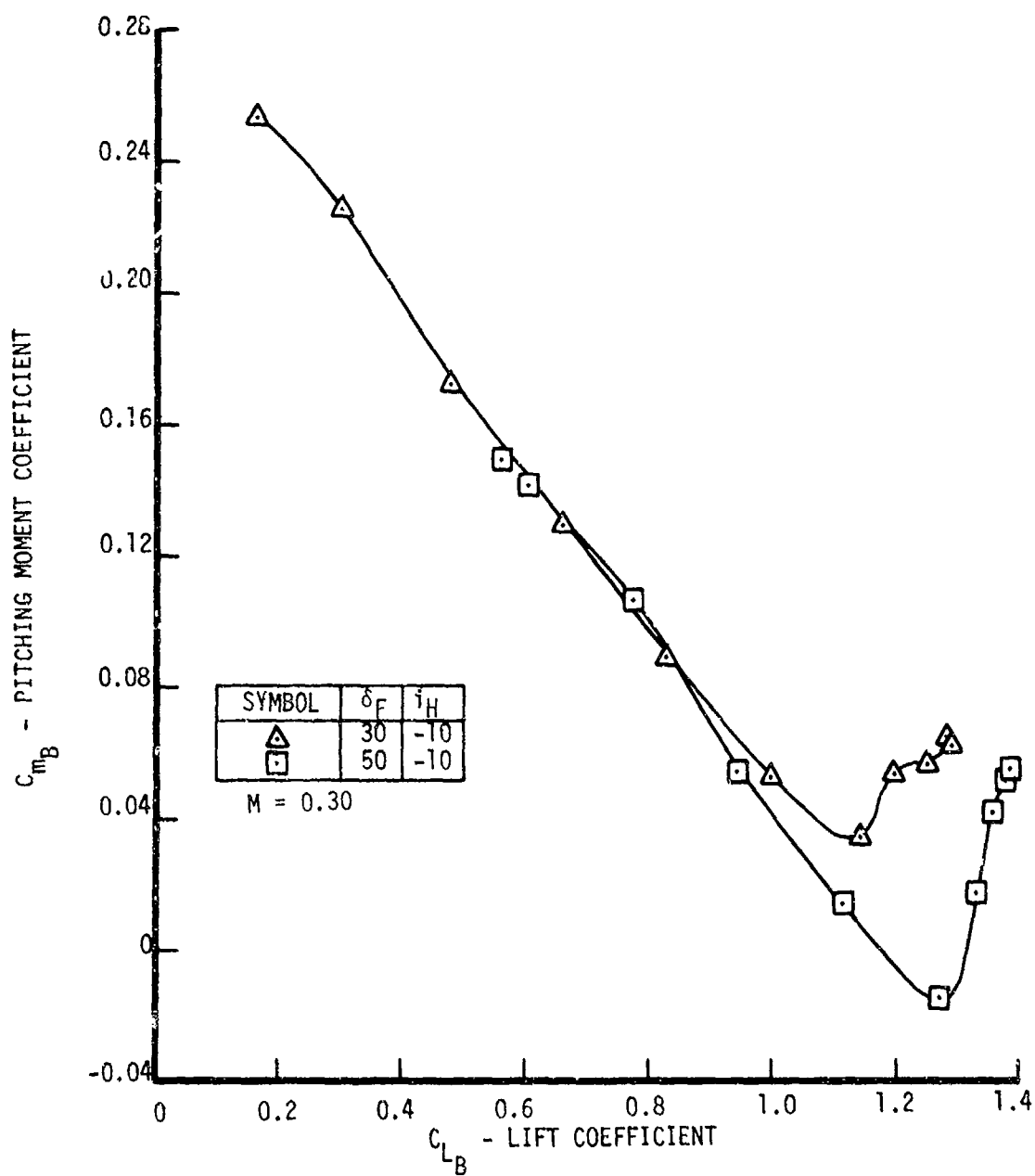
Figure 86. Variation of Pitching Moment of Basic KC-135A
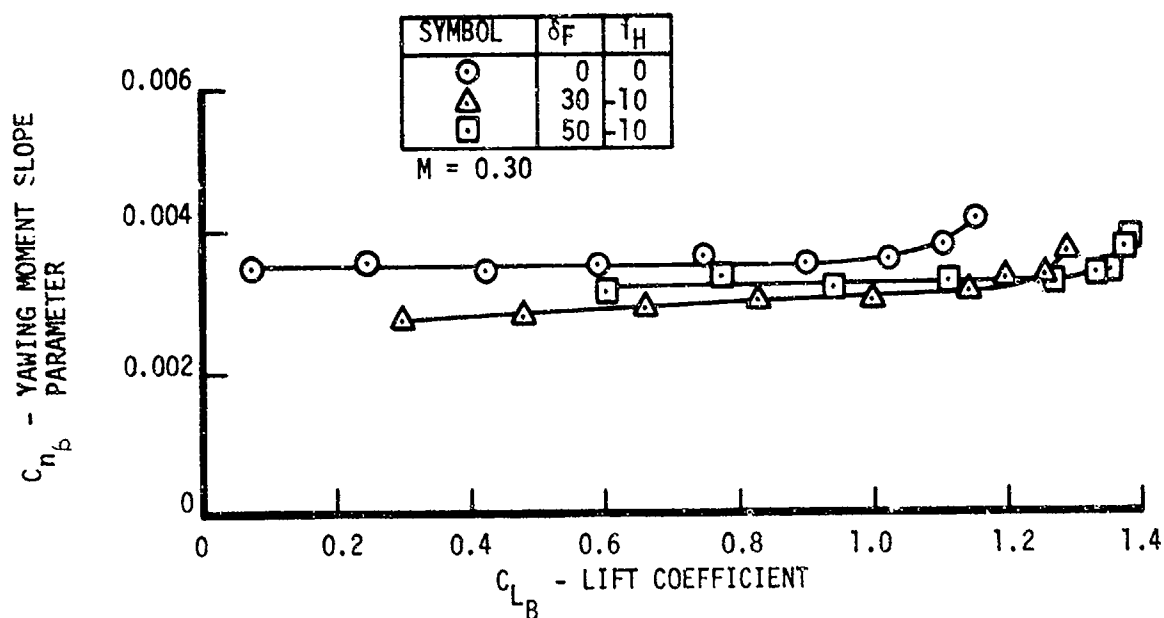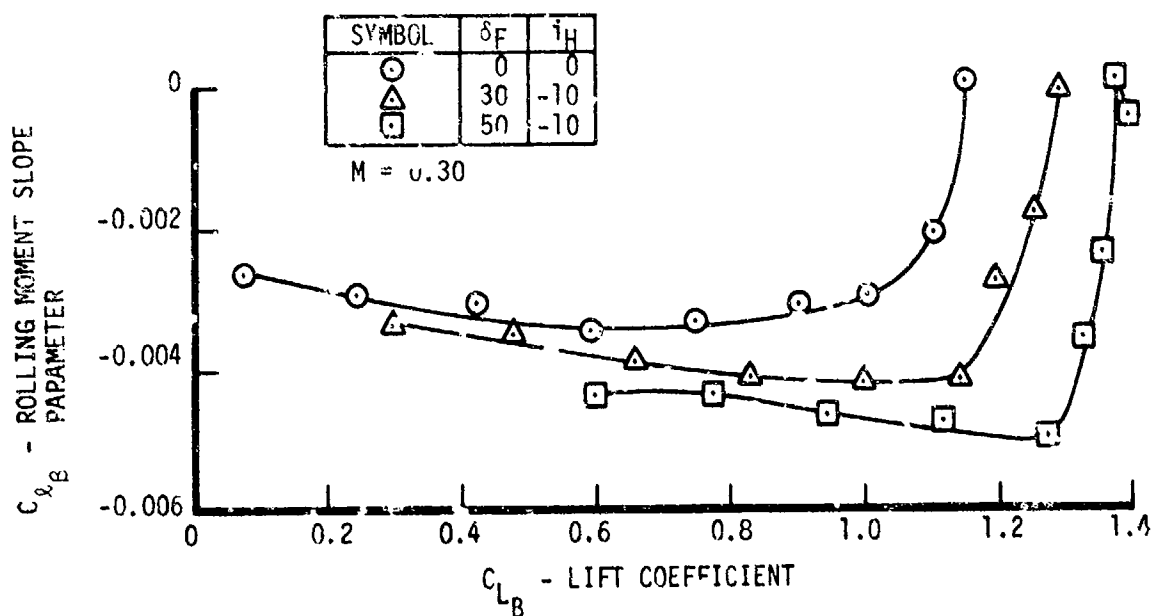Model with Lift and Flap Deflection. M = 0.30.
i_H = -10 Degrees

93
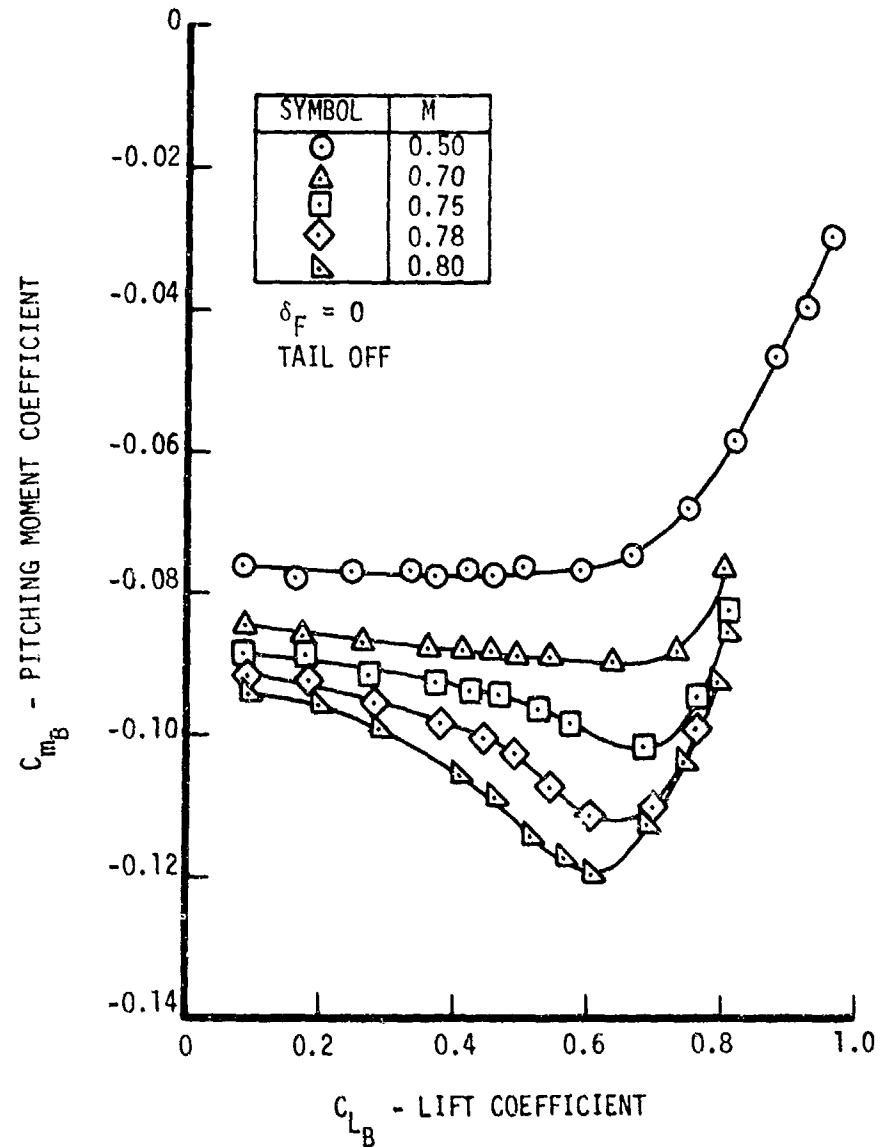
Figure 87. Variation of Pitching Moment of Basic KC-135A
Model with Lift Near Cruise Conditions. $\delta_F = 0$
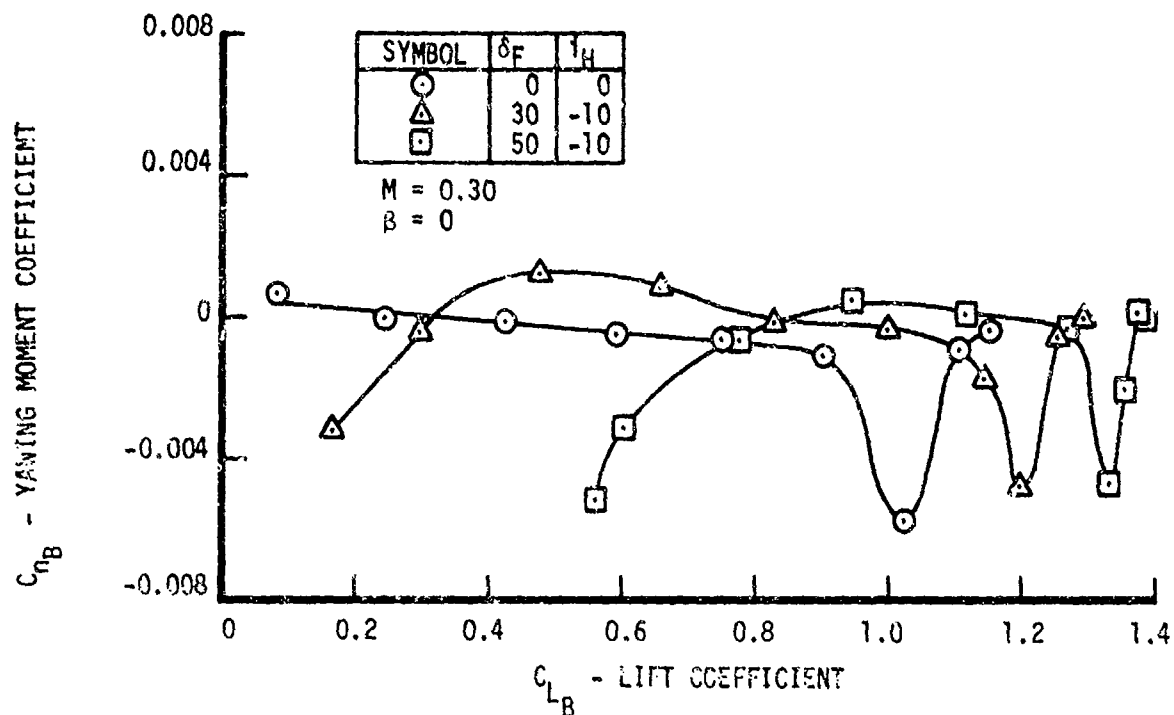
Figure 88.   Variation of Yawing Moment of Basic KC-135A
Model with Lift and Flap Deflection.   M = 0.30.
β = 0
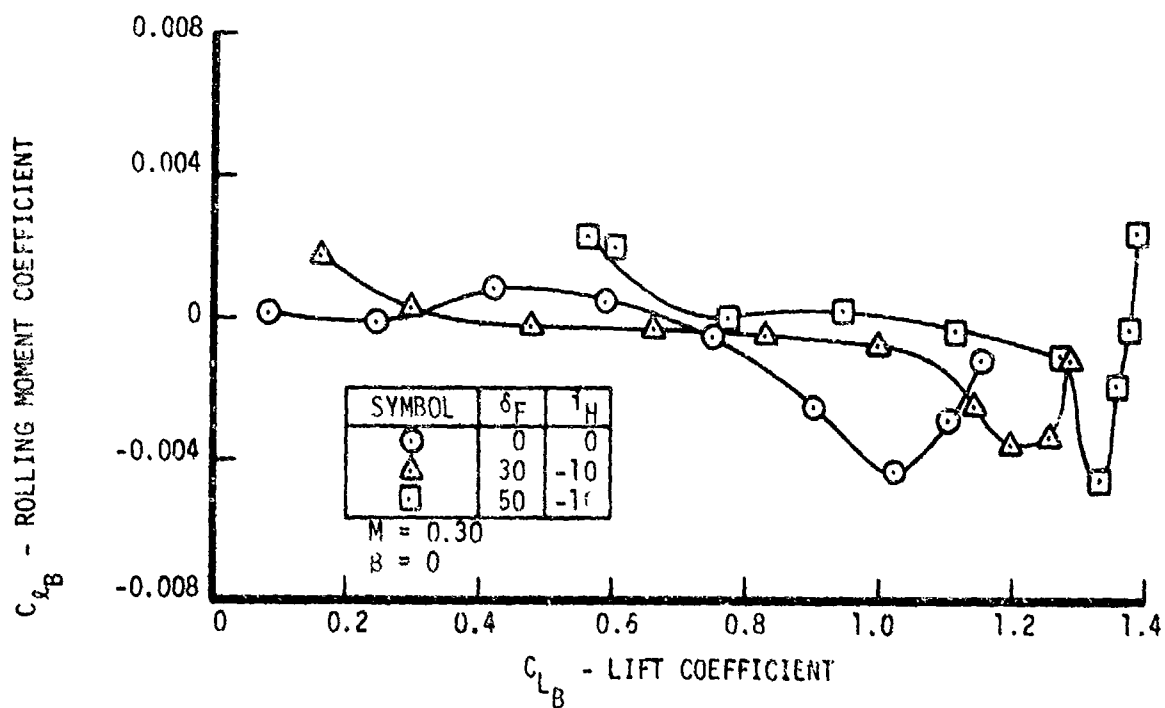
Figure 89.   Variation of Rolling Moment of Basic KC-135A
Model with Lift and Flap Deflection.   M = 0.30.
β = 0

Figure 90.   Variation of Yawing Moment Slope Parameter of
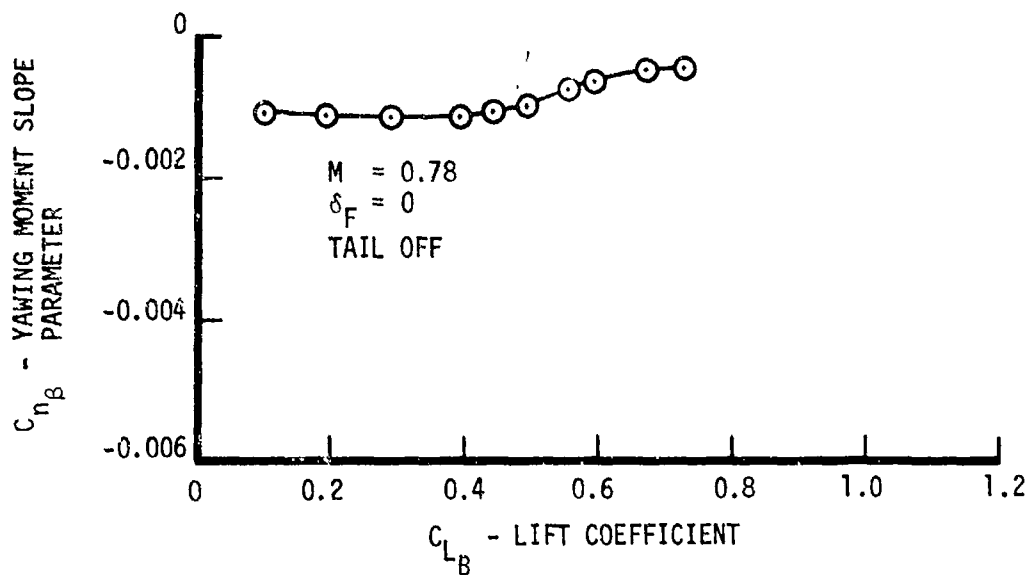Basic KC-135A Model with Lift and Flap Deflection.
M = 0.30

Figure 91.   Variation of Rolling Moment Slope Parameter of
Basic KC-135A Model with Lift and Flap Defection.
M = 0.30

Figure 92. Variation of Yawing Moment Slope Parameter of
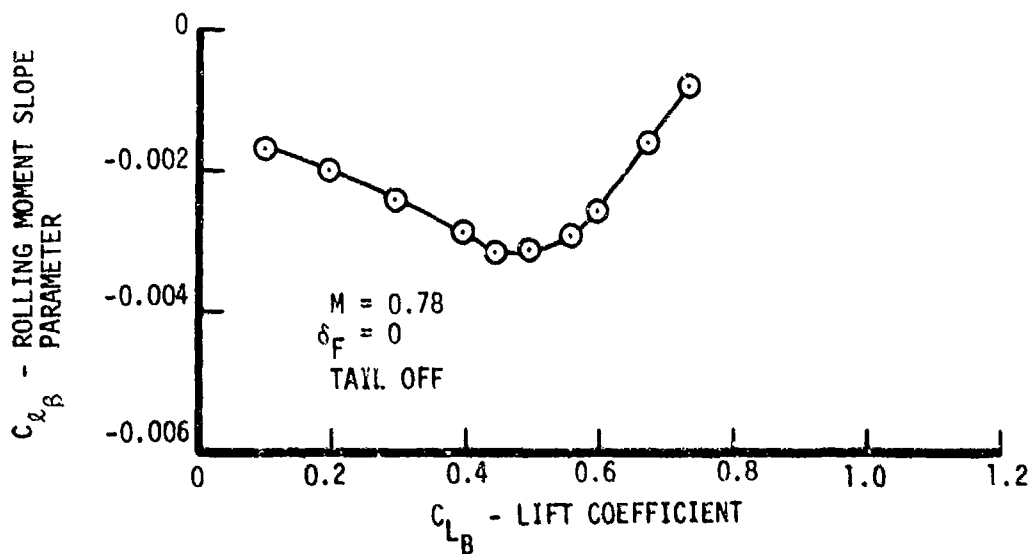Basic KC-135A Model with Lift Near Cruise
Conditions. $\delta_F = 0$

Figure 93. Variation of Rolling Moment Slope Parameter
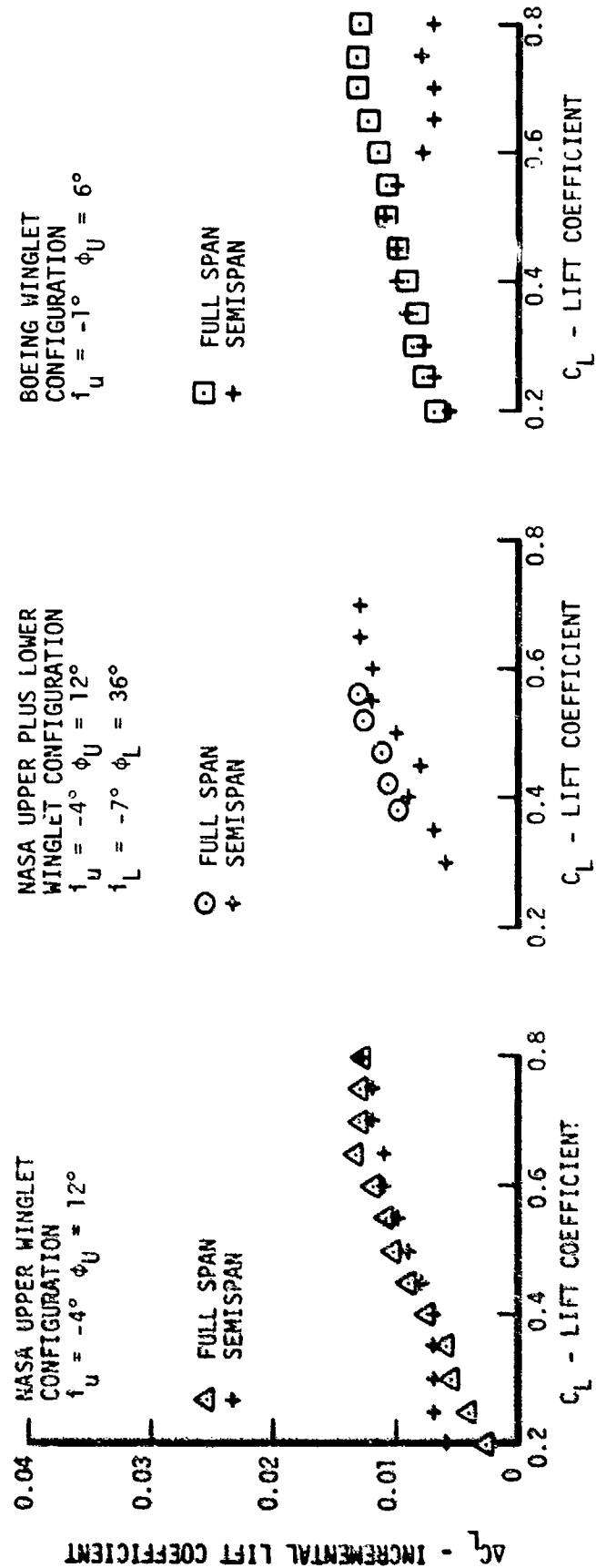of Basic KC-135A Model with Lift Near Cruise
Condition. $\delta_F = 0$

97

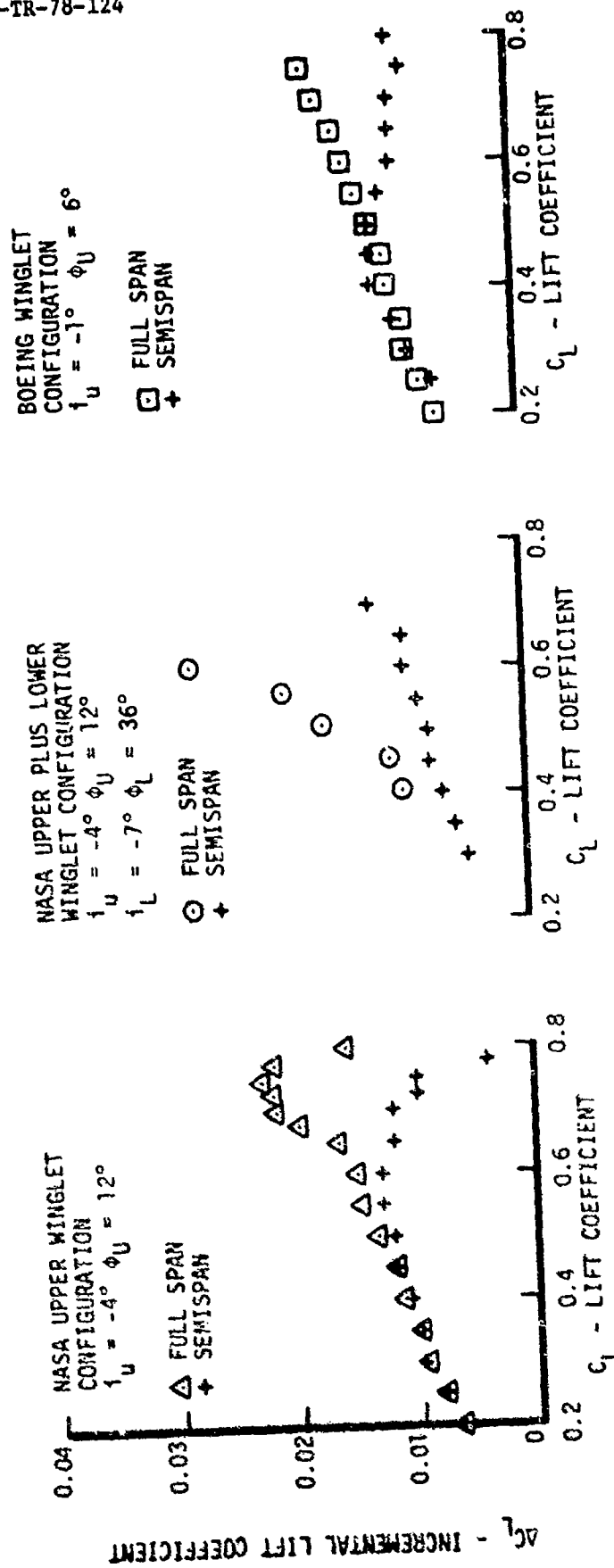Figure 94. Comparison of Full-Span and Semispan Model Incremental Lift. M = 0.70

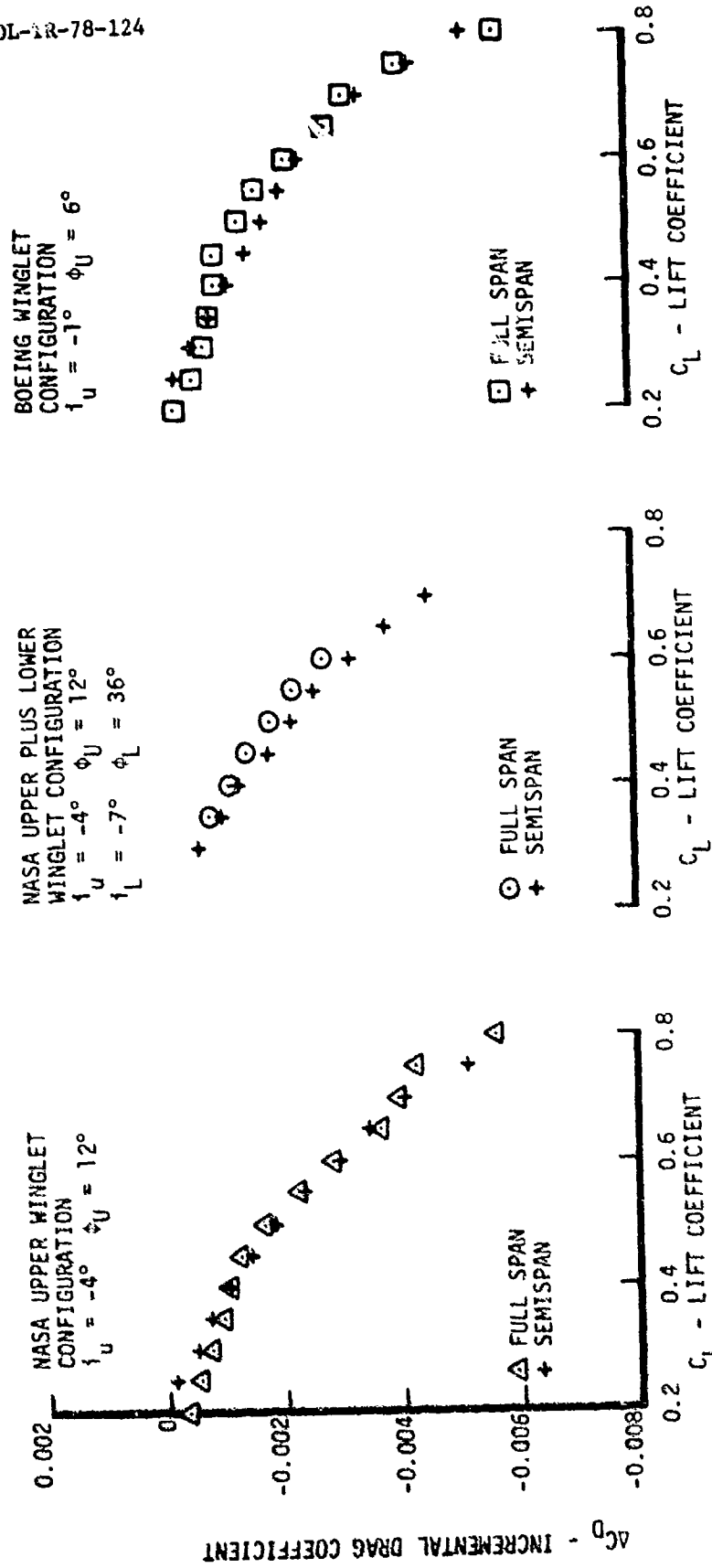Figure 95. Comparison of Full-Span and Semispan Model
Incremental Lift. M = 0.78

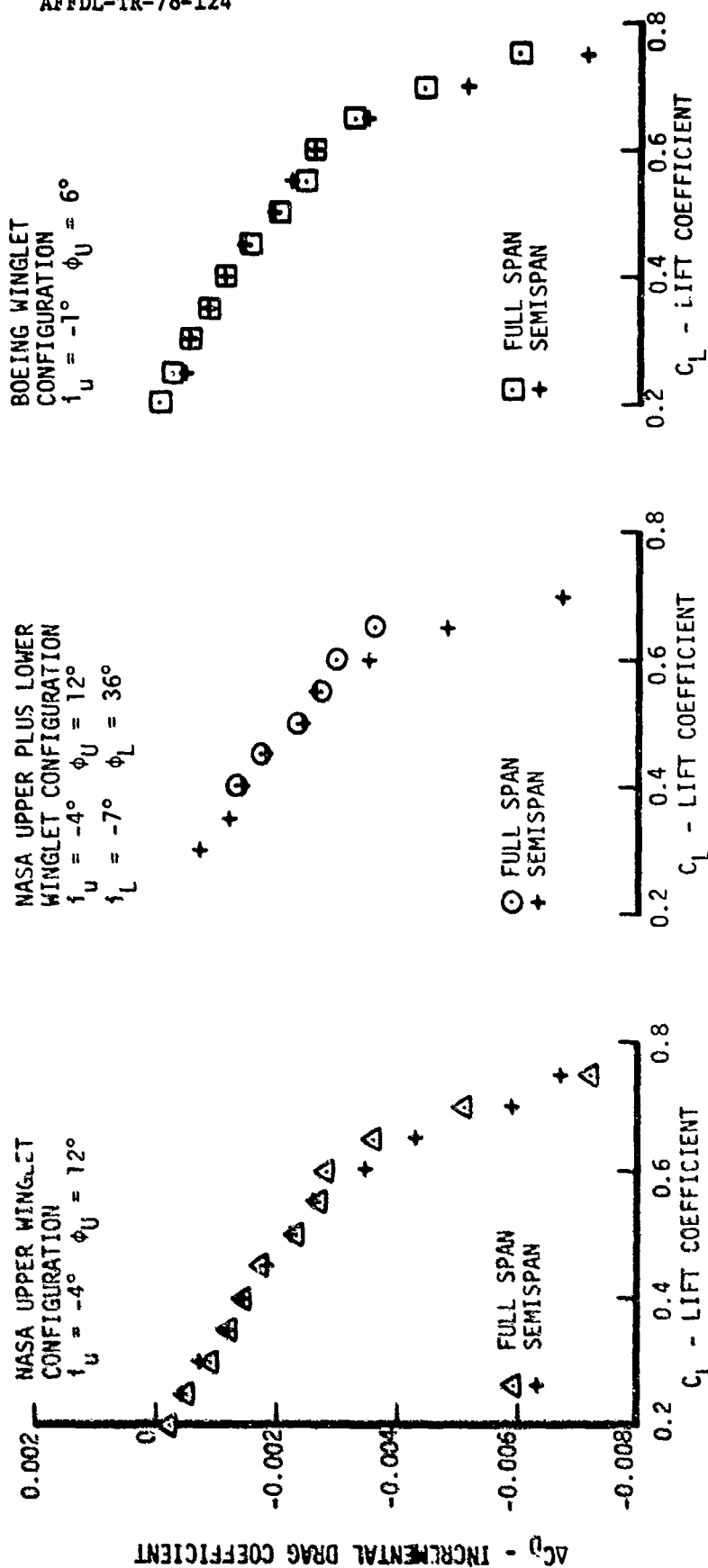Figure 96. Comparison of Full-Span and Semispan Model
Incremental Drag. M = 0.70

AFFDL-TR-78-124

Figure 97. Comparison of Full-Span and Semispan Model
Incremental Drag. M = 0.78

101

REFERENCES

1. Ishimitsu, K. K., Van Devender, N., Dodson, R., et al, "Design and Analysis of Winglets for Military Aircraft," AFFDL-TR-76-6, February 1976.

2. Goldhammer, M. I., "Nonplanar Lifting Systems Method," Douglas Aircraft Company Report MDC J 6985, January 1976.

3. Whitcomb, Richard T., "A Design Approach and Selected Wind Tunnel Results at High Subsonic Speeds for Wing Tip Mounted Winglets," NASA TN D-8260, July 1976.

4. Ramlow, H. D., "Substantiation Data for the KC-135A Flight Manual," Boeing Document D6-5599, December 1964.